Mari Voldsund

Exergy analysis of offshore oil and gas processing

Thesis for the degree of Philosophiae Doctor

Trondheim, May 2014

Norwegian University of Science and Technology
Faculty of Natural Sciences and Technology
Department of Chemistry

NTNU – Trondheim
Norwegian University of
Science and Technology

NTNU
Norwegian University of Science and Technology

Thesis for the degree of Philosophiae Doctor

Faculty of Natural Sciences and Technology
Department of Chemistry

ISBN 978-82-326-0232-2 (printed ver.)
ISBN 978-82-326-0233-9 (electronic ver.)
ISSN 1503-8181

Doctoral theses at NTNU, 2014:155

Printed by NTNU-trykk

Acknowledgements

To work on this PhD thesis has sometimes been really enjoyable and sometimes very challenging. There are several persons that I would like to acknowledge for their important contributions along the way.

My main supervisor Signe Kjelstrup initiated this project. She is thanked for all inspiration, help and guidance, for teaching me thermodynamics, introducing me to science, and last but not least for always believing in me. Ivar S. Ertesvåg has been my co-supervisor, and he is thanked for teaching me exergy analysis, for backing me up through the work on this thesis, and for always answering my questions and reading my manuscripts very thoroughly.

Cooperation with the Norwegian oil company Statoil has meant a lot for this project. Wei He and Audun Røsjorde are thanked for being my contact persons, helping out both with administrative issues, and with matters concerning offshore oil and gas processing. Thanks to Wei I could spend a summer on Statoil in Sandsli, and this was really valuable.

At one point I got an email from Tuong-Van Nguyen from the Technical University of Denmark, who had discovered that we were working on similar topics. That was the start of a very fruitful and inspiring cooperation. Thanks for all the hours on skype and email discussing ideas, simulations and papers.

All members of the "NTNU exergy interest group" are thanked for valuable input and inspiration, while Knut Jøssang and Jonas Reier Kaasa are thanked for their contributions during their work on their master theses.

I would like to thank all my friends and colleagues at the Department of Chemistry for creating a really nice working environment. Thanks for the approximately 1200 10 o'clock coffee breaks, for cabin trips and board-game nights, and for support and encouragement when this was needed.

My family and friends are thanked for all support. Everything from nice Sunday dinners and cafe visits to traveling, skiing and climbing was perfect for recreation and highly appreciated.

And Anders, you are the kindest and most patient person I know. I am so happy to have you by my side.

Summary

The objectives of this thesis were to: (i) establish exergy analyses of the oil and gas processing plants on different types of North Sea platforms; (ii) identify and discuss improvement potentials for each case, compare them and draw general conclusions if possible; and (iii) define meaningful thermodynamic performance parameters for evaluation of the platforms.

Four real platforms (Platforms A–D) and one generic platform of the North Sea type were simulated with the process simulators Aspen HYSYS and Aspen Plus. The real platforms were simulated using process data provided by the oil companies. The generic platform was simulated based on literature data, with six different feed compositions (Cases 1–6). These five platforms presented different process conditions; they differed for instance by their exported products, gas-to-oil ratios, reservoir characteristics and recovery strategies.

Exergy analyses were carried out, and it was shown that for the cases studied in this work, the power consumption was in the range of 5.5–30 MW, or 20–660 MJ/Sm^3 o.e. exported. The heat demand was very small and covered by electric heating for two of the platforms, and higher, but low enough to be covered by waste heat recovery from the power turbines and by heat integration between process streams, for the other three platforms. The main part of the power was consumed by compressors in the gas treatment section for all cases, except Platform B and Case 4 of the generic model. Platform B had lower pressures in the products than in the feeds, resulting in a low compression demand. Case 4 of the generic model had a high content of heavy hydrocarbons in the feed, resulting in large power demand in the oil export pumping section. The recompression- and oil pumping sections appear to be the other major power consumers, together with the seawater injection system, if installed.

The total exergy destruction was in the range of 12–32 MW, or 43–517 MJ/Sm^3 o.e. exported. Most exergy destruction was related to pressure increase or decrease. Exergy destruction in the gas treatment section made up 8–57% of the total amount, destruction in the recompression section accounted for 11–29%, while 10–28% took place in the production manifolds. Exergy losses due to flaring varied in the range of 0–13 MW.

Platforms with high gas-to-oil ratios and high pressures required in the gas product presented the highest power consumption and exergy destruction.

Several measures were proposed for reduction of exergy destruction and losses. Two alternatives included use of mature technologies with potential to increase

efficiency significantly: (i) limit flaring by installation of gas recovery systems, and (ii) improve gas compression performance by updating/exchanging the compressors.

Several thermodynamic performance indicators were discussed, with Platforms A–D as case studies. None of the indicators could at the same time evaluate (i) utilisation of technical achievable potential, (ii) utilisation of theoretical achievable potential and (iii) total use of energy resources. It was concluded that a set of indicators had to be used to evaluate the thermodynamic performance. The following indicators were suggested: specific exergy destruction, BAT efficiency on exergy basis, and exergy efficiency.

The formulation of exergy efficiency for offshore processing plants is difficult because of (i) the high throughput of chemical exergy, (ii) the large variety of chemical components and (iii) the differences in operating conditions. Approaches found in the literature for similar processes were applied to Platforms A–D. These approaches had several drawbacks when applied to offshore processing plants; they showed low sensitivity to performance improvements, gave inconsistent results, or favoured platforms operating under certain conditions. A new exergy efficiency, called the component-by-component efficiency, was proposed. This efficiency could sucessfully evaluate the theoretical improvement potential.

Contents

Chapter 1

Introduction

1.1 Motivation

The well-being of the world's population depends on uninterrupted availability of energy resources. Today, fossil fuels make up the bulk of the energy mix. These energy reserves will be exhausted and they result in greenhouse gas emissions that most likely are causing climate change.

The share of oil and natural gas as fuel in the world's total primary energy mix was 57% in 2012. The share of coal was 30%, while nuclear and renewables accounted for only 13% [15][1]. The primary world energy use by source the last 25 years is shown in Fig. 1.1.

According to the International Energy Agency, natural gas and oil will remain important to the global energy system for decades. In *"Energy Technology Perspectives 2012"* [36], three different scenarios for 2012 to 2050 are presented: one with a sustainable energy system and 2 °C rise in global temperature; one reflecting pledges by countries to cut emissions and boost energy efficiency, resulting in 4 °C rise in global temperature; and one without implementing measures to cut emissions further, giving a 6 °C rise in global temperature. It is forecasted that the share of natural gas will initially increase, displacing coal and some growth in nuclear power. In the most optimistic scenario, gas-powered generation will increasingly serve as peak-load power after 2030, while oil use will fall by more than 50% by 2050. However, even in this scenario oil will remain an important energy carrier in transport and as a feedstock in industry.

In Norway oil and gas extraction make up the major contribution to the country's total value creation (more than 23% came from the petroleum sector in 2012).

[1] Biomass is not included in these statistics.

In 2011, Norway was the seventh largest exporter of oil and the third largest gas exporter in the world [4]. The Norwegian greenhouse gas emissions from 1990 to 2011 are shown in Fig. 1.2, distributed on source. From 1990 to 2001, emissions from oil and gas extraction increased steadily, and from 2001 to 2011 they made up 25%–28% of the total emissions. The part from offshore oil and gas production, including power production, flaring, and cold ventilation on production platforms, accounted for 20%–22%. Power production was the main source of these emissions, accounting for more than four-fifths of them, while flaring was the second biggest source [105].

The development on the Norwegian continental shelf is heading towards more mature fields and longer distances for gas transport. Processing and transport of produced gas are more energy-demanding than production and transport of liquids, and gas production accounts for an increasing share on the Norwegian continental shelf. In addition, the fields' reservoir pressures are decreasing [4]. These elements will most probably increase the power consumption, and thereby the emissions, in this section.

CO_2 emissions from fuel combustion in energy-producing industries (which includes oil and gas extraction) made up 5% of the world's total CO_2 emissions in 2011 [38].

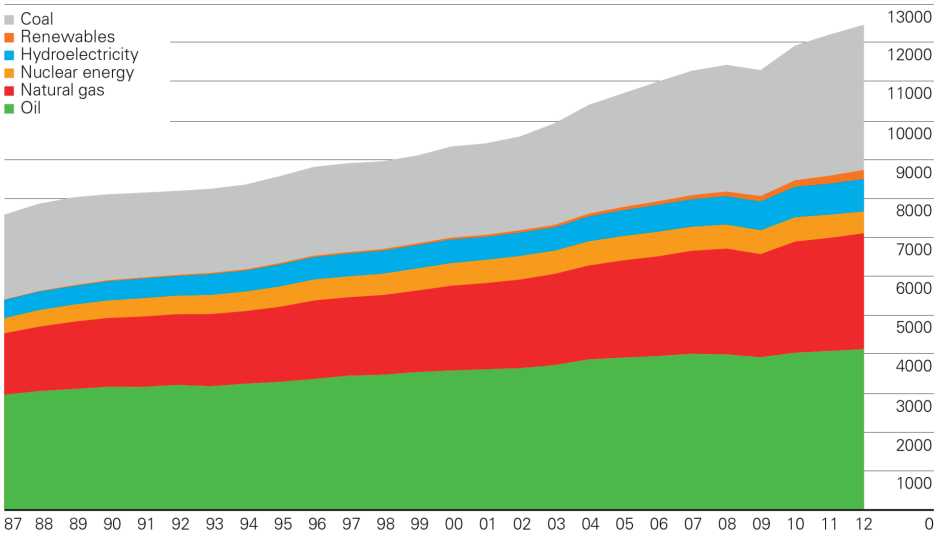

Figure 1.1: Primary world energy use (excluding biomass) by source from 1987 to 2012 given in million tonnes oil equivalents [15].

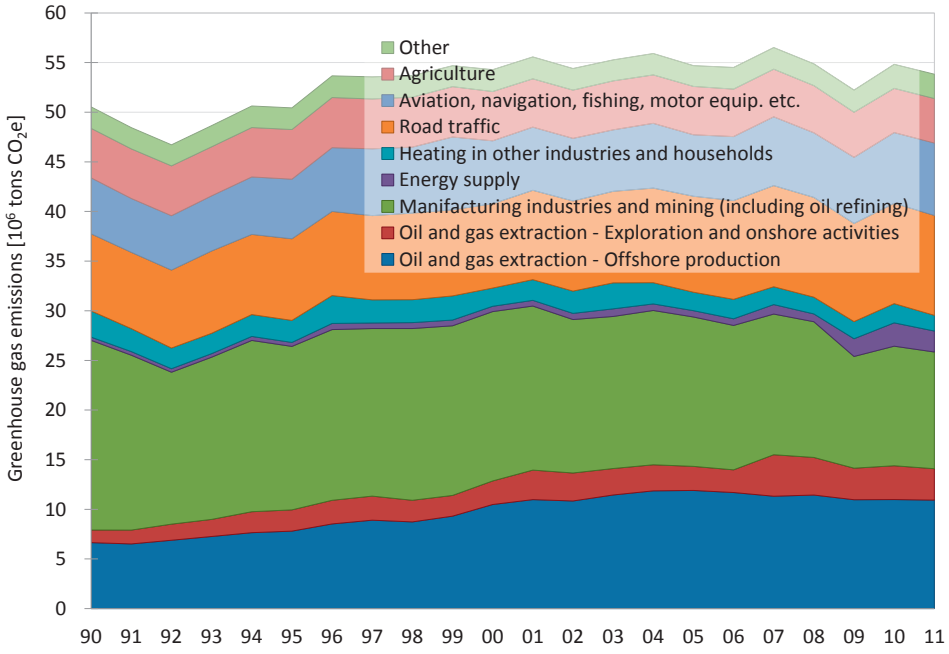

Figure 1.2: Greenhouse gas emissions in Norway by source from 1990 to 2011 [105].

1.2 Energy efficiency

One way to enhance energy security and to cut greenhouse gas emissions is to increase energy efficiency. A process is more energy efficient if it delivers more products or services for the same energy input, or the same products or services for less energy input. Thus, increasing energy efficiency can lower the energy demand, leading to a lower consumption of fossil fuels.

Increasing energy efficiency is widely recognised as a key option in the hands of policy makers, but according to the International Energy Agency [37] the option is still not used to its full potential. It states that energy efficiency must help reduce the energy intensity (energy input per unit of gross domestic product) of the global economy by two-thirds by 2050, and that the annual improvements in energy intensity must double, from 1.2% over the last 40 years to 2.4% in the coming four decades [36]. It also presents increasing energy efficiency in the industry, buildings and transport sectors as one out of four policy measures that can help limit the global temperature increase to 2 °C through to 2020 [39].

The term 'energy efficiency' is used in numerous contexts, and the exact meaning of the term may vary depending on the context. In the field of thermodynamics, energy efficiency is linked to energy analysis, which is based on the 1st law of ther-

modynamics. In this kind of analysis, loss of efficiency in a process due to loss of energy is quantified. The 1st law states that energy is conserved, and in energy analysis all kinds of energy are treated as equal. For instance, low-temperature thermal energy is treated as equivalent to high-temperature thermal energy. Furthermore, energy analysis gives no information on internal losses caused by irreversibilities, and process units such as throttling valves, heat exchangers or combustion chambers give the impression of being free of losses of any kind [50]. Nevertheless, it is common to evaluate the energy efficiency of industrial processes using energy analysis and the 1st law.

The 2nd law of thermodynamics states that in all real processes, entropy is produced. This implies that the potential to perform work decreases. Moreover, in reversible processes the entropy production is zero, implying that the potential to perform work stays unchanged. A combination of the 1st and 2nd laws allows us to measure this potential, and in *exergy analysis* this is assessed systematically. Exergy analysis provides a better evaluation of the utilisation of resources than energy analysis, and gives the possibility to pinpoint where in a process inefficiencies occur: both losses to the surroundings and internal irreversibilities.

1.3 Exergy analysis

In exergy analysis, both the 1st and the 2nd Laws of Thermodynamics are taken into use. Szargut [111] defined exergy the following way:

> *"Exergy is the amount of work obtainable when some matter is brought to a state of thermodynamic equilibrium with the common components of the natural surroundings by means of reversible processes, involving interaction only with the abovementioned components of nature."*

Thus, high-temperature thermal energy is rated higher than low-temperature energy, because it provides a higher potential to perform work. Moreover, internal losses due to irreversibilities are accounted for, and the locations of these process inefficiencies can be found. As stated by Moran and Shapiro [63], the method of exergy analysis is particularly suited for furthering the goal of more efficient resource use, since it enables the locations, types, and true magnitudes of waste and loss to be determined, while the energy conservation idea alone is inadequate for depicting some important aspects of resource utilization.

The concept of exergy has its roots in classical thermodynamics developed in the 19th century. Important milestones were Carnot's work published in 1824 on heat engines [17], where the limitations of converting thermal energy into work were described, as well as Gibbs' work from 1873 where an equation for *available work* was given that is in correspondence with the present definition of exergy [94]. The modern development of exergy analysis was initiated by Bošnjaković with the slogan "fight against irreversibilities" in 1938 [114], and the term *exergy* was

introduced by Rant in 1953 [94]. In the period 1950 to 1970, the theoretical basis of exergy analysis was enlargened and many works presenting exergy analysis of industrial processes were published (see Szargut et al. [114] or Sciubba and Wall [94] for references to the major contributions). After 1970, there was an exponential growth of applications of exergy analysis, and Sciubba and Wall [94] argue that the two main reasons for this are good textbooks developed in the 1960's and the oil crisis in 1973 that forced governments and industries to concentrate on the energy use.

The first exergy analysis of a chemical process was an analysis of a soda plant presented by Rant in 1947, and another early work was the analysis of an ammonia oxidation process presented in 1956 by Denbigh [24]. Oliveira and Van Hombeeck [22] published in 1997 the first exergy analysis of an offshore oil platform. Exergy analysis of other petroleum processes like crude oil distillation and refining were presented by Cornelissen [19], Rivero et al. [85, 83, 84] and Al-Muslim and Dincer [3].

In real processes, some exergy destruction will always take place due to practical limitations. Tsatsaronis and Park [121] defined the *unavoidable exergy destruction* of a process component as the exergy that is destroyed when the component is operated at its maximum efficiency, considering technological limitations that could not be overcome in the near future, regardless of investment costs. Johannessen et al. [40, 41] suggested to set a state of *minimum entropy production*, or minimum exergy destruction, for a given operation target, and the difference between the current value and this minimum would be considered as an excess loss.

One line of research developed from the concept of exergy is the *exergetic life cycle assessment*. In this approach the concept of exergy is introduced into the framework of the life cycle assessment and it can be seen as the exergy analysis of a complete life cycle [19, 20]. The exergy destruction of a product from cradle to grave is calculated, including the utilisation of raw materials and energy resources in the production of the product, the production of process equipment used in the production and exergy destruction related to waste products. Thus it is shown in which part(s) of the life cycle the depletion of natural resources is most severe.

The concept of exergy can also be used for resource accounting and to describe the degradation of natural capital [23]. Exergy allows us to value all types of natural resources, e.g. fossil fuels, minerals, water and biomass, on the same basis. In the *exergoecology* approach introduced by Valero, natural resources are assessed by quantifying the exergy and the exergy costs of the resources. While the exergy measures the minimum (reversible) work required to extract and concentrate the materials from a reference environment, the exergy cost accounts for the actual exergy required for accomplishing the same process with available technologies [124]. The world has a finite number of exergy resources, and the extraction of these resources implies the use of other exergy resources. As the resources are depleted, the quantity of exergy resources required to extract more goods increases [23].

1.4 Offshore oil and gas platforms

The purpose of oil and gas production platforms is to extract, process, and export petroleum. A typical North Sea offshore platform consists of a processing section, a utility system, drilling modules, and a living quarter (Fig. 1.3).

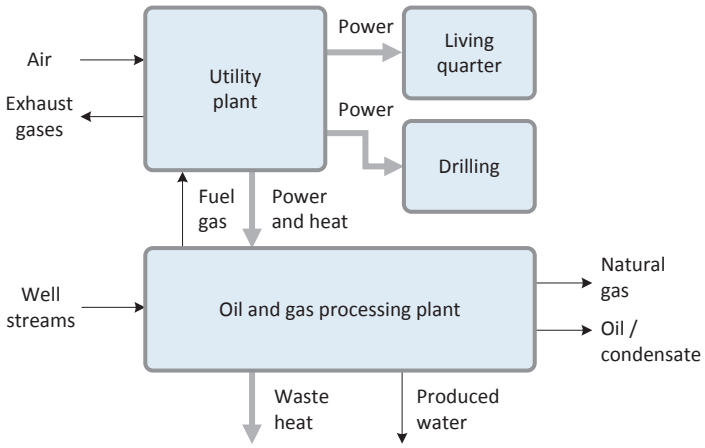

Figure 1.3: Schematic overview of a typical North Sea oil and gas platform. Black arrows represent material streams, while grey arrows represent energy streams.

In the processing section, well streams consisting of a mixture of light and heavy hydrocarbons as well as water are separated into produced water, oil/condensate and gas. The water is purified and discharged or disposed. The petroleum is processed and delivered at the required quality. In addition, seawater may be compressed and injected to enhance oil recovery. Power is needed for compression and pumping, and heat may be needed to ease separation and for gas dehydration. Power and heat are delivered by the utility system, normally by combusting gas produced at the platform. The utility system also delivers power to the living quarter and to the drilling modules.

Different platforms operate under different conditions. Both input and output material streams may have different temperatures, pressures, compositions and flow rates, resulting in different boundary conditions for the oil and gas processing sections. Factors contributing to these differences are:

- product specifications (e.g. specified vapour pressure, dew point, water content and export pressure);
- operating strategy (e.g. recovery strategy, gas treatment, exported products);
- reservoir characteristics (e.g. reservoir temperature and pressure);
- reservoir fluid properties (e.g. chemical composition, gas-to-oil ratio and water-to-oil ratio).

In the petroleum industry, the purpose is to provide customers with a fuel, which is a carrier of chemical exergy. In the case of offshore platforms, this fuel only extracted and processed with no chemical reactions involved. Thus, a typical feature of a petroleum platform is that it has a high throughput of exergy that does not take part in any thermodynamic conversion, but just passes through the system (Fig. 1.4). It is important to keep in mind that even if exergy losses and exergy destruction are low compared to the high throughput of exergy of the system, the power consumption of platforms in the North Sea vary between approximately 10 MW to several hundred MW, and that CO_2 emissions from oil installations account for one of the major contributions to greenhouse gas emissions in Norway.

As mentioned, increased power consumption is expected on North Sea installations, illustrating that as the world's exergy capital is depleting, more exergy is required in order to extract what remains.

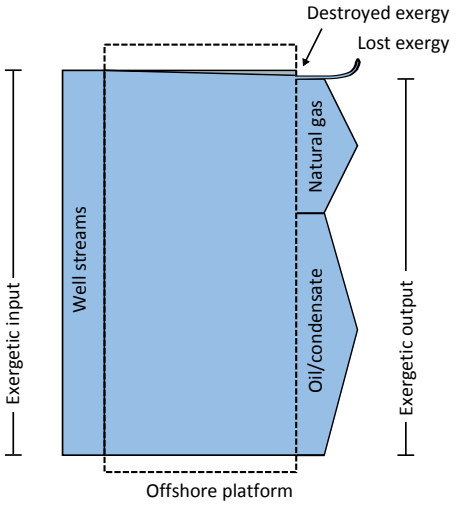

Figure 1.4: Exergy input, output, destruction and losses for a typical oil and gas platform.

1.5 Research objectives

Given that the decision of using a certain part of the oil and gas reserves is taken, the extraction of this petroleum should be carried out while destroying a minimum of exergy. This would maximise the utilisation of the resources and limit greenhouse gas emissions. One step in this direction is to map the sources to exergy destruction and exergy losses, and on this basis evaluate options for process improvements. Another step is to define suitable performance indicators that can motivate optimal operation. These topics are addressed in this thesis, with focus on the oil and gas processing on North Sea platforms.

At the start of this project, no exergy analyses of North Sea type offshore platforms could be found in the literature. The first objective of this thesis was therefore to establish exergy analyses of the oil and gas processing plants on different types of North Sea platforms, in order to obtain knowledge on exergy consumption, exergy flows, exergy destruction and exergy losses on such installations.

The second objective was to use the exergy analyses to identify and discuss improvement potentials for each case, to compare cases, and draw general conclusions if possible.

The third objective was to define meaningful thermodynamic performance indicators in order to evaluate the platforms. Such indicators should make possible to compare the performance of different platforms regarding resource use and thermodynamic perfection.

1.6 Thesis outline

This thesis is organised as a paper collection, and Chapters 2–6 are published or submitted journal papers. Conclusions are drawn in Chapter 7.

In Chapters 2–4, exergy analyses of offshore processes and discussions of improvement options are presented. A thorough exergy analysis of the oil and gas processing plant on one real North Sea oil platform is performed and discussed in Chapter 2. A model of a generic North Sea platform exporting oil and dehydrated gas is established based on literature data, and an exergy analysis is carried out in Chapter 3. The oil and gas processing plants on four real North Sea offshore platforms are analysed and compared in Chapter 4.

The topic of Chapters 5–6 is discussion and development of possible performance indicators for offshore oil and gas processing. In Chapter 5 the focus is on different types of energy-based and exergy-based indicators, while in Chapter 6 the exergy efficiency for petroleum systems is discussed in particular, and a new formulation is suggested.

1.7 List of publications

The publications made during this PhD work are listed below. Most of the conference proceedings were further developed and submitted to journals at a later stage.

1.7.1 Conference proceedings

The following articles were presented on conferences and included in the conference proceedings.

1. M. Voldsund, I. S. Ertesvåg, A. Røsjorde, W. He and S. Kjelstrup. Exergy analysis of the oil and gas separation processes on a north sea oil platform. *Proceedings of ECOS 2010 – The 23rd International Conference on Efficiency, Cost, Optimization, Simulation and Environmental Impact of Energy Systems*, Lausanne, Switzerland, 2010.
2. M. Voldsund, W. He, A. Røsjorde, I. S. Ertesvåg and S. Kjelstrup. Evaluation of the oil and gas processing at a real production day on a North Sea oil platform using exergy analysis. *Proceedings of ECOS 2012 – The 25th International Conference on Efficiency, Cost, Optimization, Simulation and Environmental Impact of Energy Systems*, Perugia, Italy, 2012.
3. M. Voldsund, T.-V. Nguyen, B. Elmegaard, I. S. Ertesvåg, A. Røsjorde, K. Jøssang and S. Kjelstrup. Comparative study of the sources of exergy destruction on four North Sea oil and gas platforms. *Proceedings of ECOS 2013 – The 26th International Conference on Efficiency, Cost, Optimization, Simulation and Environmental Impact of Energy Systems*, Guilin, China, 2013.
4. M. Voldsund, T.-V. Nguyen, B. Elmegaard, I. S. Ertesvåg, A. Røsjorde, W. He and S. Kjelstrup. Performance indicators for evaluation of North Sea oil and gas platforms. *Proceedings of ECOS 2013 – The 26th International Conference on Efficiency, Cost, Optimization, Simulation and Environmental Impact of Energy Systems*, Guilin, China, 2013.

1.7.2 Journal articles

The following articles are published in or submitted to international journals. These articles are included as Chapters 2–6 in this thesis.

1. M. Voldsund, I. S. Ertesvåg, W. He and S. Kjelstrup. Exergy analysis of the oil and gas processing a real production day on a North Sea oil platform. *Energy*, 55:716–727, 2013.
2. T.-V. Nguyen, L. Pierobon, B. Elmegaard, F. Haglind, P. Breuhaus and M. Voldsund. Exergetic assessment of energy systems on North Sea oil and gas platforms. *Energy*, 62:23–36, 2013.
3. M. Voldsund, T.-V. Nguyen, B. Elmegaard, I. S. Ertesvåg, A. Røsjorde, K. Jøssang and S. Kjelstrup. Exergy destruction and losses on four North Sea offshore platforms: A comparative study of the oil and gas processing plants. *Energy*, accepted for publication.

4. M. Voldsund, T.-V. Nguyen, B. Elmegaard, I. S. Ertesvåg and S. Kjelstrup. Thermodynamic performance indicators for offshore oil and gas processing: Application to four North Sea facilities. *Oil and gas facilities*, submitted.

5. T.-V. Nguyen, M. Voldsund, B. Elmegaard, I. S. Ertesvåg and S. Kjelstrup. On the definition of exergy efficiency for petroleum processes: Application to offshore oil and gas processing. *Energy*, submitted.

1.7.3 Book chapter

1. S. Kjelstrup, M. Voldsund and M. Takla. Towards a more resource-efficient society - The concept of exergy. In R. H. Gabrielsen and J. Grue (eds.), *Norwegian energy policy in context of the global energy situation*, pages 117–126. Novus forlag, 2012.

1.8 Thesis author contributions

This PhD thesis consists of journal articles 1–5.

M. Voldsund (the author of this thesis) has performed the process modelling and analysis, as well as the writing of journal article 1. The co-authors of this publication have contributed by defining the problem, helping to choose methodology, and by thoroughly reading and commenting the manuscript.

Similarly, the work presented in journal article 2 was carried out mainly by T.-V. Nguyen. The other co-authors, including M. Voldsund, contributed with scientific discussions and by reading and commenting the manuscript.

Journal articles 3–5 are results of a cooperation between M. Voldsund and T.-V. Nguyen, and the work loads of these publications were shared equally between these two authors. Out of the three new installations analysed and introduced in journal article 3, the modelling and exergy analysis of Platform B was performed by M. Voldsund, for Platform C it was performed by MSc. student K. Jøssang under supervision of M. Voldsund, and for Platform D it was performed by T.-V. Nguyen. The additional calculations for journal articles 4–5, the development of the new exergy efficiency and the writing of these papers, were done by both M. Voldsund and T.-V. Nguyen. S. Kjelstrup wrote parts of the discussion in journal article 4. Kjelstrup and the other co-authors contributed with scientific discussions and by reading and commenting the manuscripts.

Chapter 2

Exergy analysis of the oil and gas processing on a North Sea oil platform a real production day

Mari Voldsund[1], Ivar Ståle Ertesvåg[2], Wei He[3] and Signe Kjelstrup[1]

1. Department of Chemistry,
Norwegian University of Science and Technology,
NO-7491 Trondheim, Norway

2. Department of Energy and Process Engineering,
Norwegian University of Science and Technology,
NO-7491 Trondheim, Norway

3. Statoil ASA,
NO-5254 Sandsli, Norway

This chapter has been published in
Energy - The International Journal
Volume 55 (2013), Pages 716–727

Abstract

We explore the applicability of exergy analysis as an evaluation and monitoring tool for the oil and gas processing on an offshore platform. A real production day on a particular North Sea platform is analysed. A process flowsheet is simulated using measured process data. We distinguish between temperature-based exergy, pressure-based exergy and the mixing part of the chemical exergy. It is shown that physical exergy in the material streams mainly is pressure-based exergy, and most exergy destruction is related to decrease or increase in pressure. The sub-processes with most destroyed exergy are the production manifold (4600 kW), the recompression train (4150 kW) and the reinjection trains (10,400 kW). At this platform 260 kW separation work is done, where a considerable part is done in the compression trains in addition to in the separation train. The specific power consumption is 179 $\pm$ 3 kWh/Sm^3 and the exergetic efficiency is 0.13 $\pm$ 0.02. We propose measures to decrease exergy destruction, and that exergy analysis should be taken into regular use by the oil and gas industry. This study serve as a showcase on how to do an exact analysis of an existing offshore platform using measured process data.

2.1 Introduction

In 2009, gas turbines and diesel engines on oil and gas platforms were responsible for 21% of Norway's total CO_2-emissions [104]. Most platforms generate their own power with gas turbines, and the typical power consumption at a North Sea offshore platform varies from around 10 MW to several hundred MW. There is a general agreement that the world's CO_2 emissions should be reduced and that the world's resources should be utilised in a sustainable way. Improvement of energy efficiency is a challenge in the petroleum sector, as in the industry in general. The sector is therefore in need for a tool to monitor the energy performance of the platform processes.

Today, specific CO_2 emissions (CO_2 emission per unit produced oil) is often used as a performance parameter by the oil and gas industry. This parameter reflects the aim of reducing the world's CO_2 emissions - it encourages energy efficiency and use of renewable energy sources. However, it does not account for the varying operating conditions for offshore platforms. Different platforms have different well stream conditions, different pressure requirements for export oil and injection/export gas etc. The same platform also operates under varying conditions, e.g. well streams that change over time.

In Norway, as well as in a number of other countries, the industry has to pay tax for CO_2 and NO_x emissions. At the same time increased recovery and extended lifetimes in mature fields is encouraged. However, measures designed to improve

recovery often require significant amounts of power and may entail additional emissions to air [72]. The taxes do then punish measures that are encouraged by the authorities [34].

Exergy analysis is a thermodynamic method which is not yet systematically used by the oil and gas industry. The exergetic efficiency takes into account the minimum theoretical work that has to be done for a given process, and gives thus another perspective than specific CO_2 emissions. By using exergy analysis, one can also calculate the destroyed exergy in different parts of the process and indicate possibilities for improvement. We want to explore the use of exergy analysis as a tool for platform performance benchmarking and as an everyday tool to evaluate performance. We therefore analyse the oil and gas processing a real production day on a North Sea oil platform. We use measured process data for the specific day to simulate a process flowsheet for that day and calculate destroyed exergy and exergetic efficiency. To gain more insight about the process, we also distinguish between temperature-based exergy, pressure-based exergy and the mixing part of the chemical exergy. This is the first study using exergy analysis on a North Sea platform, which is the main motivation for this study.

There is one other exergy analysis of an offshore platform known in the literature. This is an analysis of the oil and gas processing of a Brazilian platform performed by de Oliveira Junior and van Hombeeck [22]. On this platform, power was consumed in order to heat the petroleum for separation, to compress natural gas and to pump oil to the coast. A heat recovery system was installed in order to recover heat from exhaust gases for the petroleum heating. Both the petroleum heating, despite the heat recovery system, and the compression operations gave considerable exergy destruction. The separation process, that required heating, was pointed out as a place to do improvements.

The North Sea oil platform we analyse was built more than 20 years ago. The platform was chosen because it is a relatively simple one, but contains still all processes typical for such platforms. It exports oil and reinjects gas in the reservoir for pressure maintenance. The power consumption of the entire platform varies around 34 MW and in the oil and gas processing part, which is analysed here, it varies around 24 MW. The boundary conditions of the system are dictated by the conditions of the well streams, specifications on vapour pressure and water content for the produced oil, pressure required for the export through the export pipelines, pressure required in the injection gas and pressure- and temperature specifications for the fuel gas. Initial studies of the oil and gas processing at this platform were presented by Voldsund *et al.* [127, 128].

This is the first study based on measured process data, and it can serve as a showcase on how to do an exact assessment of a specific platform using exergy analysis.

2.2 Theoretical background

2.2.1 Exergy

The exergy of a system is defined as the maximum theoretical work obtainable when the system interacts with the environment to reach equilibrium. This maximum theoretical work is obtained when all processes involved are reversible. In all real processes some exergy will be destroyed. In an exergy analysis of a process, thermodynamic inefficiencies can be identified. For a comprehensive introduction to exergy analysis, see the textbook of Kotas [50] or Moran and Shapiro [63]. For a thorough review of applications of exergy analysis, see the textbook of Dincer [26]. Important quantities in exergy analysis are:

- The *product exergy*, E_{P}, is the desired result expressed in terms of exergy.
- The *utilized exergy*, E_{U}, is the resources in terms of exergy used to provide the product exergy.
- *Exergy loss*, E_{L}, is thermodynamic inefficiencies of a system associated with the transfer of exergy with energy and material streams to the surroundings.
- *Exergy destruction*, E_{D}, is thermodynamic inefficiencies of a system associated with the irreversibilities (entropy generation) within the system boundaries.

For a system in steady state the destroyed exergy for a certain time period, E_D, is the exergy entering the system minus the exergy leaving the system:

$$E_{\mathrm{D}} = W + \sum_k \int_{T_k} \left(1 - \frac{T_0}{T_k}\right) \mathrm{d}Q_k + \sum_j n_j e_j, \tag{2.1}$$

where W is the work added, Q_k the heat transferred into the system at temperature T_k, T_0 the ambient temperature, n_j the number of moles in material stream j and e_j the molar exergy in material stream j. Some of the terms in Eq. 2.1 correspond to product exergy, some correspond to utilized exergy and some correspond to exergy loss, depending on the system considered, $E_{\mathrm{D}} = E_{\mathrm{U}} - E_{\mathrm{P}} - E_{\mathrm{L}}$.

Exergy in a material stream can be split into physical (thermomechanical) exergy, chemical exergy, kinetic exergy and potential exergy. Given on molar form, we have: $e = e^{\mathrm{ph}} + e^{\mathrm{ch}} + e^{\mathrm{kin}} + e^{\mathrm{pot}}$.

The molar physical exergy accounts for deviation from thermal and mechanical equilibrium with the environment and is given by:

$$e^{\mathrm{ph}} = h - h_0 - T_0(s - s_0), \tag{2.2}$$

where h and s are the molar enthalpy and entropy, and h_0 and s_0 are the molar enthalpy and entropy for the same stream but at T_0 and p_0, where p_0 is the ambient pressure.

The physical exergy can be divided into temperature-based and pressure-based exergy, e^{T} and e^{P}, respectively. The most common way to do this is:

$$e^{\mathrm{T}} = h - h(T_0) - T_0(s - s(T_0)), \tag{2.3}$$

and

$$e^{\mathrm{P}} = h(T_0) - h_0 - T_0(s(T_0) - s_0), \tag{2.4}$$

where $h(T_0)$ and $s(T_0)$ is enthalpy and entropy evaluated at the initial pressure of the stream and T_0.

The molar chemical exergy accounts for deviation from a state with only thermal and mechanical equilibrium with the environment to a state with also chemical equilibrium with the environment, and is given by:

$$e^{\mathrm{ch}} = \underbrace{\sum_i x_i \bar{e}_i}_{\mathrm{I}} + \underbrace{\left(h_0 - \sum_i x_i h_{i,0} - T_0 \left(s_0 - \sum_i x_i s_{i,0} \right) \right)}_{\mathrm{II}}, \tag{2.5}$$

where term I accounts for the molar chemical exergy of each of the components when they are pure and term II accounts for mixing effects. The symbol x_i is the mole fraction of chemical component i, $\bar{e}_i$ the molar chemical exergy of pure i, $h_{i,0}$ the molar enthalpy of pure i at T_0 and p_0 and $s_{i,0}$ the molar entropy of pure i at T_0 and p_0.

The kinetic and potential exergy of a material stream is equal to the kinetic and potential energy of the material stream.

2.2.2 Process performance parameters

There exists a variety of ways to define performance parameters for industrial processes based on energy and exergy. We present some parameters that are useful for oil and gas processing:

- The specific power consumption we define as consumed power per unit oil produced. As long as all power comes from the same fossil fuel source, this is proportional to specific CO_2 emissions.
- The exergetic efficiency, ε, is:

$$\varepsilon = \frac{E_{\mathrm{P}}}{E_{\mathrm{U}}}. \tag{2.6}$$

This parameter takes into account the minimum theoretical work that has to be done for a given process. The interpretation of E_{P} and E_{U} vary. We define E_{P} and E_{U} for our system in Section 2.4.2.

- The efficiency defect, δ_i, of subsystem i is the fraction of the input exergy to the whole system which is lost through irreversibilities in the subsystem [50]:

$$\delta_i = \frac{E_{\mathrm{D},i}}{E_{\mathrm{U}}}. \tag{2.7}$$

This parameter shows how different subsystems contribute to reduction of the exergetic efficiency.

2.3 System description

The studied North Sea platform is an oil producing platform that has been in production for more than 20 years. Two power turbines produce electric power that covers all power needed at the platform. Fuel gas for the power turbines is taken from the gas produced at the platform (approximately 3%). In the oil and gas processing, reservoir fluids are separated into oil, gas and water. The produced oil is pumped 18 km to a nearby platform for export, the water is rinsed and released to the sea, and the produced gas is recompressed and reinjected into the reservoir for pressure maintenance. Pressure maintenance is also achieved by injection of high pressure water, but this water is provided by a nearby platform. An overview of the oil and gas processing and characteristics for the studied day are given below.

2.3.1 Process overview

A schematic overview of the oil and gas processing at the studied platform is given in Fig. 2.1.

A number of production wells are connected to the platform and the well streams have different temperatures, pressures and oil-, gas- and water fractions. The wells are connected to the oil and gas processing section via a production manifold. In the manifold a selection of the wells are set into production. For the day we study, the pressures of the producing wells vary between 80 and 170 bar. The pressures are reduced to approximately 70 bar before the streams are mixed. The resulting stream consists of reservoir fluids with 78 mol% gas, and is sent to a separation train.

In the separation train gas and water are separated from the crude oil using gravitational separators and an electrostatic coalescer. The train consists of three stages where in the first two stages there are three-phase separators, and in the third stage there is a two-phase separator and an electrostatic coalescer. For each

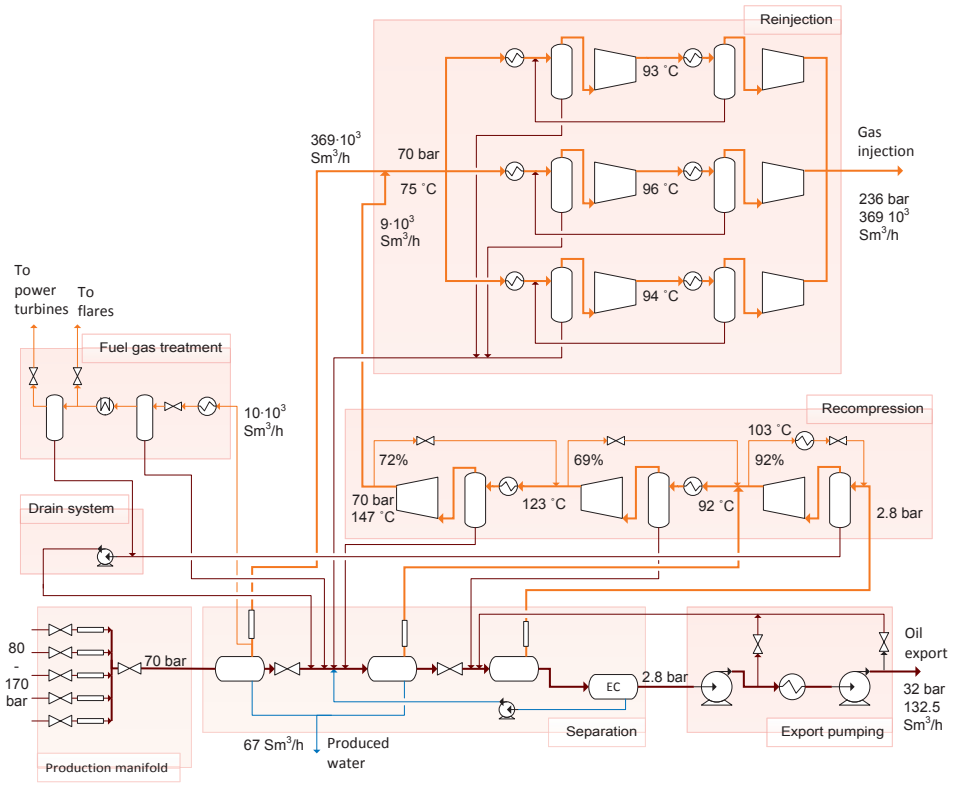

Figure 2.1: Process flowsheet of the oil and gas processing for the studied production day. Gas streams are orange, water streams are blue and oil, condensate or mixed streams are brown. Well streams (well 7, 16, 23, 24 and 26) enter the process in a production manifold where the pressures are decreased and the streams are mixed. The resulting mixed stream enters the separation train where it is separated into gas, oil and water. The water is sent out of the process, the oil is sent to the export pumping section where it is pumped for export, high pressure gas is sent to the reinjection trains and low pressure gas is sent to the recompression train where it is compressed before it is sent to the reinjection trains. In the reinjection trains the gas is further compressed before it is reinjected into the reservoir. Fuel gas is taken from the 1st separation stage, and treated in the fuel gas system. It is combusted in power turbines and in pilot flames in the flare system. There is a drain system where some small liquid streams are collected and pumped back to the separation train. It consists of several units, but a simplified version is used in this study.

separator, the pressure is reduced, so that more gas is released from the oil. The oil shall meet specifications of basic sediment content, water content and vapour pressure. In total the pressure is reduced from 71 to 2.8 bar during this section. Oily water from the separators is sent to a water treatment process where traces of oil are removed. This process is not included in this analysis. Water from the electrostatic coalescer is pumped back to the 2nd-stage separator. In contrast to the platform studied by de Oliveira Junior and van Hombeeck [22], no heating is required in the separation process.

The remaining, stabilised oil is pumped via two pumps with cooling of the oil between, to meet the pressure conditions in the transportation pipeline. A minimum flow is required through the pumps, and to achieve this, some of the oil is recycled back to right after the 2nd-stage separator.

The gas that is released in each stage in the separation train is sent to the recompression train. The train consists of three stages, each with a cooler, a scrubber and a compressor. The gas is cooled for a more efficient compression. The scrubber is a separator that removes small amounts of condensed liquid. Scrubbing protects the compressor and allows more optimal compression. In the end of the train the pressure has reached the 1st-stage separation pressure.

Since the platform is more than 20 years old, and the gas to oil ratio (GOR) in the feed has changed over time, the flow rates in the recompression train is lower than what the train was designed for. A minimum flow of gas is required through the compressors to prevent surging, and some of the gas is therefore recycled around each stage (anti-surge recycling). The fractions of gas that are recycled are 92%, 69% and 72% in the 1st, 2nd and 3rd recompression stages, respectively.

After recompression, the gas enters the reinjection trains. These are three parallel trains where the gas is compressed up to injection well pressure. In each of these trains there are two stages, each with a cooler, a scrubber and a compressor - the same way as in the recompression train. The train is run at maximum capacity, so there is no need for anti-surge recycling. High pressure gas leaves the system for injection back into the reservoir through 5 injection wells.

Fuel gas is taken from the 1st-stage separator and is cooled and fed through a pressure reducing control valve to a scrubber for liquid removal. After the scrubber, the gas is heated with an electrical heater before a last possible liquid removal, before it is sent to the power turbines. Gas for a pilot flame at the flare is also taken from this section. For normal process conditions, the amount of gas to the flare from other parts of the processes is negligible.

Condensate from scrubbers throughout the processes is sent back to the 2nd separation stage, either directly or through a drain system. The drain system consists of several tanks and small pumps, but is for simplicity looked upon as only one mixer and one pump in this study.

2.3.2 Process characteristics

We had available process data measured from 2009 to 2011. Many process variables change from day to day due to variation in the well conditions and since the operators switch between different wells during production. To obtain a consistent and representative flowsheet we decided to use the average values for a period of one day with stable conditions. We defined the 85 % of the days that were closest to the median value for selected process variables as 'normal production days', since it was found that with this criterion, days with shutdowns or other major disturbances were excluded. The day studied here is one of these 'normal production days'. The process conditions were stable throughout this day in the sense that the standard deviation in measured produced oil flow rate is less than 10 Sm^3/h (for an average flow rate of 132.5 Sm^3/h) and the injected gas flow rate measured in each of the in total 5 injection wells is less than 10^3 Sm^3/h (for an average *total* flow rate of 369 $\cdot 10^3$ Sm^3/h).

The varying well conditions lead to variation in several parameters, which are important for the performance of the oil platform. The variation in these parameters are summarised in Table 2.1. The studied day has a medium gas injection flow rate, a low oil production flow rate and a high gas injection pressure.

Table 2.1: Process parameters important for the performance of the oil platform for all normal production days from 2009 to 2011. Maximum and minimum levels of the parameters are given, together with values for the studied production day.

Process parameter	Max	Min	Studied day
Gas injection flow rate, 10^3 Sm^3/h	323	392	369
Oil production flow rate, Sm^3/h	121.6	302.6	132.5
Gas injection pressure, bar	210	240	236

The adiabatic efficiencies calculated from measured inlet and outlet temperatures and pressures for the real production day are given in Table 2.2.

Table 2.2: Adiabatic compressor efficiencies for the production day analysed. The efficiencies are calculated from the measured inlet and outlet temperatures and pressures of the compressors, given in Table 2.12 and Table 2.13 in Appendix 2.A.

Compressor	Adiabatic efficiency	Compressor	Adiabatic efficiency
Recompression		*Reinjection B*	
1st stage	47%	1st stage	64%
2nd stage	69%	2nd stage	57%
3rd stage	56%		
Reinjection A		*Reinjection C*	
1st stage	64%	1st stage	69%
2nd stage	54%	2nd stage	64%

2.4 Methodology

2.4.1 Simulation of the process flowsheet

The chemical processes were simulated using the process simulator Aspen HYSYS. We used the property package where the Peng-Robinson equation of state [77] is used to calculate thermodynamic properties. This package is the recommended property package for oil and gas applications [9]. The HYSYS PR option was chosen and liquid densities were calculated with the COSTALD method. The HYSYS PR option has several enhancements to the original Peng-Robinson equation and the COSTALD method calculates better liquid densities than the equation of state [9]. Interaction coefficients were taken from the HYSYS library and the interaction parameters unavailable from the library were set as estimated by HYSYS. Hypothetical components were used to simulate the heavy oil fractions. Hypothetical components are made-up components that represent oil fractions that can consist of a number of different real components.

Mean values for measured process variables like flow rates, temperatures and pressures for the studied production day were used as input variables in the simulation together with some values found in documentation of equipment (pump efficiencies and a pressure drop over a scrubber). The hypothetical components used to describe the heavy oil fractions and the composition of the oil-, gas- and water phases were taken as developed by the oil company. It was assumed that these compositions do not change over time. Other measured process variables were used to validate the model. Details about the hypothetical components, the composition of the reservoir fluids, and the measured process variables, used as input variables and for validation, are given in Appendix 2.A.

2.4.2 Exergy analysis

The ambient temperature was set to 8 °C, as this is the average temperature for the North Sea throughout the year [73].

The exergy destruction in each process unit was found using the exergy balance of the unit. Exergy in the material streams were calculated creating user variables in HYSYS programmed with Visual Basic. Physical exergy was calculated as described by Abdollahi-Demneh *et al.* [2]. Temperature- and pressure-based exergy was calculated by modifying the same code. New code was developed that calculated the mixing part of the chemical exergy (term II in Eq. 2.5). The component chemical exergy (term I in Eq. 2.5) was not taken into consideration, since this exergy only passes through the system. Contributions from kinetic and potential exergy were neglected.

All cooling in the system is done with cooling water discharged irreversibly to the sea. The exergy leaving the system in form of thermal energy was therefore

regarded as destroyed exergy. This means in practice that the system boundaries were drawn around the points where cooling water and sea water are mixed. The small amount of heating that is required is done with an electric fuel gas heater. Since no thermal energy enters the system and all thermal energy leaving the system was regarded destroyed, the exergy balance (Eq. 2.1) reduced to:

$$E_{\mathrm{D}} = W + \sum_j n_j e_j. \tag{2.8}$$

For the calculation of the exergetic efficiency, E_P was defined as the exergy difference between process streams leaving and entering the system and E_U as the power delivered to the process units (after electrical and mechanical losses). This is identical to the exergetic efficiency defined by de Oliveira Junior and van Hombeeck for their system, except for that they used the exergy of the fuel gas as utilised exergy, not the power consumption, meaning that they included the power turbines in the analysis. The exergetic efficiency defined this way corresponds to the theoretical minimum exergy input required to drive the process with the current boundary conditions for the material streams, divided by the actual exergy input. No streams leaving the system were considered as exergy loss, giving $E_L = 0$.

2.4.3 Uncertainty analysis

The dominant contributions to uncertainty in the calculations were the uncertainty in measured process variables and uncertainty from inaccuracies in the equation of state.

Uncertainties (with 95 % confidence interval) were determined for all measured process variables. At the platform, some measurements (fiscal measurements) are subject to requirements for uncertainty set by the authorities (The Norwegian Petroleum Directorate and The Climate and Pollution Agency). For these variables we assumed that the real measurement uncertainties were equal to the set limits. For the remaining measured variables, uncertainties were taken as set in the oil company's own guidelines for accuracy. However, for some of these variables the uncertainties were adjusted after discussions with the operators of the platform and in accordance with the authors' experience with the dataset.

When all errors are independent and random, the magnitude of the uncertainty σ_A in variable A is given by:

$$\sigma_A = \sqrt{\sum_{i=1}^{n} \left(\frac{\partial A}{\partial x_i} \sigma_{x_i} \right)^2}, \tag{2.9}$$

where A depends on n other variables x_i, each with uncertainty σ_{x_i} [115]. Propagation of uncertainty from measured variables to the calculated performance parameters and destroyed exergies was calculated using Eq. 2.9 with the following

approximation:

$$\frac{\partial A}{\partial x_i} = \frac{A(x_i + \sigma_{x_i}) - A(x_i - \sigma_{x_i})}{2\sigma_{x_i}}. \tag{2.10}$$

The values for $A(x_i + \sigma_{x_i})$ and $A(x_i - \sigma_{x_i})$ were found for each x_i by simulating the process with the value of x_i changed and everything else kept constant.

Inaccuracies in calculated destroyed exergy, power consumption and performance parameters originating from the chosen equation of state (Peng-Robinson) were found by focusing on methane, which is a key component in the process. Enthalpy and physical exergy for methane at relevant temperatures and pressures calculated with the Peng-Robinson equation of state was compared with enthalpy and physical exergy for methane at the same temperatures and pressures calculated with a presumably more accurate equation of state developed by Setzmann and Wagner [95]. The magnitude of the uncertainty of calculated power consumption was assessed by the difference in calculated enthalpy change for methane with the two equations of state for the temperature and pressure in and out of the unit. The magnitude of the uncertainty of calculated destroyed exergy was assessed by the difference in calculated destroyed exergy, taking physical exergy in, physical exergy out and (if relevant) power in to the unit into account, for methane with the two equations of state.

The uncertainty reported, $\sigma_{A,\mathrm{comb}}$, was a combination of the uncertainty from measurements, $\sigma_{A,\mathrm{m}}$, and the uncertainty from the state equation, $\sigma_{A,\mathrm{eos}}$:

$$\sigma_{A,\mathrm{comb}} = \sqrt{\sigma_{A,\mathrm{m}}^2 + \sigma_{A,\mathrm{eos}}^2}. \tag{2.11}$$

2.5 Results

2.5.1 Exergy flows entering and leaving the process

Different types of exergy entering and leaving the process are given in Table 2.3. The component part of the chemical exergy, term I in Eq. 2.5, is not included in the analysis. This is a high value due to the high energy content in the oil and the natural gas, but it has no impact on calculated exergy differences, since the chemical components entering and leaving each control volume are the same. Term II in Eq. 2.5 expresses the mixing effects on the chemical exergy and is shown for each flow. The difference in chemical exergy for the system is due to mixing effects. When positive, a change in the mixing exergy is the minimum exergy (work) theoretically required to conduct the separation in the system. A negative value means that mixing takes place.

We see from Table 2.3 that around 49 MW enter the system in form of physical exergy in the well streams. This physical exergy is mainly due to high well

Table 2.3: Mass and exergy flows entering and leaving the oil and gas processing at the platform for the analysed production day. For chemical exergy only the mixing part is given (term II in Eq. 2.5). The power exergy is power added to the process units after electric and mechanical losses (ΔH for the units).

Exergy stream	Mass flow, ton/h	Chemical exergy, mixing part, kW	Physical exergy, kW	Power, kW
In				
Well 7	90	−1220	7940	
Well 16	99	−1840	11,200	
Well 23	112	−1680	11,260	
Well 24	103	−1780	10,150	
Well 26	89	−1500	8810	
Power				23,800
Total in	494	−8020	49,350	23,800
Out				
Oil export	108	−891	298	
Gas injection	310	−6680	50,580	
Produced water	68	−1	539	
Flare gas	0.3	−6	21	
Fuel gas	8	−174	763	
Total out	494	−7750	52,210	0

Table 2.4: Percentage of temperature- and pressure-based exergy components in the physical exergy entering and leaving the process.

Exergy stream	Temperature-based exergy, %	Pressure-based exergy, %	Exergy stream	Temperature-based exergy, %	Pressure-based exergy, %
In			*Out*		
Well 7	10	90	Oil export	55	45
Well 16	7	93	Gas injection	4	96
Well 23	9	91	Produced water	97	3
Well 24	7	93	Flare gas	2	98
Well 26	7	93	Fuel gas	2	98
Total in	7	93	Total out	5	95

stream pressures. The percentage of temperature- and pressure-based exergy in the physical exergy entering and leaving the process is given in Table 2.4, and we see that the pressure-based exergy dominates the physical exergy in the well streams. Through process units like pumps and compressors 23.8 MW power enter the process. The gas injection stream contains around 51 MW physical exergy. Due to the high injection pressure, this stream is also dominated by pressure-based exergy, see Table 2.4. Most of the exergy that enter the system, and that is not destroyed, leave the system with the injection gas. The other streams leaving the system contain less than 1 MW physical exergy.

2.5.2 Exergy transformations and exergy destruction in each sub-system

Power consumption, exergy destruction and efficiency defects in the different sub-processes are given in Table 2.5. The change in different types of exergy in the

sub-processes are given in Table 2.6. The major destroyed exergies distributed on the type of process units in each sub-process are given in Fig. 2.2.

Table 2.5: Power consumption, destroyed exergy and efficiency defect for each sub-process in the oil and gas processing at the platform for the analysed production day. 'Power consumption' is power added to the process units (ΔH), after electric and mechanical losses.

Sub-process	Power consumption, kW	Destroyed exergy, kW	Efficiency defect, −
Production manifold	0	4600 ± 400	0.195 ± 0.017
Separation train	0.117 ± 0.017	800 ± 200	0.034 ± 0.008
Export section	320 ± 150	240 ± 190	0.009 ± 0.008
Recompression train	4700 ± 30	4150 ± 190	0.173 ± 0.008
Reinjection trains	$18,640 \pm 180$	$10,400 \pm 500$	0.43 ± 0.02
Fuel gas system	156 ± 2	508 ± 5	0.0214 ± 0.0004
Total	$23,800 \pm 400$	$20,700 \pm 500$	0.867 ± 0.013

Table 2.6: Change in chemical exergy and temperature- and pressure-based exergy for each sub-process. The power consumption minus the sum of the change in each of these three exergy types equals the exergy destruction given in Table 2.5.

Sub-process	Chemical exergy change, kW	Temperature-based exergy change, kW	Pressure-based exergy change, kW
Production manifold	−0.014	−960	−3660
Separation train	50	−280	−590
Export section	0	−50	130
Recompression train	20	140	390
Reinjection trains	190	110	7990
Fuel gas system	4	−30	−320

Table 2.5 and Fig. 2.2 show that exergy destruction take place mainly in the reinjection trains, the recompression train and in the production manifold. Efficiency defects, cf. Eq. 2.7, for these subsystems are 0.43, 0.17 and 0.19 respectively. If we compare with de Oliveira Junior and van Hombeeck [22] we see the same high exergy loss due to compression. In addition they calculated a high exergy loss due to heating, which we do not have at this platform, since there is no need for heating to separate the well streams. They did not include the production manifold in their analysis.

In the reinjection trains the pressure is increased from 70 bar to 236 bar. In Table 2.5 and Table 2.6 we see that from the 18,640 kW power used in this section, 7990 kW is used to increase pressure-based exergy, 300 kW is used to increase chemical exergy and temperature-based exergy while 10,400 kW is destroyed. Fig. 2.2 shows that the destroyed exergy in the reinjection train is mainly exergy destruction in compressors and due to cooling, while a small amount of exergy is destroyed in

mixers. Exergy is destroyed in the compressors because the compressor efficiencies are not 100%, so all power input is not used to increase the pressure. Some power is transformed into thermal energy, giving exergy destruction. Higher compressor efficiencies will give less exergy destruction, but this is only possible up to a certain point with today's technology. A large part of this exergy destruction can therefore be looked upon as 'unavoidable'. In the coolers thermal energy is removed, and since the cooling water is mixed irreversibly with the sea, the associated exergy is destroyed.

The pressure is increased from 2.8 bar to 70 bar in the recompression train. In Table 2.5 and Table 2.6 we see that for the 4700 kW power used in this section, the chemical and physical exergy is only increased with 550 kW while the remaining 4150 kW is destroyed. Exergy is destroyed for the same reasons as in the reinjection train, but in addition there is exergy destruction due to the anti-surge recycling around the compressors. This recycling gives the largest contribution to the total exergy destruction in the reinjection train, mainly due to lost pressure in the recycle streams. In addition, the exergy destruction in the compressors and coolers are much higher than necessary, since much more gas than necessary is cooled and compressed. This exergy destruction is a direct result of the fact that there are different flow rates in this sub-process compared to what the process equipment was designed for. This is the same situation as observed in a study of an Italian onshore gas treatment facility by Margarone *et al.* [58], where the system for power production was dimensioned for a higher production than the current, due to the natural depletion of the gas reservoirs.

In the production manifold, the pressures of the well streams are reduced, and this is the reason for the destroyed exergy. The major part of the exergy destruction is destruction of pressure-based exergy; 3660 kW.

The efficiency defect of the separation train is only around 0.03, see Table 2.5. The purpose of the separation train is to separate oil, gas and water, and thus increase the chemical exergy of the material streams. This is done in several stages with reducing pressure, so physical exergy is used to do separation work. In Table 2.5 and Table 2.6 we see that 870 kW physical exergy is used, and out of this 800 kW is destroyed and 50 kW is transformed into chemical exergy. In Fig. 2.2 the destroyed exergy labeled 'valves' is exergy destroyed only due to pressure reduction in the main oil stream. The destroyed exergy labeled 'mixing' is both exergy destruction due to pressure reduction, since pressure is reduced in high pressure streams that are mixed with low pressure streams, and exergy destruction due to mixing of streams with different temperatures and concentrations. The small amount of power consumption in the separation train is due to the small water pump.

The efficiency defect of the fuel gas system is near 0.2 and the amount of destroyed exergy is 508 kW, see Table 2.5. We see in Fig. 2.2 that this exergy destruction mainly take place in the electrical heater and in valves. In the electrical heater 156 kW high quality power is transformed into thermal energy.

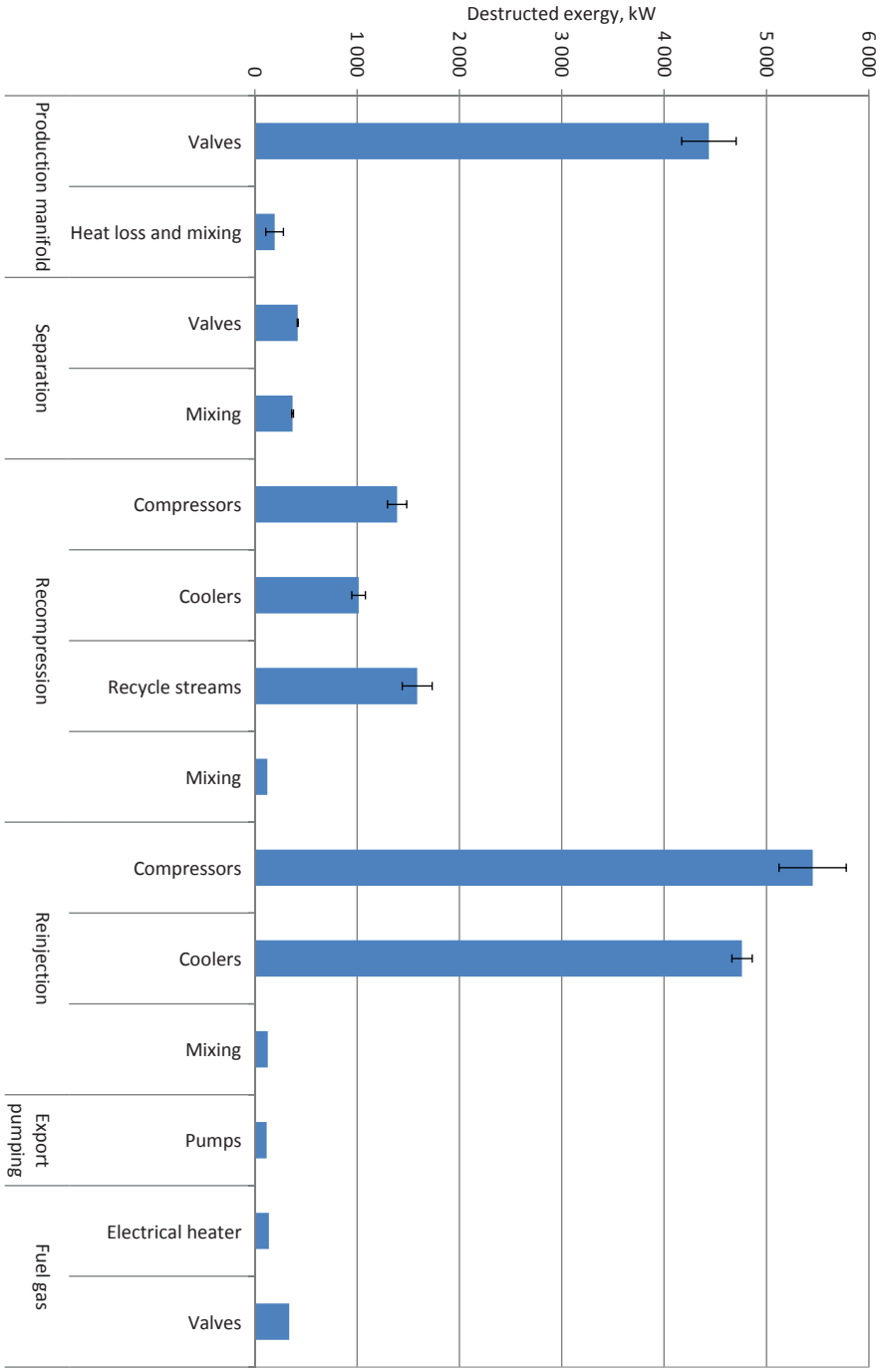

Figure 2.2: The major contributions to exergy destruction distributed on type of process unit in the different sub-processes of the oil and gas processing at the platform for the day analysed.

In the export pumping section 320 kW power is used to increase the pressure of the export oil. The efficiencies of the pumps are low, see Table 2.16, but since the fluid is liquid, not gas, and the flow rates are low in this section, the exergy destruction here is low compared to other parts of the process and this sub-process has the lowest efficiency defect.

2.5.3 Separation work

We can see from Table 2.6 that approximately 260 kW separation work is done. Both the reinjection trains and the recompression train give significant contributions to this increase in chemical exergy, in addition to the separation train. The recompression trains give the highest contribution with 190 kW. The chemical exergy increases of the separation train and the recompression train are also considerable, with 50 and 20 kW respectively. The scrubbing in the compression trains is of high relative importance for the overall separation. The high gas to oil ratio (GOR) at this particular platform gives a high significance to the exergy transformations and exergy destruction in the compression sections. With high gas flow rates, high flow rates of condensate are separated in these sections, and this gives an important contribution to the overall separation of components.

2.5.4 Performance parameters

Calculated performance parameters for the process are given in Table 2.7. The specific power consumption is proportional to the part of the specific CO_2 emissions originating from the oil and gas processing part of the platform when natural gas is used for power production. The parameter evaluates the power consumption without taking the boundary conditions of the system into account. The exergetic efficiency compares the power used in the process with the power needed if all internal processes were reversible. The management of the process with set boundary conditions for the material streams is thus evaluated. The specific power consumption and the exergetic efficiency show different features of the process, and both parameters should be kept low.

Table 2.7: Performance parameters for the oil and gas processing at the platform for the analysed production day. 'Power consumption' is power added to the process units, after electric losses and mechanical losses in gears etc.

Parameter	Value
Specific power consumption, kWh/Sm^3	179 ± 3
Exergetic efficiency, -	0.13 ± 0.02

2.5.5 Accuracy

The calculated uncertainties of destroyed exergy from measurements and inaccuracies in the equation of state were of the same order of magnitude. For some sub-systems uncertainty from measurements dominated, while for other sub-systems uncertainty from inaccuracies in the equation of state dominated.

The absolute difference between enthalpy calculated for methane with the equation of state developed by Setzmann and Wagner [95] and the Peng-Robinson equation of state varied between 0 and 13 kJ/kg for relevant temperatures and pressures (pressures between 1 atm and 500 bar and temperatures between 25 °C and 175 °C). The same difference for physical exergy varied between 0 and 14 kJ/kg. The relative deviation of physical exergy varied between 0 and 1.6×10^{-2}.

For the mass- and energy balances, the relative deviations between mass and energy flow in and out of the system were 1.2×10^{-5} and 1.6×10^{-5}, respectively. Errors from the mass- and energy balance were negligible compared to the calculated uncertainties.

The neglect of contributions from potential exergy has no impact on the overall exergy destruction and exergetic efficiency, since the feed- and product streams of the process (except for the small fuel gas stream) enter and leave the process at the same elevation. However, it can be seen in Table 2.18 that the neglect of height differences has led to a small error in the simulation. Some exergy destruction might have been assigned to wrong process units, since measured process data is used as input in the simulation, and we have pressure increases and decreases due to height differences. The process units are spread on 3 different levels with a total height difference of approximately 30 m. Physical exergy that in reality is transferred into potential exergy will give a higher calculated destroyed exergy, and vice versa. In most cases this error is negligible compared to calculated uncertainties. The exception is the separation train and the export pumping section, where calculated uncertainties are lower than the contribution from neglect of potential exergy. However, these sub-processes have small efficiency defects, see Table 2.5, and the accuracy of these values are thus not critical for the overall results.

It was assumed that the compositions of the different phases in the well streams were constant over time, so the compositions and hypothetical components developed by the oil company could be used in the simulation of the process the studied day. To test the impact on the results, compositions and hypothetical components developed by the oil company for a nearby reservoir was used. The differences in the results were mostly within calculated uncertainties.

2.6 Discussion

Exergy analysis is a systematic approach that localises thermodynamic losses and quantifies theoretical saving potential. It makes possible to compare the magnitude of different types of losses. The results presented above can be used directly to improve the process at this platform as discussed in Section 2.6.1, or they can be used for evaluation of performance as discussed in Section 2.6.2.

2.6.1 Reduction of exergy destruction

The exergy destruction map in Fig. 2.2 raises some important issues.

Measures should be done to increase compressor efficiencies and to reduce the anti-surge recycling, for instance by modifying the existing compressors or by replacing them with new compressors. Higher efficiencies and design for flow rates relevant for current and future production are of big importance. Although some exergy destruction is unavoidable, Table 2.2 shows room for improvement.

The high exergy destruction due to cooling of compressed gas and dissipation of cooling water (with temperature higher than T_0) into the sea indicates that the potential to exploit this exergy should be examined. The temperatures of the warm streams are relatively low (between 70 and 150 °C, see Fig. 2.1) and the exergy related to this is therefore hard to utilize due to technical reasons. The demand for thermal energy is limited at this specific platform, but it should be possible to eliminate the electric heater in the fuel gas system by heat integration with one of the warmest compressed process streams. However, waste heat from the power turbines is available at higher temperatures, and might be preferred for heating purposes.

Attention should be drawn to the exergy destruction due to pressure reduction in the production manifold. The possibility to exploit this exergy in ejectors and expanders should be reviewed. Multiphase ejectors can use the exergy in high pressure wells to enhance recovery and flow rates in depleted wells [5]. Expanders for multiphase flow is under development [80, 75, 18, 28, 76], and this might be an application. Similarly, the exergy destroyed in the valves in the fuel gas system and in the separation train could have been recovered in expanders. In the fuel gas system, we have lower potential for savings, but it is easier since we have expansion of gas, which is a mature technology. For the separation train, it might be interesting to assess the concept of separator turbines, which in addition to production of power gives separation with more compact equipment [80, 75].

The suggestions above are of different nature; updating existing process units, modifying the configuration of the process and developing new process units. The benefits of the measures proposed are dependent on the remaining lifetime of the installation, and will always be evaluated against investment costs. The feasibility

of the suggested measures will also be influenced by the general demand for simple and compact processes on offshore installations.

2.6.2 Performance parameters and exergy analysis in the oil industry

In this study we have calculated the exergetic efficiency of the oil- and gas processing of an existing offshore platform. This parameter can add to the industry's own measures of performance, like the specific CO_2 emissions. The exergetic efficiency can be used to both quantify and justify best practices. It can also be used by the public sector to set standards for performance, that all should adhere to. Such standards may eventually lead to developments of more energy efficient technologies and to the best operation of these.

Under the introduction of other power sources for offshore platforms, for instance electric power from land or power from offshore windmills [33], specific CO_2 emissions are no longer proportional to specific power consumption. Tax on specific CO_2 emissions encourages the use of renewable power sources, but once such a source is taken into use, this parameter does not say anything about the performance of the process anymore. Specific power consumption will always evaluate the power demand and exergetic efficiency will always evaluate the management of the process with given boundary conditions.

We have so far only looked at the oil and gas processing at one platform. We propose that more platforms should be analysed, to explore the applicability of exergy analysis when comparing different platforms. We also propose that one platform should be monitored over time, to see how exergy analysis can be used to evaluate efforts on adapting to changing process conditions or on increasing the process efficiency.

2.7 Conclusion

An exergy analysis has been performed on the oil and gas processing on a North Sea oil platform for a real production day. The day was simulated using measured process data. The magnitude of changes in different types of exergy was quantified. It was shown that physical exergy in the material streams are mainly due to high pressures, and most exergy destruction take place in processes that increase pressure (compressors and cooling in the compression trains) or decrease pressure (in pressure reduction valves and recycling). It was also shown that at this particular platform a large part of the separation work is done in the recompression and reinjection trains (20 and 190 kW), not only in the separation train (50 kW). The overall process consumes 23.8 MW electric power. The sub-processes with most destroyed exergy are the production manifold (4600 kW), the recompression train

(4150 kW) and the reinjection trains (10,400 kW). The specific power consumption is 179 kWh/Sm^3 and the exergetic efficiency is 0.13. We propose measures to decrease exergy destruction, and thus increase the exergetic efficiency, of the process. We show the usefulness of performing exergy analysis on offshore platforms, and propose that this should be taken into regular use by the oil and gas industry.

Acknowledgements

The motivation from Statoil's new-idea project of reducing CO_2 emissions from offshore oil and gas platforms is essential to this study. Kirstin Hosaas, Laila Anita Gangstad, Alf Gunnar Edwardsen and Hanne Lied Larsen from Statoil are thanked for help with issues regarding the process flowsheet. Tuong-Van Nguyen is thanked for valuable discussions. The Faculty of Natural Sciences and Technology at the Norwegian University of Science and Technology is acknowledged for financial support.

Nomenclature

e	molar exergy, J/mol
$\bar{e}$	molar chemical exergy of pure component, J/mol
E	exergy flow, kW
h	molar enthalpy
n	molar flow rate, mol/s
P	pressure, bar
Q	heat, kW
s	molar entropy, J/mol-K
T	temperature, K
W	work, kW
x	mole fraction, -
δ	efficiency defect, -
σ	uncertainty

Subscript

ch	chemical
comb	combined uncertainty
D	destruction
eos	related to equation of state
i	chemical component, subsystem
j	mass stream
k	heat transfer
L	loss
m	related to measurements

P	product
U	utilised
0	environmental temperature and pressure

Superscript

P	pressure-based
ph	physical
T	temperature-based

2.A Process flowsheet

The simulation of the process flowsheet of the oil- and gas processing at the studied platform is explained in detail in this appendix. Fig. 2.1 in Section 2.3 showed the simulated process flowsheet. Details regarding the simulation are listed in 2.A.1, while input data are given in 2.A.2 and the validity of the simulation is discussed in 2.A.3. The reported uncertainties for measured process variables are the 95 % confidence intervals for the measurements, determined as described in Section 2.4.3.

2.A.1 Simulation details

When simulating the process flowsheet, the following simplifications and manipulations were done:

- In the real process there are two separators in the 1st separation stage; one normal and one test separator (both are continously in use). For simplicity they were merged into one separator.
- The HYSYS separators overpredicted the separation of water and oil in the separation train, so in the simulation a part of the separated water from each of the separators was split off and added to the oil stream, to correct for this.
- In the drain system small amounts of liquid from knock out drums in the flare system and from scrubbers with low liquid flow rates are collected in a reclaimed oil sump. When the liquid here reaches a certain level, it is pumped to the 2nd separation stage. For simplicity this was simulated as a small pump that continously pumps liquid from the scrubbers to the 2nd separation stage. Since we study a normal production day with a stable production, we neglected liquid from the flare system.

2.A.2 Input data

The feed of the system is reservoir fluids, and hypothetical components were used to simulate these fluids. The properties of the hypothetical components are given in Table 2.8. The composition of each phase in the reservoir fluids are given in Table 2.9. This description of the reservoir fluids is developed by the oil company.

Table 2.8: Molecular weight, M, normal boiling point, T_b, and ideal liquid density, $\rho_{\text{id.liq.}}$, for the hypothetical components used to describe the heavy oil fractions.

Name	M, g/mol	T_b, °C	$\rho_{\text{id.liq.}}$, kg/m^3
HypoA-1	81	73	721.2
HypoA-2	108	99	740.1
HypoA-3	125	152	774.6
HypoA-4	171	230	817.1
HypoA-5	247	316	859.3
HypoA-6	388	437	906.2
HypoA-7	640	618	988.5

Table 2.9: Composition of the three phases of the reservoir fluids, given as molar fractions.

Component	Gas	Liquid	Water
CO_2	9.18e-3	8.61e-3	0
Methane	0.83	0.78	0
Ethane	6.81e-2	6.41e-2	0
Propane	3.74e-2	3.55e-2	0
i-Butane	5.71e-3	5.52e-3	0
n-Butane	1.34e-2	1.30e-2	0
i-Pentane	4.28e-3	4.39e-3	0
n-Pentane	5.51e-3	5.80e-3	0
H_2O	0	0	1
N_2	9.18e-3	8.61e-3	0
HypoA-1	9.07e-3	1.34e-2	0
HypoA-2	3.47e-3	1.17e-2	0
HypoA-3	7.14e-4	1.49e-2	0
HypoA-4	0	1.24e-2	0
HypoA-5	0	9.01e-3	0
HypoA-6	0	5.22e-3	0
HypoA-7	0	3.44e-3	0

The reservoir fluids enter the process from the wells through the production manifold. The flow rates of oil, gas and water in each well stream were initially set as the allocated flow rates calculated by the oil company, given in Table 2.10. After all the input parameters of the rest of the process were set, these flow rates were scaled so that the simulated flow rates of export oil, injection gas and produced water fitted with measured flow rates for these streams, given in Table 2.11. The values of these measured flow rates are more exact than the allocated flow rates.

Table 2.10: Allocated flow rates of gas, oil and water for each well stream for the studied production day.

Well	Gas 10^3 Sm^3/h	Oil Sm^3/h	Water m^3/h
7	57.6	20.6	13.8
16	87.5	27.2	1.5
23	80.5	21.1	13.9
24	81.9	40.1	1.9
26	71.3	23.5	5.4

Table 2.11: Measured flow rates in process streams leaving the platform.

Produced fluid	Unit	Flow rate
Export oil	Sm^3/h	132.5 ± 0.4
Injection gas	10^3 Sm^3/h	369 ± 17
Produced water	Sm^3/h	67 ± 5

Temperatures, pressures and flow rates that were set as measured throughout the process are given in Table 2.12, Table 2.13 and Table 2.14. In the reinjection trains, the total gas flow rate is determined by the measured gas injection rate. Flow rates are in addition measured several places through each of the injection trains, and the flow rate of each train is set to make the simulated flow rates as close to all of the measured flow rates as possible (least squares). Measured and simulated flow rates in this sub-process are given in Table 2.15. In the export pumping section and fuel gas system, not enough process variables were measured, so the efficiencies of the export pumps were found from the performance curves of the pumps, and the pressure drop over the fuel gas cooler was taken from the cooler data sheet, see Table 2.16. Efficiencies of the small pump in the drain system and the water pump were set to the assumed value 75 %, and pressure drops over all separators where this was not given by measured pressures were set to 0 kPa.

2.A.3 Validation

Measured flow rates are compared with simulated flow rates in Table 2.15 and Table 2.17. The simulated flow rates were within the uncertainty of the measured flow rates, when the uncertainty was known.

A measured pressure in the separation train was compared with a simulated pressure in Table 2.18. The deviation between these numbers is due to the fact that height differences are not included in the simulation, as discussed in Section 2.5.5. The pressure difference corresponds to a height difference of 17 m within the separation train. This is however of minor importance for the overall results.

Table 2.12: Measured temperatures for the studied production day. Where values other than measured values are used in the simulated process flowsheet, for instance because measured values were not available for the studied day, this is indicated in footnotes.

Description	Temperature, °C	Description	Temperature, °C
Production manifold		*Export pumping*	
From well 7, valve, in	85.8 ± 1.0	2nd pump, in	48.1 ± 1.0
From well 16, valve, in	84.7 ± 1.0	*Reinjection, Train A*	
From well 23, valve, in	87.1 ± 1.0	1st cooler, out	28.0[a]
From well 24, valve, in	81.0 ± 1.0	1st compressor, out	94.0 ± 1.0
From well 26, valve, in	79.6 ± 1.0	2nd cooler, out	28.0 ± 1.0
From well 7[b]	76.6 ± 1.0	2nd compressor, out	77.1 ± 1.0
From well 16[b]	75.6 ± 1.0	*Reinjection, Train B*	
From well 23[b]	71.3 ± 1.0	1st cooler, out	28.0 ± 1.0
From well 24[b]	76.8 ± 1.0	1st compressor, out	95.6 ± 1.0
From well 26[b]	74.3 ± 1.0	2nd cooler, out	28.0 ± 1.0
Separation train		2nd compressor, out	74.4 ± 1.0
Gas from 1st separator[b]	73.6 ± 1.0[c]	*Reinjection, Train C*	
Gas from 2nd separator[b]	59.2 ± 1.0	1st cooler, out	30.0[d]
Gas from 3rd separator[b]	46.9 ± 1.0	1st compressor, out	93.4 ± 1.0
Recompression train		2nd cooler, out	30.0[d]
1st cooler, out	39.9 ± 1.0	2nd compressor, out	80.7 ± 1.0
1st compressor, out	104.9 ± 1.0	*Fuel gas system*	
2nd cooler, out	21.0 ± 1.0	1st scrubber, gas out	35.0 ± 1.0
2nd compressor, out	111.8 ± 1.0	2nd scrubber, in	63.0 ± 1.0
3rd cooler, out	24.0 ± 1.0		
3rd compressor, out	146.5 ± 1.0		

[a]This temperature is not measured for the studied production day, so the set point of the cooler is used.
[b]After heat loss.
[c]The weighted mean based on mass flow rate for the two separators that in the simulated flowsheet is merged into one.
[d]This temperature is not measured and the set point for the cooler is not known for the studied production day, so the set point for the cooler a few weeks earlier is used.

In Table 2.19 the measured power consumption of each compression train is compared with the summed enthalpy change, ΔH, over the compressors in each train. The differences between the power consumption and the enthalpy changes are electric and mechanical losses. The numbers indicate that 84 - 90 % of the power consumed in each train end up in the process streams, and this is considered realistic.

Table 2.13: Measured pressures for the studied production day. Where values other than measured values are used in the simulated process flowsheet, for instance because measured values were not available for the studied day, this is indicated in footnotes.

Description	Pressure, bar	Description	Pressure, bar
Production manifold		*Reinjection, Train A*	
From well 7, valve, in	130.1 ± 1.3	1st compressor, in	68.8 ± 0.7
From well 16, valve, in	113.0 ± 1.1	1st compressor, out	137.4 ± 1.4
From well 23, valve, in	165.1 ± 1.7	2nd compressor, in	137.5 ± 1.4[a]
From well 24, valve, in	87.6 ± 0.9	2nd compressor, out	236 ± 2
From well 26, valve, in	88.8 ± 0.9	*Reinjection, Train B*	
From well 7, valve, out	73.0 ± 0.7	1st compressor, in	68.9 ± 0.7
From well 16, valve, out	73.0 ± 0.7	1st compressor, out	139.8 ± 1.4
From well 23, valve, out	73.1 ± 0.7	2nd compressor, in	139.1 ± 1.4
From well 24, valve, out	72.7 ± 0.7	2nd compressor, out	236 ± 2
From well 26, valve, out	72.3 ± 0.7	*Reinjection, Train C*	
Separation train		1st compressor, out	131.9 ± 1.3
1st separator, in	70.4 ± 0.7[b]	1st compressor, in	66.1 ± 0.7
2nd separator, in	8.50 ± 0.08	2nd compressor, in	129.2 ± 1.3
3rd separator, in	2.80 ± 0.03	2nd compressor, out	236 ± 2
Water pump, out	8.77 ± 0.09	*Fuel gas system*	
Recompression train		1st scrubber, in	38.8 ± 0.4
1st compressor, in	2.41 ± 0.02	2nd scrubber, in	38.4 ± 0.4
1st compressor, out	5.72 ± 0.06	2nd scrubber, gas out	38.0 ± 0.4
2nd compressor, in	5.20 ± 0.05	To flare	9.30 ± 0.09
2nd compressor, out	18.75 ± 0.19	To turbine	18.25 ± 0.18
3rd compressor, in	18.29 ± 0.18	*Drain system*	
3rd compressor, out	70.0 ± 0.7	Drain pump, out	8.52 ± 0.09[c]
Export pumping			
1st pump, out	13.30 ± 0.13		
2nd pump, in	12.81 ± 0.13		
2nd pump, out	32.1 ± 0.3		

[a]This pressure was measured to 137.5 < 1.4 bar, but can not be higher than the pressure out from the 1st separator, so in the simulation it is instead set to 137.4 bar.
[b]The weighted mean based on mass flow rate for the mesured values in the gas flow from the two separators that in the simulated flowsheet is merged into one.
[c]This is the pressure measured in the most recent pumping period.

Table 2.14: Measured flow rates set in the simulated process flowsheet for the studied production day.

Description	Unit	Flow rate
Separation train		
Water from 1st separator	Sm^3/h	54 ± 5
Water from 2nd separator	m^3/h	12.6 ± 1.3
Water pump, out	m^3/h	0.53 ± 0.05
Recompression train		
1st compressor, in	m^3/h	7100 ± 700
2nd compressor, in	m^3/h	5800 ± 600
3rd compressor, in	m^3/h	1560 ± 160
Export pumping section		
1st pump, out	m^3/h	230 ± 20
2nd pump, out	m^3/h	176 ± 18
Fuel gas system		
To flares	Sm^3/h	335 ± 14[a]
To power turbines	Sm^3/h	9630 ± 170

[a]Sum of pilot flame for high pressure and low pressure flare, where it is assumed that half of the measured flow rate for low pressure flare is for pilot flame while the rest is from other places in the system, and is negligible these places.

Table 2.15: Measured and simulated flow rates of gas for the studied production day in the reinjection trains.

Description	Measured flow rate, m^3/h	Simulated flow rate, m^3/h
Train A		
1st compressor, in	1210 ± 120	1140
1st compressor, out	750 ± 70	750
2nd compressor, in	510 ± 50	503
Train B		
1st compressor, in	1300 ± 130	1213
1st compressor, out	770 ± 80	790
2nd compressor, in	530 ± 50	529
Train C		
1st compressor, in	2400 ± 200	2348
2nd compressor, in	1040 ± 100	1059

Table 2.16: Efficiencies, η, of pumps in the export pumping section found from the performance curves of the pumps, and pressure drop, ΔP, of cooler found from cooler data sheet.

Process unit	Variable	Value
Booster export pump	η, %	55
Main export pump	η, %	48
Fuel gas cooler	ΔP, kPa	50

Table 2.17: Measured and simulated flow rates of gas for the studied production day in the separation train. The uncertainties for the two last gas flows in the separation train are not known, because the flow rates are lower than what the flowmeters are designed for.

Description	Measured flow rate, ton/h	Simulated flow rate, ton/h
Gas from 1st separator	320 ± 30^a	318
Gas from 2nd separator	8.1	10.4
Gas from 3rd separator	2.2	2.2

[a]The sum of the gas flow from the two separators that in the simulated flowsheet is merged into one.

Table 2.18: Measured and simulated pressure for the studied production day in the separation train.

Description	Measured pressure, bar	Simulated pressure, bar
Oil from electrostatic coalescer	4.25 ± 0.04	2.80

Table 2.19: Measured power consumption in compression trains and sum of simulated enthalpy change, ΔH, over the compressors for each train.

Compressor train	Measured power consumption, kW	Sum of simulated ΔH, kW
Recompression	5200 ± 100	4703
Reinjection A	5550 ± 110	4781
Reinjection B	5940 ± 120	5008
Reinjection C	9800 ± 200	8847

Chapter 3

Exergetic assessment of energy systems on North Sea oil and gas platforms

Tuong-Van Nguyen[1], Leonardo Pierobon[1], Brian Elmegaard[1], Fredrik Haglind[1], Peter Breuhaus[2] and Mari Voldsund[3]

1. Department of Mechanical Engineering,
Technical University of Denmark,
DK-2800 Kongens Lyngby, Denmark

2. Department of Energy,
International Research Institute of Stavanger,
NO-4021 Stavanger, Norway

3. Department of Chemistry,
Norwegian University of Science and Technology,
NO-7491 Trondheim, Norway

This chapter has been published in
Energy - The International Journal
Volume 62 (2013), Pages 23–36

Abstract

Oil and gas platforms in the North Sea region are associated with high power consumption and large CO_2 emissions, as the processing and utility plants suffer from significant changes in production rates and performance losses over the field lifespan. In this paper, a generic model of the overall offshore system is described: its thermodynamic performance is assessed by performing an exergy accounting and rules of thumb for oil and gas platforms are derived. Simulations are built and conducted with the tools Aspen Plus®, Dynamic Network Analysis and Aspen HYSYS®. 62–65% of the total exergy destruction of an offshore platform is attributable to the power generation and waste heat recovery system, and 35–38% to the oil and gas processing. The variability of the feed composition has little effect on the split of the thermodynamic irreversibilities between both plants. The rejection of high-temperature gases from the utility and flaring systems is the major contributor to the exergy losses. These findings suggest to focus efforts on a better use of the waste heat contained in the exhaust gases and on the ways in which the gas compression performance can be improved.

3.1 Introduction

The oil and gas extraction sector was responsible for nearly 26% of the total greenhouse gas emissions of Norway in 2011 [106], since the combustion of natural gas or diesel oil for power generation on offshore installations produces significant amounts of carbon dioxide. The environmental impact and the energy intensity of these facilities are expected to increase in the coming years, as a direct consequence of greater onsite energy use to separate and transport oil and gas to the shore and to inject gas or water into the reservoirs for enhanced oil recovery [14, 109, 110]. As environmental awareness has increased in recent decades, more attention has been paid to the ways in which the greenhouse gas emissions and the energy demand of industrial activities can be reduced, by for instance promoting efficiency measures.

However, oil and gas platforms are usually designed for the early life of a petroleum field. The onsite processes suffer from significant changes in production flows and operating conditions over time. They become inevitably less performant, besides the normal process of efficiency reduction due to aging. The performance of this type of facilities is generally expressed in terms of environmental impact, such as the amount of carbon dioxide produced per unit of oil equivalent, or with energy metrics, such as the specific power consumption per unit of oil produced [110, 128].

Svalheim and King [110] stressed the large energy demand of the compression, pumping and injection (gas or seawater) processes and pointed out the benefits that resulted from applying energy-efficiency measures (e.g. operating gas turbines

at high load and reducing flaring practices). Their study mentioned that the performance of an offshore platform can be defined as the ratio of the gas consumed onsite to the quantity of oil and gas exported onshore. It was emphasised that the interest of this indicator is limited, as each oil field has different natural characteristics (e.g. gas-to-oil ratio, well-fluid composition, field size): comparing different facilities based on this metric could therefore be misleading.

The other indicators discussed by Svalheim and King [110] are also based either on environmental impact studies or on conventional energy assessments. The latter illustrate the changes from one form of energy to another within a given system and derives from the 1st principle of thermodynamics. This approach has limitations as it does not allow the quantification of the irreversibilities of a system, since energy cannot be destroyed. This shortcoming can be addressed by conducting an exergy analysis, which is based on both the 1st and 2nd principles of thermodynamics.

Unlike energy, exergy can and to a certain extent is destroyed in real processes. An exergy analysis reveals the locations and extents of the thermodynamic irreversibilities present in a system, and exergy destruction accounts for fuel use throughout successive processes. This method is described in Bejan *et al.* [13, 12] and has been applied extensively to evaluate the performance of various industrial processes [130, 83, 22, 127, 128, 48, 49, 50, 44].

However, there are only a few studies on exergy and offshore processes and relatively little information exists regarding the thermodynamic inefficiencies of the *complete* offshore plant. Examples of exergy analyses on oil platforms are the studies by Oliveira and Van Hombeeck [22] and by Voldsund *et al.* [127, 128]. Oliveira and Van Hombeeck carried out an exergy analysis of a Brazilian petroleum plant and focused exclusively on the separation, compression and pumping modules. Their study indicated that the most exergy-consuming processes were the petroleum heating and the gas compression steps, whereas the separation step had the lowest exergetic efficiency.

Voldsund *et al.* [127, 128] used a similar approach and simulated the oil and gas processing plant of a Norwegian offshore platform. The sub-systems investigated in their research comprised the separation, recompression and reinjection trains, as well as the fuel gas and oil export processes. Their work demonstrated that the largest exergy destruction took place in the gas reinjection and recompression trains.

The literature seems to contain neither generic analyses considering both the processing and utility systems, nor investigations of the effects of different reservoir fluid compositions on the platform performance.

The goal of this study is to help address these gaps: this paper aims therefore at deriving generic conclusions on the thermodynamic performance of oil and gas platforms in the North Sea region. This research work is originally part of a larger project dealing with the optimisation of electrical energy production on offshore

platforms and builds on previous work conducted by the same authors [70]. Three main steps were followed in this study:

- development and validation of a generic model of North Sea oil and gas offshore platforms to generate realistic and reliable production profiles;
- simulation of various operating conditions and well-fluid flows to investigate the overall system behaviour and evaluate the material and energy flows;
- analysis of the energy and exergy consumption patterns with fluctuations of the reservoir fluid composition.

The methodology and the model developed are described and documented in Section 3.2. Section 3.3 reports the results obtained for different simulation cases, which are discussed and criticised in Section 3.4. Concluding remarks are outlined in Section 3.5.

3.2 Methodology

3.2.1 System description

Reservoir fluids are complex multiphase mixtures with a large variety of chemical components. They contain (i) petroleum, also named crude oil, which exhibits a high content of heavy hydrocarbons, (ii) natural gas, which is mostly methane and light hydrocarbons, and (iii) water. Efficient offshore separation of the oil, gas and water phases is required to maximise the oil production and to minimise its contents of water and gas.

Crude oil is transported to the shore, via pipelines or shuffle tanks, while produced water is cleaned and either discharged overboard or injected into the reservoir for pressure maintenance. Gas may (i) be exported to the coast via a specific pipeline network to be treated onshore, (ii) reinjected into the reservoir via dedicated wells to enhance the oil production or (iii) injected into the oil wells to ease the reservoir fluid lift. Variations and differences across oil and gas platforms may be related to:

- reservoir characteristics (e.g. temperature and pressure, gas-to-oil (GOR) and water-to-oil (WOR) ratios);
- reservoir fluid properties (e.g. chemical composition, thermophysical properties, critical point);
- technical requirements (e.g. crude oil content of gas and water, export temperature and pressure);

- technological choices (e.g. number of trains, gas export, gas lift, system consideration).

However, the conceptual design of these offshore facilities stays similar: although design differences exist from one platform to another, gas purification and exportation, wastewater treatment and seawater injection are the most common gas and water processing technologies in the North Sea region. Moreover, as North Sea crude oil and natural gas have a low content of carbon dioxide, hydrogen sulphide and salt, neither desalting nor sweetening units are necessary onsite. According to [14, 21, 74], a typical offshore oil and gas platform of this region consists of the following sub-systems:

- Production manifold
- Crude oil separation
- Oil pumping and export
- Gas recompression and purification
- Gas compression and exportation
- Wastewater treatment
- Seawater injection
- Power generation and heat recovery
- Heating, ventilation and air conditioning (HVAC)
- Miscellaneous utilities (e.g. sewage)

The model of the generic offshore platform developed within this study includes the aforementioned processes, excluding the HVAC system and the connected utilities (Fig. 3.1 and Fig. 3.2), which may differ significantly from one platform to another. It was built based on the system configurations presented in the open literature: [14, 42, 57, 78] for the crude oil processing, [57, 78] for the gas treatment process and [1, 125] for the water processing. Gas lift and injection were not considered within this study.

The approach of this work assumes an oil and gas processing plant designed for each simulation case investigated, as one of the goals of this study is to provide a basis for comparison between various reservoir fluid compositions. Therefore, the off-design behaviour of the processing plant was not investigated whereas the part-load behaviour of the gas turbines was considered. The design conditions for each component and sub-system modelled in this work are presented further (Table 3.1).

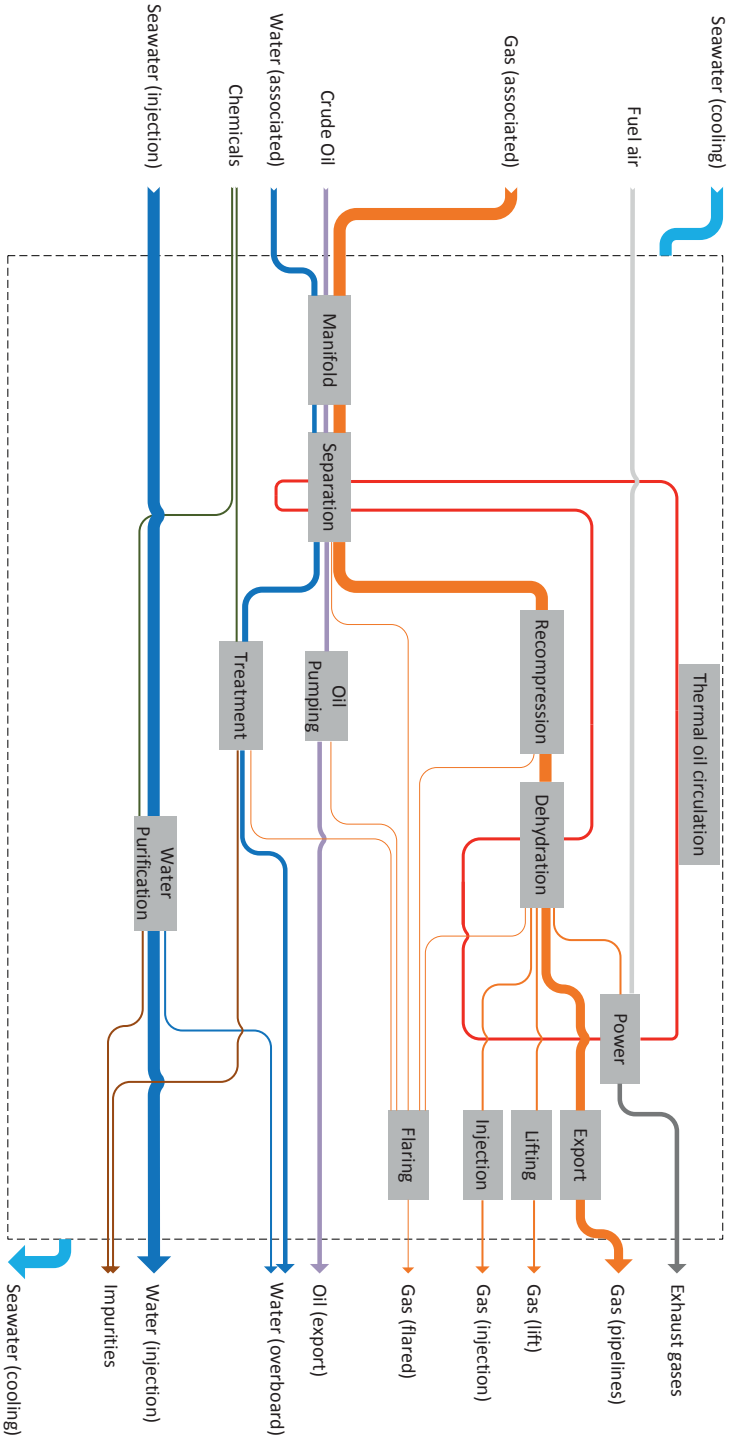

Figure 3.1: Conceptual layout of processes on North Sea oil and gas platforms.

3.2.2 System model

Fluid modelling

Crude oil contains hydrocarbons ranging from light alkanes to heavy aromatics, naphtenes and paraffins and various impurities such as nickel, nitrogen and sulphur compounds. Complete compositional analyses of this mixture are rarely carried out, which means that the exact chemical composition is unknown. In general, petroleum is characterised by carrying out a true boiling point (TBP) analysis, which gives an approximation of its physical and chemical properties. Molecular weight, viscosity, specific density and gravity are measured, while thermal properties such as heating value and thermal conductivity are estimated by empirical correlations. Petroleum is modelled as a group of known and hypothetical (also called *pseudo-components*) whose properties are derived from the true boiling curve [42, 1].

In this study, crude oil was modelled as a mixture of 83 chemical compounds: CO_2, H_2O, O_2, N_2, Ar, H_2S, 47 hydrocarbons and 29 pseudo-components. It had the following bulk properties: an American Petroleum Institute (API) gravity of 39.9, a specific gravity of 0.826, a density of 825.5 kg/m^3 and a content of light hydrocarbons of 27.2 vol%. It was assumed that it is extracted along with associated free gas, with this molar composition: 4.37% N_2, 1.34% CO_2, 75.7% CH_4, 7.22% C_2H_6, 6.70% C_3H_8, 3.89% n-C_4H_{10} and 3.70% n-C_5H_{12}. Standard air, with a molar composition of 77.29% N_2, 20.75% O_2, 1.01% H_2O, 0.92% Ar and 0.03% CO_2, and standard seawater, with a molar concentration, in mol/L, of 0.002 HCO_3^-, 0.525 Cl^-, 0.024 SO_4^{2-}, 0.045 Mg^{2+}, 0.013 Ca^{2+}, 0.450 Na^+ and 0.01 K^+, were considered. The reservoir fluid compositions are presented further in this work (Table 3.2).

Processing plant model

The reservoir fluid is transferred to the platform complex via a network of pipelines and a system of production manifolds **(1)**. The individual streams pass through choke boxes, which consist of valves and chokes, in which they are mixed and depressurised to ease further gas and liquid separation in the separation train **(2)**.

Oil, gas and water are separated by gravity in three stages. Since low pressures and high temperatures ease the separation of these three phases, the pressure of the well-fluid is decreased by throttling valves and its temperature is increased by preheating with a heat medium at the inlet of each stage. The two first stages consist of three-phase separators, the third one consists of a two-phase separator and an electrostatic coalescer. It was assumed that the gravity separators are continuously operated, that physical equilibrium is reached and that no solids are entrained in the gas vapour phase. The power needed to sustain the electric field

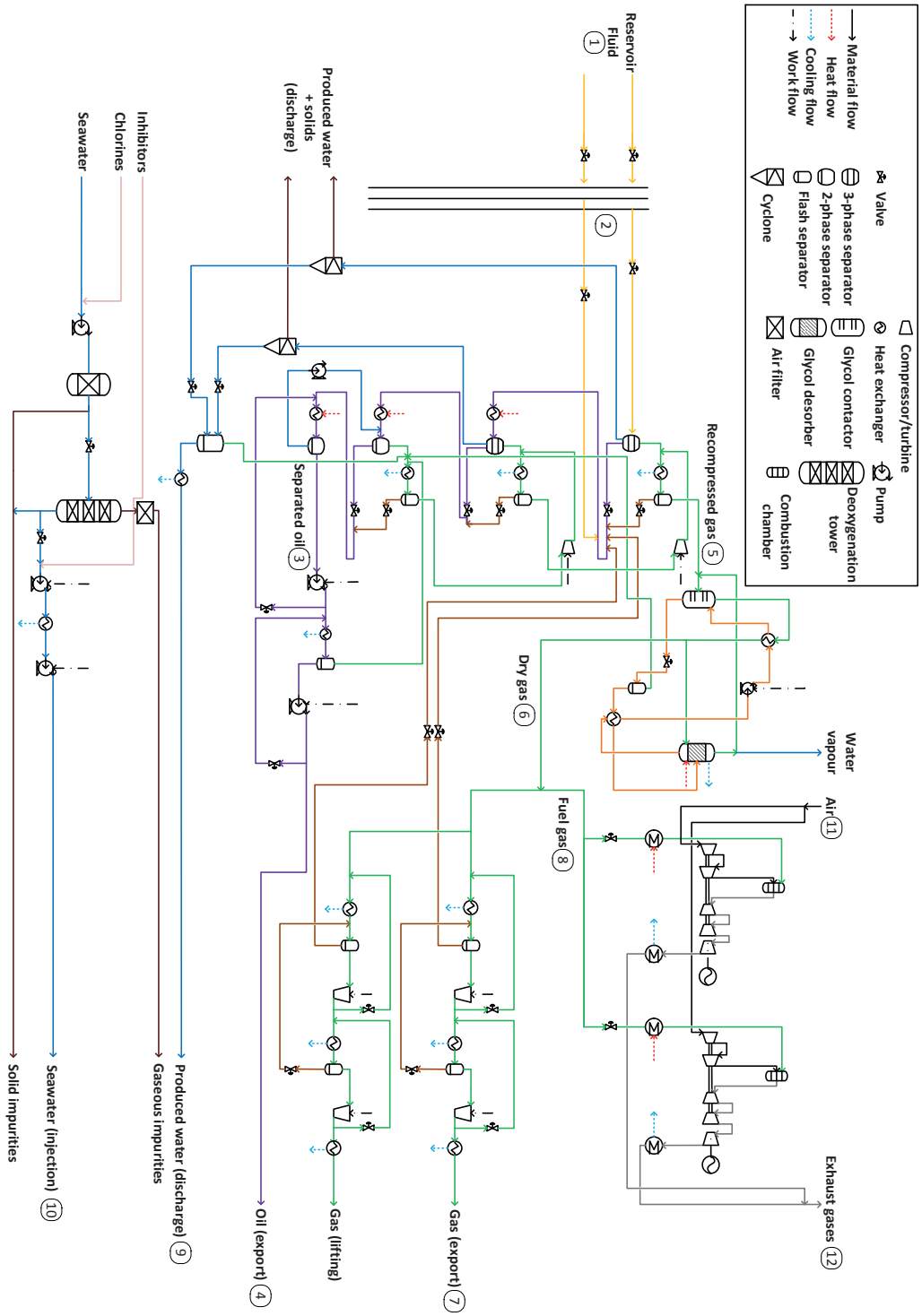

Figure 3.2: Simplified flow diagram of the offshore platform model.

in the coalescer is ignored, because its contribution to the total power consumption is negligible.

The oil from the separation train enters the export pumping system **(3)**, after having been mixed with oil and condensate that is removed in other parts of the processing plant. It is then pumped and stored in a tank, where the last traces of gas and water are removed by flashing, and finally exported onshore **(4)**.

The gas leaving the separation and oil pumping steps is cooled by heat exchange with seawater, is sent to a scrubber where condensate and water droplets are partly removed and is recompressed to the pressure of the previous separation stage **(5)**. Wet gas enters at the bottom of a packed contactor, in which water is captured by physical absorption with liquid triethylene glycol (TEG).

The water content of the gas after this dehydration **(6)** is usually below 0.01 mol%, which prevents severe corrosion issues in gas pipelines. The wet glycol is depressurised to nearly atmospheric pressure and cleaned of water vapour in a desorption column. A small fraction of dry natural gas is sent for stripping in this unit in order to increase the glycol purity to at least 98.5 mol%. Regenerated glycol is pumped to its initial pressure and preheated before re-entering the absorber.

Most of the dry gas is sent to the compression train **(7)** where it is cooled and scrubbed to further remove heavy hydrocarbons, and compressed for storage and export to the shore. A certain fraction of the dry gas is usually recycled to control the volume of gas entering the compressors and to prevent surge issues. The remaining gas that is not processed is used for power generation directly onsite **(8)**. It is expanded through a succession of valves and combusted with air in gas turbine engines.

The water from the separation and purification trains, also denoted produced water, enters hydrocyclones in which suspended particulates and dissolved hydrocarbons are removed. It then passes through valves and flows through degassers where the last oil and gas traces are recovered before disposal to the sea **(9)**.

In parallel with the oil and gas processing, seawater is treated on the platform for further injection into the reservoir, in order to sustain high pressure conditions and to enhance oil production. The injection fluid must meet strict quality requirements to prevent corrosion and reservoir degradation: it is thus cleaned before being pumped into the reservoir **(10)**. The seawater injection train includes a succession of filters to remove solid impurities such as sand particles and algae, deoxygenation towers to reduce the oxygen content, booster and high pressure pumps.

Utility plant model

The electrical power required onsite is produced by gas turbines, fuelled with a fraction of the natural gas extracted along with oil, and atmospheric air **(11)**.

These engines are typically selected on the basis of the maximum expected power demand. They must also, because of the specific features of an offshore plant, satisfy those major requirements:

- high compactness (e.g. small weight and footprint, to lower the capital costs of the oil and gas platform);
- high reliability and availability (e.g. robust gas turbine operation, since the production flows may vary significantly);
- high fuel flexibility (e.g. adaptability to different types of fuels while maintaining an acceptable efficiency).

Hence, the selection of a gas turbine for offshore applications may be a compromise between these three criteria and the engine thermal efficiency. In general, the electrical demand of an offshore platform is supported by multiple and redundant gas turbines running in part-load conditions, which gives additional benefits in terms of plant flexibility and reliability. In this study, the utility system was modelled as two twin-spool gas turbines complemented by power turbines sharing equally the electrical power supply. They are based on the performance characteristics of the SGT-500 engines developed by SIEMENS [96], which are claimed to be highly suitable for offshore and marine applications.

The compressor off-design characteristics are derived by applying a stage-stacking analysis [99, 66, 103]. The calculations of the isentropic efficiency of each stage are based on the assumption, presented in Templalexis *et al.* [116], that total pressure drop can be distinguished in three different components, namely profile (primary) losses, secondary losses and shock losses. Calculations of the primary losses are based on the approach developed in Lieblein [54] and additional losses due to annulus drag, tip clearance and trailing vortices are included based on Saravanamuttoo *et al.* [87]. The turbine off-design performance is derived by applying the method introduced in Stodola [107] and in Traupel [117].

The waste heat from the exhaust gases is partly used to increase the temperature of a heating medium, such as glycol-water or hot oils, and the remaining is released to the atmosphere via the stack **(12)**. The heating medium circulates in a closed-loop system and provides the heat required on the platform. The highest temperature level of the different process modules is generally found at the reboiler of the desorption column, where triethylene glycol and water are separated. Seawater is processed on the platform as a cooling media, to decrease the amount of heavy hydrocarbons entrained with natural gas in the recompression process, and to prevent foaming and low loads in the separation system.

3.2.3 System simulation and validation

Simulation basis

The process simulations (Fig. 3.2) were carried out with Aspen Plus® version 7.2 [6], with the exception of the power generation and the glycol dehydration systems. Simulations of the production manifolds, petroleum separation, oil pumping, gas recompression and flaring were based on the Peng-Robinson (PR) equation of state (EOS) [77], while simulations of the water purification and injection processes were based on the Non-Random Two Liquid (NRTL) model [81], which is more suited for electrolyte system modelling. Glycol dehydration was simulated with Aspen HYSYS® [7], using the glycol property package, claimed to predict more accurately the behaviour of the triethylene glycol-water mixture [8]. Power generation was simulated by using the in-house tool Dynamic Network Analysis (DNA), which is a program developed at the Technical University of Denmark [27]. The assumptions and parameters are based on the compilation of various data from literature ([42, 110, 78, 56, 132, 21, 57, 25]) (Table 3.1).

Table 3.1: Process design assumptions.

Reservoir fluid	71°C and 16.5 MPa
Production manifold	Pressure levels: 12 MPa and 7 MPa
Separation train	Pressure levels: 7 MPa, 2.9 MPa, 0.72 MPa and 0.18 MPa Temperature levels: feed temperature (1st stage), between 65 and 85°C (others) Pressure drops: 0.5-0.3-0.05 bar (3-phase separators), 0.05-0.02 bar (mixers), 0.25-0.1-0.025 bar (heat exchangers), 0.5-0.3-0.05 bar (flash separators)
Crude oil/glycol heat exchangers	Temperature increase (cold side): 5 K, ΔT_{min} = 10 K
Compression train	Intermediate pressure level: 11.4 MPa Recycling: 75 m^3/hr
Gas/seawater heat exchangers	Temperature outlet (hot side): 30-20°C, ΔT_{min} = 10 K
Centrifugal compressors	η_{is} = 63-67%, η_{mec} = 93% (recompression train), η_{is} = 65%, η_{mec} = 95% (compression train)
Centrifugal oil pumps	η_{pp} = 62%, η_{dr} = 98% (export train)
Centrifugal water pumps	η_{pp} = 81%, η_{dr} = 98% (injection train)
Produced water/seawater heat exchangers	Temperature outlet (hot side) = 25°C, ΔT_{min} = 10 K
Skim vessel/degasser	Operating pressure: 1.2 bar
Glycol contactor	Packed column, operating pressure: 7 MPa
Glycol regenerator	1.2 bar, 5 stages, kettle reboiler: 204.4°C, overhead condenser: 98.5°C
Glycol/glycol heat exchangers	Pressure drops: 0.2-0.025 bar
Waste-heat recovery system	Temperature outlet (cold side): 210-220°C
Seawater injection	Standard volume flow rate: 1300 Sm^3/hr
Seawater quality	Oxygen level: 10 ppb, solids content: 5 ppm
Cooling water	Standard volume flow rate: 2400 Sm^3/hr
Flaring-to-fuel gas ratio	12.4 vol% (based on statistical data from the Danish Energy Agency [21])
Export and injection pressures	12.5 MPa (seawater), 14.5 MPa (oil) and 18.5 MPa (gas)

Case studies

Six cases were investigated within this study, corresponding to the same processes and operating conditions – but with different reservoir fluid compositions and loads (Table 3.2). As emphasised by Svalheim and King [110], production flows are strongly time-dependent: it is thus unlikely to find, for one platform, six distinct situations with sensibly similar flow rates and sensibly different gas-to-oil (GOR) and water-to-oil (WOR) ratios. In practice, the operating pressures and temperatures of the separation train are adapted to the reservoir fluid composition. Each simulation case was defined on the same well-fluid molar flow rate, fixed at 18450 kmol/hr, as well as identical design conditions (Table 3.1).

Case 1, referred as the baseline case in the rest of this study, was intended to represent a reservoir fluid containing oil, associated free gas and water with a cut of 15 mol%. Gas- and water-to-oil ratios were chosen based on the production data of different oil platforms operating in the North Sea region in order to simulate a volatile oil. *Case 2* and *Case 3* differ from *Case 1* by the content of water, which was increased by 10 mol% points and decreased by 5 mol% points, respectively.

Cases 4,*5* and *6* were intended to represent three different types of oils, respectively black, near-critical (NC) and condensate, which differ in their content of heavy hydrocarbons [132]. Black oil has a low API gravity, a large fraction of heavy hydrocarbons, and a relatively low content of methane, whereas near-critical and condensate oils are characterised by a high API gravity ($\geq 40°$) and light hydrocarbons content. The latter are generally located at greater depths, which results in higher reservoir pressures [89, 132]. These differences in physical properties across petroleum reservoirs were not considered in the process modelling, and the impact of this assumption is briefly discussed further (Section 3.4).

Table 3.2: Simulation specifications – reservoir fluid properties.

	Case 1	Case 2	Case 3	Case 4	Case 5	Case 6
Flow						
Mass (t/hr)	738	757	963	1783	649	543
Volume (m^3/hr)	2044	1750	2153	2567	2093	2147
Mole fraction						
CH_4	49.2	42.9	49.0	29.5	59.0	62.2
C_2H_6	4.70	4.10	6.30	3.60	6.72	6.64
C_3H_8	4.70	4.10	4.03	2.00	3.82	3.18
n-C_4H_{10}	3.40	3.00	3.53	3.90	3.09	2.26
n-C_5H_{12}	1.40	1.20	2.35	3.30	2.21	1.52
n-C_6H_{14}	0.60	0.50	2.36	2.80	1.55	1.12
CO_2	0.90	0.80	0.02	0.02	1.11	0.26
N_2	2.80	2.50	1.55	0.30	0.47	2.01
C_7+ and others	12.3	10.7	15.9	39.6	7.01	5.81
H_2O	20.0	30.2	15.0	15.0	15.0	15.0
Exergy						
$\bar{e}_{ch}$ (GJ/kmol)	1.88	1.64	2.31	4.32	1.54	1.37
$\bar{e}_{ph}$ (MJ/kmol)	7.87	6.90	7.81	6.26	8.66	9.04
$\dot{E}$ (GW)	9.62	8.40	11.9	22.2	7.91	7.04

Error analysis

Simulation results and calibrated values presented in the open literature, in [57, 56, 22, 127, 128, 96], were used to validate the models and tools developed within this work. Eight model variables were tested (Table 3.3) and the relative errors were calculated based on the following definition:

$$\epsilon = \left| \frac{v_{\text{simulation}} - v_{\text{expected}}}{v_{\text{expected}}} \right|. \tag{3.1}$$

Table 3.3: Error analysis parameters.

Parameter	Unit	Description
$\dot{V}_{\text{water}}$	Sm^3/hr	Produced water flow
$\dot{V}_{\text{gas}}$	Sm^3/hr	Export gas flow
$\dot{V}_{\text{oil}}$	Sm^3/hr	Export oil flow
P	MW	Power consumption
$\dot{m}_{\text{exh}}$	kg/s	Exhaust gas flow
η_{th}	%	Gas turbine – thermal efficiency
T_{exh}	°C	Gas turbine – exhaust gas temperature
TIT	°C	Gas turbine – turbine inlet temperature

Sensitivity analysis

Operating parameters, such as gas and oil export pressures, seawater injection flow rate, and pressure differ from one platform to another, depending on the physical properties of the oil field and on the pipeline network requirements. Moreover, different technological choices such as the selection of the gas compressors (e.g. centrifugal, radial or axial, depending on the volume flow and pressure ratio per stage) and of the oil pumps (e.g. centrifugal or positive displacement) apply for each platform. The effects of these different machine characteristics were investigated in a parametric study (Table 3.4), based on the values discussed in [35, 108, 22, 127, 128].

Table 3.4: Sensitivity analysis parameters.

Parameter	Description	Base value	Lower	Upper
η_{pp} (%)	Centrifugal oil pump efficiency	62	55	78
η_{is} (%)	Isentropic efficiency (compression)	65	45	80
η_{is} (%)	Isentropic efficiency (recompression)	63–67	45	80

3.2.4 Exergy analysis

An exergy analysis was performed on the offshore platform system to identify the process units with the greatest internal irreversibilities, based on the following

assumptions. The dead state conditions are taken to be $T_0 = 5°C$, $p_0 = 1$ atm and a chemical composition of X_0, as defined in the model of Szargut [112]. The system works in steady-state and no exergy is accumulated.

Flow exergy

As enthalpy and entropy, exergy is a property which can be defined for every stream of matter [13]. The specific exergy of a material stream e is a function of its physical e^{ph}, chemical e^{ch}, kinetic e^{kn} and potential e^{pt} components and is defined as:

$$e = e^{\mathrm{ph}} + e^{\mathrm{ch}} + e^{\mathrm{kn}} + e^{\mathrm{pt}}. \tag{3.2}$$

Kinetic and potential contributions on the flow exergies were assumed to be negligible toward physical and chemical exergies. Physical exergy is related to temperature and pressure differences from the dead state, and the values were computed from the process simulations by applying the Peng-Robinson and Non-Random-Two-Liquid thermodynamic equations of states:

$$e^{\mathrm{ph}} = (h - h_0) - T_0(s - s_0), \tag{3.3}$$

where h and s are the specific enthalpy and entropy of a stream of matter per unit-of-mass, respectively. Chemical exergy is related to deviations in chemical composition from reference substances present in the environment, and was calculated based on the model of Szargut [65, 112] for pure substances, and on the heuristic correlations of Rivero [85] for hypothetical components:

$$e^{\mathrm{ch,c}} = \beta NHV_{\mathrm{c}} + \sum z_{\mathrm{m}} e_{\mathrm{ch,m}}, \tag{3.4}$$

where NHV_i stands for the Net Heating Value, z_j the mass fraction of metal impurities, $e^{\mathrm{ch,c}}$ the corresponding chemical exergy and β the chemical exergy correction factor.

Exergy destruction and losses

The internal irreversibilities of a given system result in exergy destruction, which can be calculated from the global exergy balance [13]:

$$\begin{aligned} \dot{E}_{\mathrm{d}} &= \sum \dot{E}_{\mathrm{i}} - \sum \dot{E}_{\mathrm{o}} \\ &= \sum \left(1 - \frac{T_0}{T_k}\right) \dot{Q}_k - \dot{W}_{\mathrm{cv}} + \sum \dot{m}_{\mathrm{i}} e_{\mathrm{i}} - \sum \dot{m}_{\mathrm{o}} e_{\mathrm{o}}, \end{aligned} \tag{3.5}$$

where $\dot{E}_{\mathrm{d}}$, $\dot{E}_{\mathrm{i}}$ and $\dot{E}_{\mathrm{o}}$ are the destroyed, input and output exergy rates, respectively, $\dot{m}$ is the mass flow rate of a stream of matter, and $\dot{Q}_k$ and $\dot{W}_{\mathrm{cv}}$ the time rates of energy transfer by heat and work ($\dot{Q} \geq 0$ indicates heat transfer to the system,

$\dot{W} \geq 0$ work done by the system). The subscripts i and o denote inlet and outlet and the subscript k the boundary of the component of interest.

Alternatively, the exergy destruction rate can be determined from the Gouy-Stodola theorem [12]:

$$\dot{E}_{\mathrm{d}} = T_0 \dot{S}_{\mathrm{gen}}, \tag{3.6}$$

where $\dot{S}_{\mathrm{gen}}$ is the entropy generation rate.

The exergy losses, unlike the exergy destruction, do not result from internal irreversibilities of a system, but rather from the rejection of exergy to the environment without any practical use. They are also denoted external irreversibilities and are for instance associated with waste streams [13, 86]. The lost exergy is destroyed by reaching equilibrium when being mixed into the environment and the exergy loss rate $\dot{E}_{\mathrm{l}}$ is defined as:

$$\dot{E}_{\mathrm{l}} = \sum \dot{E}_{\mathrm{rejected}}. \tag{3.7}$$

Exergy efficiency and irreversibility ratio

The exergy destruction rate $\dot{E}_{\mathrm{d},k}$ within a specific process component k can then be related to the exergy destruction rate within the whole system $\dot{E}_{\mathrm{d}}$ by calculating the exergy destruction ratio y^*_{d}, defined as:

$$y^*_{\mathrm{d}} = \frac{\dot{E}_{\mathrm{d},k}}{\dot{E}_{\mathrm{d}}}. \tag{3.8}$$

Similarly, the exergy loss rate $\dot{E}_{\mathrm{l},k}$ within a specific process component k can be related to the exergy loss rate of the whole system $\dot{E}_{\mathrm{d}}$ by calculating the exergy loss ratio y^*_{l}, defined as:

$$y^*_{\mathrm{l}} = \frac{\dot{E}_{\mathrm{l},k}}{\dot{E}_{\mathrm{l}}}. \tag{3.9}$$

The thermodynamic performance of a given component k can be expressed by defining its exergetic efficiency η_k and by identifying the fuel and product of interest. It should be emphasised that fuel and product exergies $\dot{E}_{\mathrm{f},k}$ and $\dot{E}_{\mathrm{p},k}$ of the component k are not necessarily equal to its input $\dot{E}_{\mathrm{i},k}$ and output $\dot{E}_{\mathrm{o},k}$ exergies.

$$\eta_k = \frac{\dot{E}_{\mathrm{p},k}}{\dot{E}_{\mathrm{f},k}} = 1 - \frac{\dot{E}_{\mathrm{d},k} + \dot{E}_{\mathrm{l},k}}{\dot{E}_{\mathrm{f},k}}. \tag{3.10}$$

The definitions of exergetic fuels and products for the components and sub-systems investigated within this study are extensively discussed in Bejan *et al.* [13] and in Kotas [48, 49, 50].

Alternatively, for systems such as physical separation plants or that include dissipative devices, the relationship between the irreversibilities of a system and its

total exergy input can be expressed with the exergy loss ratio λ, as defined in Kotas [49, 50]. It derives from the exergetic efficiency definition proposed by Grassmann [31] and represents the proportion of the total exergy flowing into the control volume that is lost through irreversibilities. The criteria λ is denoted irreversibility ratio in the rest of the study to avoid confusion with the exergy loss ratio y_l^* defined in Bejan *et al.* [13].

$$\lambda = \frac{\dot{I}}{\dot{E}_i}, \tag{3.11}$$

where $\dot{I}$ is the rate of irreversibilities of the investigated system.

3.3 Results

3.3.1 System simulation and analysis

Process simulation

The offshore platform model was used to investigate the six case studies in order to obtain the net oil, gas and water production flows (Table 3.5) and the electrical energy demand of each module (Table 3.6). The power consumption of the offshore platform ranges from 22.6 MW to 31.1 MW and the maximum value is obtained with black oil as input (*Case 4*), as the power demand of the oil pumping section increases sharply. Results indicate that the major electricity consumer is generally the compression train, which is responsible for 42% to 56% of the total power demand in the remaining cases.

The seawater injection process ranks second with a share of 17% to 23% and a power demand of about 5.3 MW. Seawater pumped to a pressure of 12.5 MPa for further injection into the reservoir is not extracted through the oil and natural gas wells and does not enter the separation train. As the water purification and injection processes are not integrated within the other onsite systems, crude oil, produced oil, gas and water do not flow through this section of the platform. The electrical energy demand of this process is therefore independent of the composition and flow rate of the reservoir fluid. It depends exclusively on the flow rate of the seawater required for pressure maintenance and on the pressure level requirements.

The third greatest power demand of the offshore facility is either the gas re-compression process or the oil pumping, depending on the amount of gas extracted along with oil. The power consumption of these compressors is smaller in the cases with a high gas-to-oil ratio (*Cases 5 and 6*): this suggests that most of the associated gas, rich in light hydrocarbons such as methane and ethane, exits the separation train at the first stage and bypasses the booster compressors.

Case 4 is characterised by a different power consumption profile: the oil pumping section has the greatest demand, accounting for about 41% of the total plant

consumption. The results suggest that the additional power needed to pump the surplus of oil overcomes the decrease of power required in the gas compression section. The duty of the recompression train also increases in this specific case, because hydrocarbons of intermediate molecular weight (e.g. butane, pentanes, hexanes and heptanes) are not flashed at the first separation stage but at the second and third ones. This results in larger recycle flows between the separation and recompression modules and thus in a significant increase of the power and cooling demands of this section.

In contrast, a greater water fraction has a negative feedback on the electrical energy demand of the processing plant, since water is directly removed in the three-phase separators and only small amounts are carried through the plant. The effect of a higher water fraction in the wet gas leaving the recompression train is limited: the power demand of the dehydration process slightly increases because of the larger glycol flow in the absorption-desorption loop to reduce the water content of gas to the required specification.

Table 3.5: Net oil, gas and water production flow rates of the offshore platform system.

	Simulation cases					
	Case 1	Case 2	Case 3	Case 4	Case 5	Case 6
Oil (export)						
Molar (Mmol/hr)	3.2	3.0	4.5	9.9	2.3	1.7
Volume (Sm^3/hr)	614	548	843	1962	407	316
Mass (t/hr)	508	451	686	1628	325	255
Gas (export)						
Molar (Mmol/hr)	11.1	9.7	10.8	5.9	12.9	13.6
Volume (kSm^3/hr)	262	228	255	139	305	319
Mass (t/hr)	234	203	223	118	267	273
Produced water						
Molar (Mmol/hr)	3.4	4.7	2.1	1.7	2.3	2.3
Volume (Sm^3/hr)	60.9	85.2	38.0	30.2	41.4	41.6
Mass (t/hr)	61.0	85.3	38.0	30.2	41.5	41.6

Table 3.6: Power consumption (values expressed in (MW)) of the processing plant.

	Simulation cases					
	Case 1	Case 2	Case 3	Case 4	Case 5	Case 6
Compression	10.8	9.5	10.4	6.0	12.3	13.1
Recompression	2.8	4.1	4.7	6.9	3.5	3.0
Oil pumping	4.0	3.6	5.5	12.9	2.7	2.1
Seawater injection	5.3	5.3	5.3	5.3	5.3	5.3
Total (MW)	22.9	22.6	26.0	31.1	23.8	23.5
Total (MJ/Sm^3_{oil})	134	148	111	57.1	211	268
Total (MJ/t_{rf})	112	107	97	63	132	156
Total (MJ/m^3_{rf})	40	46	43	44	41	39

Error analysis

The separation, gas recompression and injection process models were verified against literature [57, 56, 22, 127, 128, 96] and the error analysis showed an average deviation smaller than 7–8% for all tested variables (Fig. 3.3). The maximum difference was found in the prediction of the power consumption of the processing plant. For loads above 50%, which is the region of interest, the maximum relative error was found in the prediction of the gas turbine thermal efficiency and was around 3.7%.

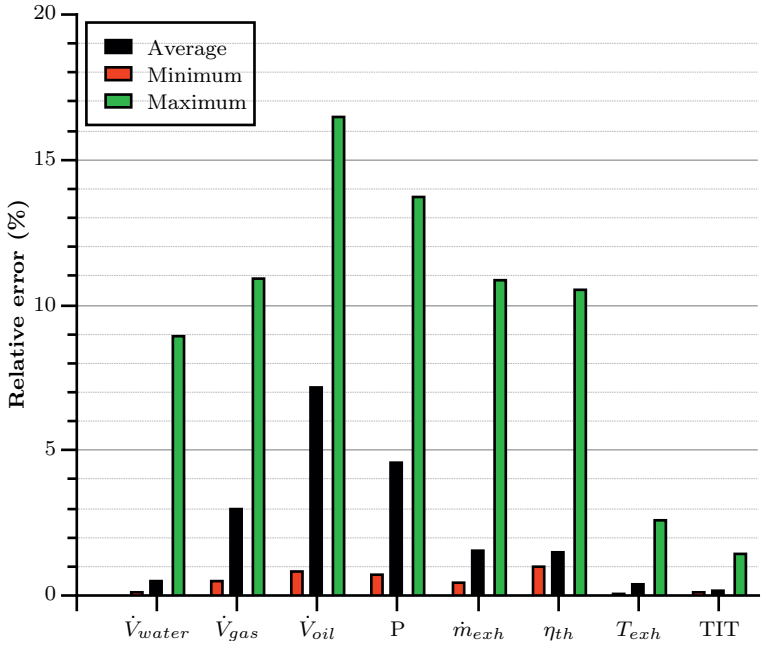

Figure 3.3: Minimum, average and maximum relative error ϵ (%) for the tested model variables (Table 3.3).

Sensitivity analysis

A sensitivity analysis on three parameters (Table 3.4) was conducted to illustrate the trends of the power consumption profile as a function of the efficiencies of the gas compressors and of the oil export pumps. The results suggest that the total power demand is mostly sensitive to the efficiency of the gas compressors in the compression train (Fig. 3.4). The power demand between a state-of-the-art centrifugal compressor operated near its design point and a poorly designed one, or operated at part-load, can vary from 3 to 9 MW. This difference is significant in all cases but is particularly marked in *Case 5* and *Case 6*, where near-critical and condensate oils are processed. The variations in power demand with the efficiencies of the oil pumps are comparatively small, with the exception of the black oil case

where the electrical power demand of the export train is much more significant (Fig. 3.5). Similar trends are found with the variations of efficiencies of the gas recompressors, although they are less marked than with the gas compressors (Fig. 3.6).

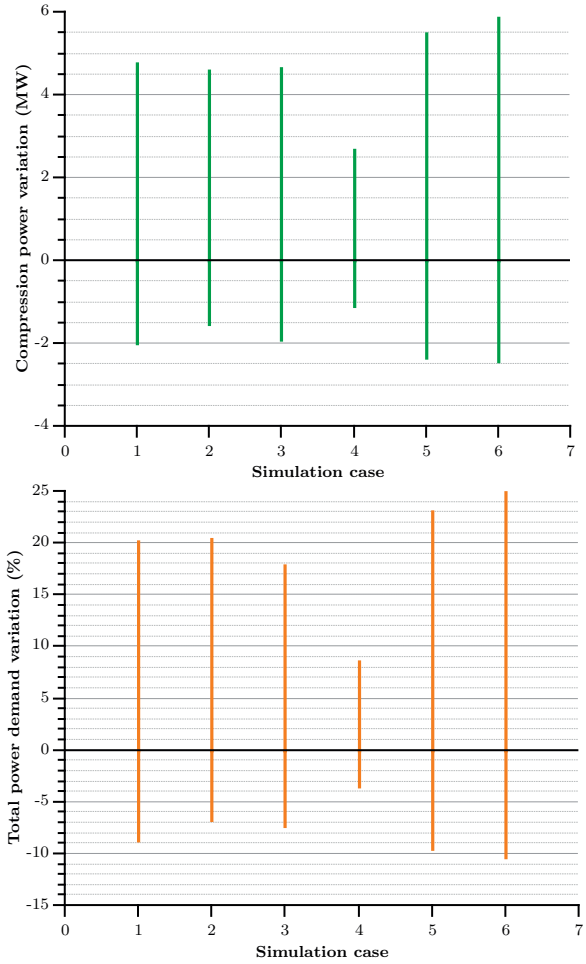

Figure 3.4: Effect of the isentropic compressors efficiency η_{is} (45–80%) on the compression train *(left)* and total *(right)* power demands.

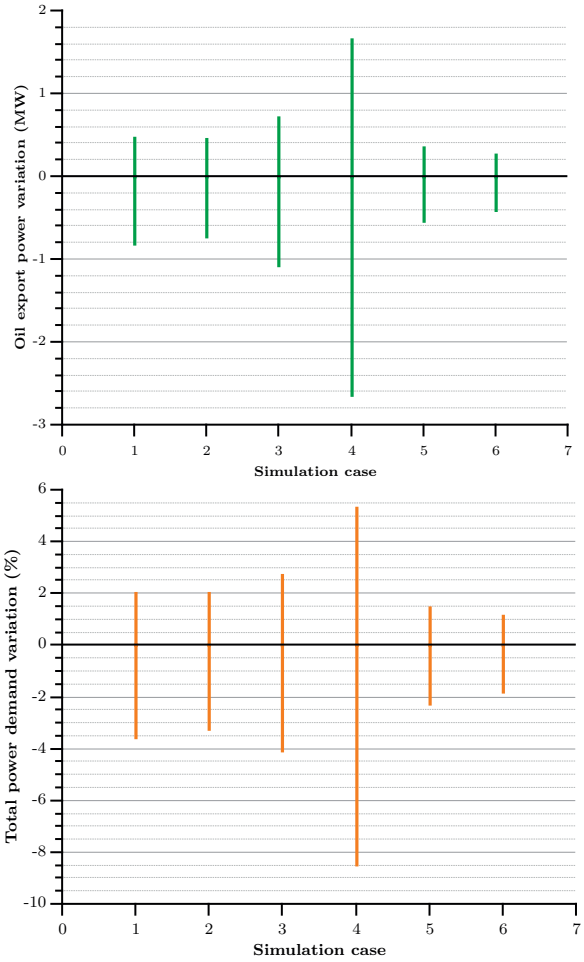

Figure 3.5: Effect of the centrifugal oil pumps efficiency η_{pp} (55–78%) on the oil export *(left)* and total *(right)* power demands.

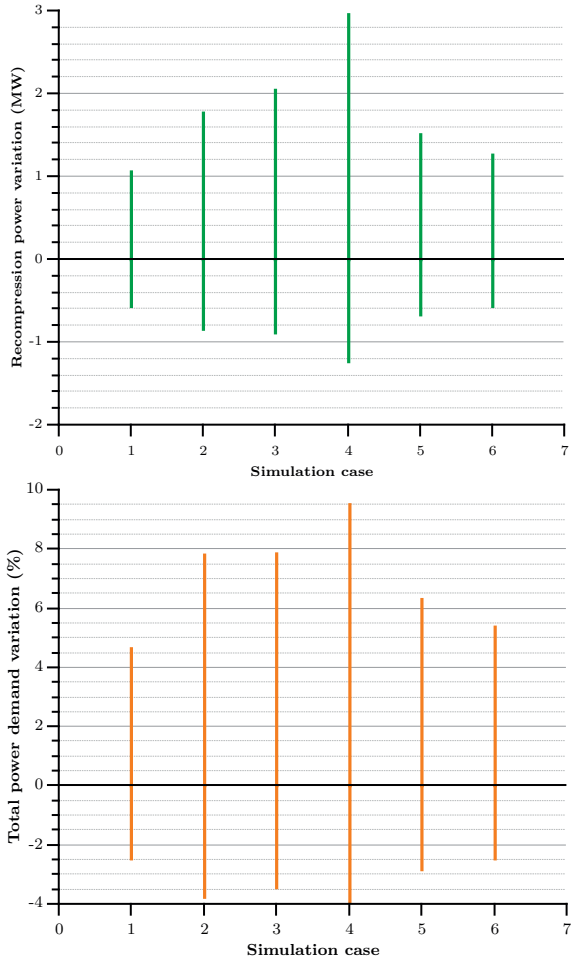

Figure 3.6: Effect of the isentropic compressors efficiency η_{is} (45–80%) on the recompression train *(left)* and total *(right)* power demands.

3.3.2 Exergy analysis

Exergy flows

The results of the combined process simulations and exergy accountings (Table 3.7) indicate that the produced water and exhaust gases from the power generation system have a small specific exergy content. Operations such as compression and pumping, which aim at increasing the physical exergy of the gas and oil flows, have a minor impact on the total specific exergy of these streams. The input and output exergies of the offshore platform system are dominated by the chemical exergy content of the oil and gas streams, which ranges from 43 to 48 MJ/kg and is at least 100 times as great as their physical exergy (Table 3.2). Most of the exergy found at the outlet of the offshore platform system is thus carried by these two streams, independently of the case considered.

Exergy destruction, losses and efficiencies

The total destroyed exergy on the overall offshore platform, i.e. including both the processing and the utility plant, is between 68 and 84 MW, with 62–65% of this being attributable to the gas turbines and waste heat recovery and 35–38% to the oil, gas and seawater processing plant (Table 3.8). The largest exergy destruction of the *complete* system lies, in *any case*, in the combustion chambers of the gas turbines and amounts to almost 50% of the total exergy destruction of the platform. It can be split into thermodynamic irreversibilities due to mixing of natural gas and compressed air and to the combustion process by itself. This exergetic analysis demonstrates that the variability of the well-fluid composition has a moderate effect on this result, but, on the opposite, has a significant impact on the share of exergy destruction across the processing plant.

The total exergy destruction of the processing plant exclusively is between 24 and 32 MW. The maximum exergy destruction is found in *Case 4* (31.6 MW), which is characterised by a crude oil poor in light hydrocarbons, while the minimum is found in *Case 6* (23.9 MW), featured by a crude oil with a high gas content. A comparison of the specific exergy destruction per unit of mass, actual volume and exergy input is presented further (Table 3.12).

The results also indicate that the largest thermodynamic irreversibilities of the processing plant occur in the production manifold and in the gas compression systems, followed by the recompression and separation modules (Table 3.9). In contrast, the contributions from the wastewater treatment and the seawater injection processes are negligible, and the exergy destruction taking place in the oil pumping step is moderate in most cases. The latter is significant only when black crude oil enters the platform (*Case 4*) because of the higher content of heavy hydrocarbons and larger oil flow at the inlet of the export pumping section.

Table 3.7: Flow rates and associated specific exergies (values given in (Mmol/hr) and (GJ/kmol), respectively) – stream numbers refer to Fig. 3.2.

Stream number (type)	**Simulation cases**											
	Case 1		Case 2		Case 3		Case 4		Case 5		Case 6	
	$\dot{n}$	$\bar{e}$	$\dot{n}$	$\bar{e}$	$\dot{n}$	$\bar{e}$	$\dot{n}$	$\bar{e}$	$\dot{n}$	$\bar{e}$	$\dot{n}$	$\bar{e}$
1 (Reservoir fluid)	18.5	1.88	18.5	1.64	18.5	2.31	18.5	4.32	18.5	1.54	18.5	1.37
2 (Reservoir fluid)	18.5	1.87	18.5	1.63	18.5	2.30	18.5	4.31	18.5	1.53	18.5	1.36
3 (Separated oil)	3.7	6.42	3.2	6.48	4.8	6.52	10.2	7.18	2.5	6.07	1.8	6.36
4 (Pumped oil)	3.2	7.17	3.0	6.77	4.5	6.80	9.9	7.37	2.3	6.40	1.7	6.63
5 (Recompressed gas)	11.7	0.96	11.6	0.96	11.9	1.04	6.4	0.99	13.6	1.00	14.9	1.02
6 (Dry gas)	11.4	0.97	9.9	0.97	11.0	1.00	6.1	1.00	13.1	1.00	13.8	0.98
7 (Compressed gas)	11.1	0.99	9.7	0.99	10.8	1.02	5.9	1.02	12.9	1.02	13.6	1.00
8 (Fuel gas)	0.18	0.97	0.17	0.97	0.19	1.00	0.22	1.00	0.18	1.00	0.18	0.98
9 (Produced water)	3.4	<0.001	4.7	<0.001	2.1	<0.001	1.7	<0.001	2.3	<0.001	2.3	<0.001
10 (Injected water)	71.1	<0.003	71.1	<0.003	71.1	<0.003	71.1	<0.003	71.1	<0.003	71.1	<0.003
11 (Air)	20.5	<0.001	20.3	<0.001	21.4	<0.001	22.8	<0.001	20.9	<0.001	20.7	<0.001
12 (Exhaust gases)	20.5	0.003	20.4	0.003	21.4	0.003	22.9	0.004	21.0	0.003	20.8	0.003
Flared and vented gases	0.02	0.96	0.02	0.96	0.02	0.99	0.03	0.99	0.02	0.99	0.02	0.97

Table 3.8: Exergy destruction (values expressed in (MW)) of the offshore platform.

	Simulation cases					
Sub-system, component	Case 1	Case 2	Case 3	Case 4	Case 5	Case 6
Production manifold	6.01	5.25	6.10	6.07	6.32	6.75
Separation	3.49	3.60	4.36	8.41	2.37	1.82
Heaters	0.85	0.73	1.16	2.32	0.63	0.47
Throttles	1.87	1.62	2.56	5.40	1.19	0.92
Mixers & others	0.77	1.25	0.64	0.69	0.55	0.43
Recompression	2.88	4.85	3.54	3.32	3.61	3.30
Coolers	1.92	3.00	1.80	1.23	2.10	2.07
Throttles	0.15	0.20	0.13	0.07	0.18	0.11
Compressors	0.62	0.82	1.04	1.58	0.74	0.60
Mixers & others	0.19	0.82	0.57	0.44	0.58	0.52
Glycol dehydration	3.18	3.23	2.75	1.76	3.24	3.68
Fuel gas and flaring	1.23	1.39	1.48	1.42	1.52	1.53
Gas compression	4.78	4.20	4.62	2.61	5.48	5.80
Coolers	1.57	1.35	1.50	0.69	1.86	1.95
Compressors	2.92	2.57	2.83	1.63	3.33	3.56
Mixers	0.02	0.02	0.02	0.02	0.02	0.02
Throttles	0.27	0.27	0.27	0.27	0.27	0.27
Oil pumping	2.29	2.29	2.94	7.69	1.06	1.12
Pumps	1.14	1.02	1.60	3.64	0.73	0.60
Coolers	1.03	1.27	1.34	4.05	0.33	0.52
Throttles & others	0.12	0.10	0.12	0.21	0.07	0.05
Wastewater treatment	0.11	0.20	0.07	0.06	0.07	0.07
Seawater injection	0.23	0.23	0.23	0.23	0.23	0.23
Processing plant	24.2	25.2	26.1	31.6	23.9	24.3
Power generation	40.8	40.2	43.4	47.8	41.5	41.3
Compressors	2.87	2.82	3.12	3.61	2.92	2.92
Turbines	4.55	4.51	4.74	5.00	4.59	4.59
Combustion chamber	33.0	32.6	35.1	38.7	33.4	33.2
Others	0.40	0.40	0.43	0.47	0.41	0.41
Heat carrier circulation	3.41	3.37	3.55	3.79	3.43	3.42
Utility system	44.2	43.6	47.0	51.6	44.9	44.7
Platform	68.4	68.8	73.1	83.2	68.8	69.0

The exergy destruction within the production manifold is caused by the well-fluid depressurisation from 16.5 to 7 MPa without generation of any useful product. The second greatest irreversibilities are found at the gas compression section: they are mainly due to the poor performances of the gas compressors and to the recycling around these components to prevent surging. Significant exergy destruction also takes place in the recompression step because the streams flowing out of the separation train are mixed at different temperatures and compositions before scrubbing and throttling.

Table 3.9: Exergy destruction ratio of the offshore platform (excl. utility system) y_{d}^{*} (%).

	Simulation cases					
Sub-system	Case 1	Case 2	Case 3	Case 4	Case 5	Case 6
Production manifold	24.8	20.8	23.4	19.2	26.4	27.8
Separation	14.4	14.3	16.7	26.6	9.9	7.5
Recompression	11.9	19.2	13.6	10.5	15.1	13.6
Dehydration	13.1	12.8	10.5	5.6	13.6	15.1
Fuel gas and flaring	5.1	5.5	5.7	4.5	6.4	6.3
Gas compression	19.8	16.6	17.7	8.3	22.9	23.9
Oil pumping	9.5	9.1	11.3	24.4	4.4	4.6
Wastewater treatment	0.5	0.8	0.3	0.2	0.3	0.3
Seawater injection	1.0	0.9	0.9	0.7	1.0	0.9

The exergy losses of the offshore platform are nearly constant in all cases: they are related to effluent streams rejected into the environment without being valorised, such as flared gases, discharged seawater, wastewater and exhaust gases from the gas turbine systems (Table 3.10). Approximatively 60% of the total exergy losses is due to the direct rejection of high-temperature exhaust gases to the environment, while about 30% is associated with the flaring and ventilation of natural gas throughout its processing. The remaining 10% is related to the exergy content of cooling and wastewater discharged overboard: these exergy losses are comparatively small, as the discharged streams are rejected at nearly environmental conditions (Table 3.11). The exergy losses associated with exhaust gases are higher in *Case 3* and *Case 4*, as the mass flow rate of exhaust gases increases with the power demand of the processing plant.

Table 3.10: Exergy losses (values expressed in (MW)) of the offshore platform.

	Simulation cases					
Waste stream	Case 1	Case 2	Case 3	Case 4	Case 5	Case 6
Exhaust gases	18.5	18.3	20.4	23.4	19.1	18.9
Cooling water	2.46	2.81	2.80	5.17	2.21	2.09
Flared gases	10.5	10.4	11.4	13.0	10.8	10.7
Wastewater	0.85	1.21	0.33	0.28	0.36	0.37
Platform	32.3	32.7	34.9	41.9	32.5	32.1

A comparison based on the irreversibility ratio λ suggests that the offshore processing becomes less performant with increasing gas-to-oil and water-to-oil ratios (Table 3.12). It also indicates that the total exergy destruction and losses within the offshore platform represent only 0.5–1.5% of the total exergy flowing into the system.

Table 3.11: Exergy loss ratio of the offshore platform y_l^* (%).

	Simulation cases					
Waste stream	Case 1	Case 2	Case 3	Case 4	Case 5	Case 6
Exhaust gases	57.3	56.0	58.5	55.8	58.8	58.9
Cooling water	7.62	8.59	8.02	12.3	6.80	6.51
Flared gases	32.5	31.8	32.7	31.0	33.2	33.3
Wastewater	2.63	3.70	0.95	0.67	1.11	1.15

Table 3.12: Specific exergy destruction, losses and irreversibility ratios.

	Simulation cases					
Irreversibilities	Case 1	Case 2	Case 3	Case 4	Case 5	Case 6
$\dot{E}_d$ (MW)	68	69	73	83	69	69
e_d (MJ/t_{rf})	334	327	273	168	382	457
e_d (MJ/m^3_{rf})	120	142	122	117	118	116
$\dot{E}_l$ (MW)	32	33	35	42	33	32
e_l (MJ/t_{rf})	158	156	130	85	180	213
e_l (MJ/m^3_{rf})	57	67	58	59	56	54
Total (MW)	101	102	108	125	101	101
Total (MJ/t_{rf})	491	483	404	253	562	670
Total (MJ/m^3_{rf})	177	209	181	175	174	170
λ (%, internal)	0.71	0.82	0.61	0.37	0.87	0.98
λ (%, total)	1.05	1.21	0.91	0.56	1.28	1.43

In the baseline case, the gas turbine system, the gas compression and the oil pumping processes have a low exergetic efficiency, of about 27%, 42% and 37% respectively, as a result of large thermodynamic irreversibilities associated with chemical reaction and heat transfer in the first process, and with mixing and friction in the second and third ones. No meaningful exergetic efficiency could be defined for the production manifold and the gas flaring modules. They mainly consist of arrangements of mixers and throttling valves, which are dissipative by design: they destroy exergy without generating any useful product. Alternatively, as the exergetic product is null, it may be argued that the exergetic efficiency is 0.

This exergetic analysis shows that exergy is introduced onsite in the form of raw materials (crude oil, fuel air, seawater and chemicals) and exits in the form of valuable products (oil and gas sent onshore) and waste streams (produced water, exhaust and flare gases) (Fig. 3.7). The chemical exergy of the reservoir fluid flows through the offshore platform system and is separated into the oil and gas chemical exergies with only minor destruction in the processing plant, as no chemical reactions take place. On the opposite, chemical exergy is consumed to a great extent in the utility plant, as a fraction of the produced natural gas is used and combusted in the gas turbines.

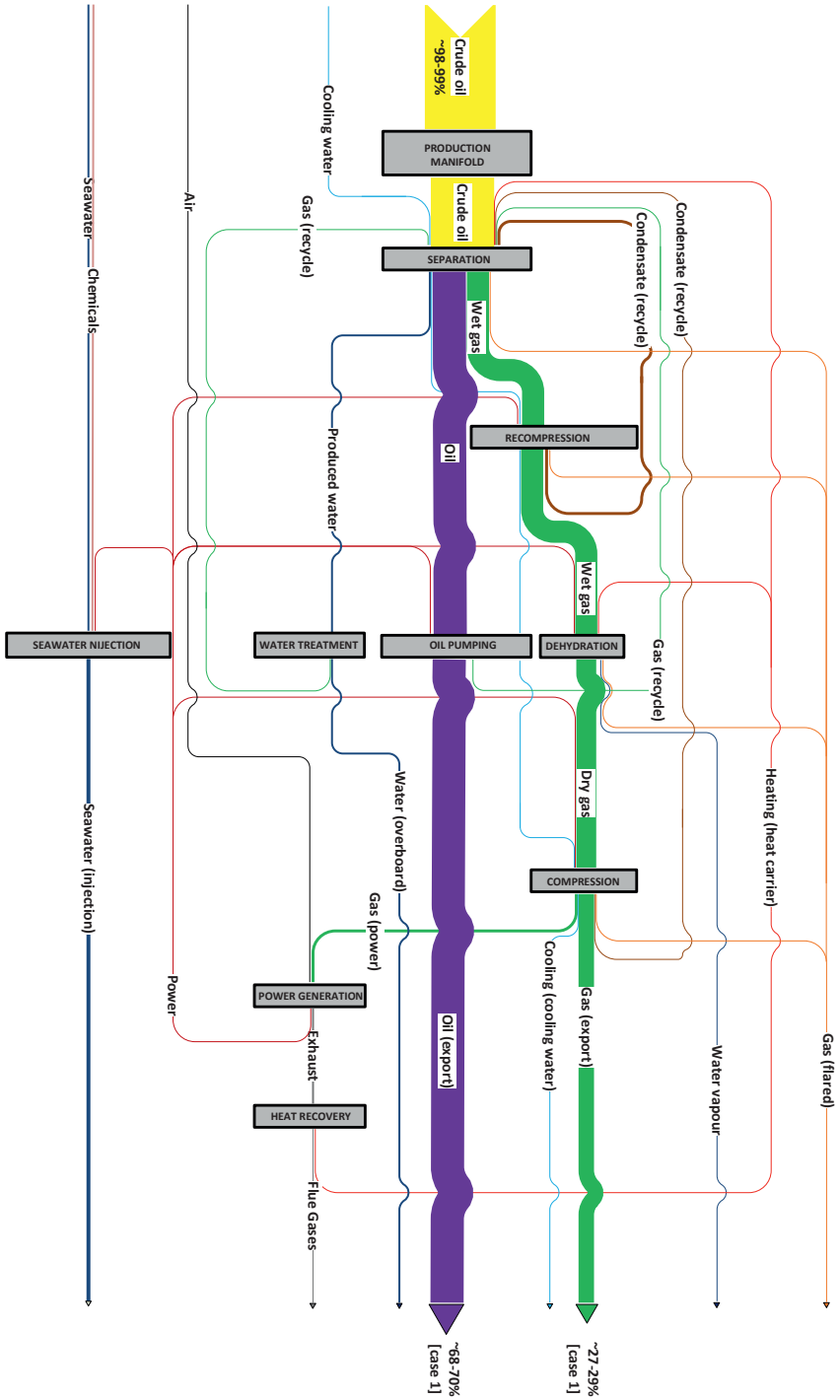

Figure 3.7: Grassmann diagram of the offshore platform system.

Possibilities for improvement

Generic recommendations for improvement of the platform performance can be derived from the exergy analysis. The overall goal is to reduce or eliminate the exergy destruction and losses of the plant and the main ones are ranked as follows:

1. Combustion chambers of the gas turbines (chemical reaction, mixing, friction, heat transfer)
2. Exhaust gases from the waste heat recovery system (high temperature and large physical exergy)
3. Flared and vented gases from the processing plant (large chemical and physical exergy contents)
4. Production manifold (mainly due to depressurisation)
5. Compressors in the gas compression train

The largest thermodynamic irreversibilities are found at the combustors. In theory, the exergy destruction taking place in the combustion chambers could be reduced by decreasing the overall air-to-fuel ratio [13]. However, it implies that the combustion temperature increases toward the adiabatic flame temperature, which causes significant thermal stress and impacts the lifetime of the components.

The exhaust gases leaving the waste heat recovery system are rejected at high temperature to the atmosphere, which represents a substantial loss of physical exergy. The excess heat contained in the flue gases could be partly recovered for producing electricity, by using a bottoming cycle such as an organic Rankine cycle. The stack temperature and the exergy loss of the platform system would decrease in consequence. The waste heat recovery system could in theory be further improved: the heat carrier is heated from 200°C to 220°C, suffers severe pressure drops in the closed-loop system, and the large temperature gaps with the exhaust gases of the gas turbine are responsible for a significant exergy destruction associated with heat transfer. However, as the highest temperature requirement of the processing plant is found at the kettle reboiler of the glycol desorber (about 200–205°C), integrating a direct heat exchange between the glycol/water mixture and the flue gases would have a limited positive impact.

The third main source of exergy destruction/losses is associated with flared gas from the processing plant: continuous flaring should therefore, if possible, be limited. The gases sent for flaring could be recovered in the processing plant: this presents the combined benefits of decreasing the exergy losses, reducing the environmental impact of the offshore facility and recovering more gas for sale.

The irreversibilities taking place in the production manifold could *a priori* hardly be reduced with the current set-up of offshore processing since a lower pressure of the well-fluid is required at the inlet of the separation train. Higher pressure

levels in the separation train would lead to smaller exergy destruction rates in the production manifold train, although this might result in lower gas recovery and conflict with the process constraints of other system sections. The integration of multiphase flow expanders would allow energy recovery from the throttling steps and would lead to smaller exergy destruction rates. However, it is a challenge to design such devices which could stand the processing of multiphase mixtures (oil, water, gas and sand) on the long term. Implementing them in the separation train might be easier, as most of the water-sand mixture is removed in the first-stage separator.

Substantial exergy destruction is associated with the gas compression train, as the compressors typically used on oil offshore platforms are featured by a relatively low isentropic efficiency and gas recirculation, since flow variations are expected and surge must be prevented. The sensitivity of the total power consumption of the processing plant to the compressors efficiency emphasises the importance of this system section: its performance could be increased by re-wheeling (removal and replacement of the compressor internals), implementing variable speed drive systems, using alternative control methods and adjusting the stagger angle of vanes. Another possibility is to integrate compressors of different sizes in parallel so that the majority of them is operated near their optimal operating point.

3.4 Discussion

3.4.1 Comparison with literature

The process simulation results are in accordance with the findings of Svalheim and King [110], who stated that the gas compression, oil pumping and seawater injection steps are the most energy-consuming steps. It was suggested to use the produced water extracted along with oil and gas instead of treated seawater [79], but it was also emphasised that the hydrocarbon content of the wastewater emulsion might result in plugging issues. Further research and quality control of the treated water are thus necessary before this option becomes viable [1].

The present results on the thermodynamic performance of oil and gas platforms can be compared to the results of Voldsund *et al.* [127, 128], which were introduced in Section 3.1. They considered a real-case offshore facility located in the North Sea region, processing a crude oil rich in methane (78%) and producing about 370 kSm^3/hr of natural gas, 135 Sm^3/hr of oil and 67 Sm^3/hr of water. In this regard, the most similar case investigated within this work was *Case 6*. The power demand was about 18.5 MW without seawater injection, which is about 20% smaller than the value calculated and presented in their paper. This difference is mainly imputable to the assumptions on the isentropic efficiency of the gas compressors in the present study, which was at first set to 65% and varied by conducting a sensitivity analysis. In their work, the isentropic efficiency was between 47% and

69% in the recompression train and between 54% and 69% in the compression section. Other differences are the total volume of gas processed in the gas compression section, which is about 15% larger, and the final pressure level, which is 23.5 MPa.

Furthermore, the comparison between these two research works also suggests that the gas compression-treatment process is one of the most exergy-destructive steps of a typical oil offshore processing. Similarly, the recompression and separation steps rank next, while the exergy destruction taking place in the oil export pumping is generally negligible. The main discrepancy lies in the accounting of the exergy associated with overboard discharge of cooling water. It is in the present work accounted as an exergy loss whereas it is considered as exergy destruction in their study, because of a different choice of the system boundaries. They suggested to focus on the gas compression and injection train, by for instance eliminating anti-surge recycling. One of the main emphases was on the performance improvement of this system section, since a more efficient gas process would induce a reduction of the power consumption and a lower exergy destruction in both the oil processing and power generation plants. There was on overall a good correspondence between the findings of both works.

Oliveira and Van Hombeeck [22], who investigated a real-case Brazilian oil platform, also stressed the great power demand and the significant exergy destruction associated with the gas compression step. However, the authors pointed out the importance of the crude oil heating operations taking place within the separation module. The considerable exergy consumption in the feed preheating is responsible for a furnace demand of about 25 MW exergy for a feed of 450 t/hr, which differs strongly from the findings of Voldsund *et al.* [127] and the present results. These discrepancies are mainly due to the temperature differences between the North Sea and the Brazilian feeds flowing out of the oil reservoir. The feed characteristics at the inlet of the separation train were 7.4°C and 10.78 bar in their work and the well-fluid should therefore be heated before oil, gas and water separation. On the opposite, it was about 65–75°C at the inlet of the first-stage separator in the present work and in the study of Voldsund *et al.* [127, 128]. These differences in results and conclusions suggest that offshore platforms located in different oil regions (e.g. North Sea, Gulf of Mexico, Brazilian Basin) may, with respect to process and exergy considerations, present highly different characteristics.

Finally, energy conservation measures on offshore installations, such as waste heat recovery, are discussed in the works of Kloster [46, 47]. It was also argued that the replacement of simple cycle gas turbines by combined cycle ones would be the most significant energy efficiency measure for oil and gas platforms, as this would greatly reduce their fuel consumption and CO_2-emissions. Moreover, the addition of a bottoming steam cycle, as suggested, could improve the performance of the overall platform in both design and part-load conditions, while maintaining a high flexibility of the power generation units.

3.4.2 Significance and limitations of the study

The results of this paper may be used as guidelines to predict the major sources of thermodynamic irreversibilities of a North Sea oil and gas platform. However, caution should be exercised in drawing conclusions for cases presenting different design setups. Although gas export is the preferred gas processing technology in the North Sea oil region [14], processing routes such as gas injection are practiced on several platforms [21] to support the reservoir pressure and enhance oil recovery. It is for instance the case of the oil platform investigated in Voldsund *et al.* [127, 128]. It may be difficult to estimate the exergy destruction profile for these cases, since it depends on factors such as the injection pressure, the compression train efficiency and the gas recirculation. The power demand and the exergy destruction are nonetheless expected to increase because the injected gas must be compressed to a higher pressure than in the reservoir to induce oil flowing [128, 32]. Similar reasoning applies to the gas lift process: the difference being that the gas is injected into the well flow in the wellhead to decrease the specific gravity of the reservoir fluid.

Another possible difference across offshore platforms is the inventory of gas turbine units. The study on which this work builds on, conducted by the same authors [70], considers two twin-spool and a single one-spool gas turbines. It is shown that the utility system accounts for about 67.3% of the total exergy destruction, which is similar to the results presented in this paper. This indicates that the exergy destruction share between the processing and the utility plants is moderately affected by the number and type of the power generation units. However, if no waste heat recovery system is integrated after the gas turbines, the exergy losses are expected to be greater, because the flue gases would be released to the environment at a higher stack temperature.

The present findings may also be used for making qualitative estimates on the magnitude of exergy destruction for different compositions and operating conditions. The investigations carried out in this work were made at specific temperatures and pressures of the reservoir and processing systems, which may not be encountered in actual cases. In practice, temperatures and pressures of the separation train are adjusted to control the oil and gas flows in each stage to prevent foaming, to ensure a minimum circulating flow and to enhance the recovery of light hydrocarbons. One of the main aims is to reduce the power consumption of the recompression system while reaching the desired crude oil vapour pressure at the outlet of the export pumping train. Pressure levels are generally lower and temperature levels in the reservoir as the API gravity of oils increases (heavy oils) [56, 132]. This suggests that the exergy destruction in the production manifold, the separation train and the recompression system may be slightly underestimated in this study.

Finally, a conventional exergy analysis, as conducted in this work, does not allow:

- the evaluation of interactions and cost flows among the system components and processes, as it does not consider their mutual interdependencies [44];
- the assessment of the environmental impact of this facility, as the exergy losses associated with the emissions of pollutants are neither proportional to their toxicity, nor to the exergy costs related to their treatments [92].

Several methods have been proposed over the last decades to increase the level of details and accuracy of an exergy analysis, with the examples of the extended exergy accounting method [92, 93], the exergoeconomic [122, 120] and the advanced exergy-based analyses [44, 60]. The readers are referred to these references for more extensive explanations of these concepts. Future work will address the limitations of the exergy analysis method by applying these approaches to the specific case of an oil and gas platform.

3.5 Conclusion

A generic North Sea offshore platform was modelled in order to establish rules of thumbs for oil and gas platforms of that region. The material outflows and energy requirements under different sets of production flows were predicted and validated. This overall model includes power generation, oil and gas processing, gas purification and seawater injection sub-models. The first sub-model was calibrated by use of published data from SIEMENS while the others were verified by comparison with open literature.

Six simulation cases were investigated to analyse the effects of different gas-to-oil and water-to-oil ratios on the thermodynamic performance of this integrated system, based on the exergy analysis method. Exergy is destroyed with a split of about 65%/35% for the utility system (power generation and waste heat recovery) and the oil, gas and water processing, respectively. Exergy losses are mostly due to the rejection of high-temperature exhaust gases from the cogeneration plant to the environment and on flaring practices. However, the exergy destruction and loss rates represent only 0.5 to 1.5% of the total input exergy because of the inherently large chemical exergy content of oil and natural gas.

At identical design conditions, the irreversibility ratio of an offshore platform is higher with increasing gas-to-oil and water-to-oil ratios, suggesting that the thermodynamic performance of this overall system is optimal with low well-fluid contents of gas and water.

Although the exact values of exergy destruction would differ from one platform to another, it is suggested that significant inefficiencies and possibilities for performance improvement of the system exist. Recovering more thermal exergy from the exhaust gases, limiting or eliminating flaring practices and monitoring the gas

compression trains could increase the thermodynamic performance of conventional oil and gas offshore platforms.

Acknowledgements

The funding from the Norwegian Research Council through the Petromaks programme, within the project 2034/E30 led by Teknova is acknowledged.

Nomenclature

e	specific exergy (mass), J/kg
$\bar{e}$	specific exergy (molar), J/mol
$\dot{E}$	exergy rate, MW
h	specific enthalpy (mass), J/kg
$\dot{I}$	irreversibilities rate, MW
P	power, MW
p	pressure, MPa
s	specific entropy (mass), J/(kg·K)
$\dot{S}$	entropy rate, MW/K
$\dot{V}$	Standard volume flow, Sm^3/hr
y	component/sub-system exergy ratio
z	pollutant mass fraction

Abbreviations

API	American Petroleum Institute
ASPEN	Advanced System for Process Engineering
DNA	Dynamic Network Analysis
EOS	equation of state
GOR	gas-to-oil ratio
HVAC	heating, ventilation and air conditioning
NC	near-critical
NHV	net heating value, kJ/kg
NRTL	non-random-two-liquid
PR	Peng-Robinson
TBP	true boiling point
TEG	triethylene glycol
TIT	turbine inlet temperature, °C
WOR	water-to-oil ratio

Greek letters

β	chemical exergy correction factor

ΔT	temperature approach, K
ϵ	relative error
η	efficiency
λ	irreversibility ratio

Superscripts

*	relative
ch	chemical
kn	kinetic
ph	physical
pt	potential

Subscripts

0	dead state
c	chemical specie
comp	compressor
cv	control volume
d	destruction
dr	driver
exh	exhaust
f	fuel
gen	generation
i	inlet
k	component
l	loss
m	metal
mec	mechanical
min	minimum
o	outlet
p	product
pp	pump
rf	reservoir fluid
th	thermal

Chapter 4

Exergy destruction and losses on four North Sea offshore platforms: A comparative study of the oil and gas processing plants

Mari Voldsund[1], Tuong-Van Nguyen[2], Brian Elmegaard[2], Ivar Ståle Ertesvåg[3], Audun Røsjorde[4], Knut Jøssang[3] and Signe Kjelstrup[1]

1. Department of Chemistry,
Norwegian University of Science and Technology,
NO-7491 Trondheim, Norway

2. Department of Mechanical Engineering,
Technical University of Denmark,
DK-2800 Kongens Lyngby, Denmark

3. Department of Energy and Process Engineering,
Norwegian University of Science and Technology,
NO-7491 Trondheim, Norway

4. Statoil ASA,
NO-1364 Fornebu, Norway

This chapter is accepted for publication in
Energy - The International Journal

Abstract

The oil and gas processing plants of four North Sea offshore platforms are analysed and compared, based on the exergy analysis method. Sources of exergy destruction and losses are identified and the findings for the different platforms are compared. Different platforms have different working conditions, which implies that some platforms *need* less heat and power than others. Reservoir properties and composition vary over the lifetime of an oil field, and therefore maintaining a high efficiency of the processing plant is challenging. The results of the analysis show that 27%–57% of the exergy destruction take place in the gas treatment sections, 13%–29% take place in the gas recompression sections and 10%–24% occur in the production manifolds. The exergy losses with flared gas are significant for two of the platforms. The exact potential for energy savings and for enhancing system performances differs across offshore platforms. However, the results indicate that the largest rooms for improvement lie in (i) gas compression systems where large amounts of gas may be compressed and recycled to prevent surge, (ii) production manifolds where well-streams are depressurised and mixed, and (iii) in the installation of flare gas recovery systems.

4.1 Introduction

Oil and gas processing on North Sea offshore platforms consumes substantial amounts of power and has a significant environmental impact, being responsible for about 26% of the total greenhouse gas emissions of Norway in 2011 [105]. Onsite processes on offshore facilities suffer from significant performance losses over the lifetime of the installation, as a consequence of substantial variations of the reservoir properties (e.g. pressure and temperature) and of the production flow rates and composition (e.g. gas-to-oil and water-to-oil ratios, crude oil properties). These off-design conditions lead to the use of control strategies such as anti-surge recycling [110], and thus to greater power consumption and larger exergy destruction. Moreover, as the oil production decreases with time, energy-intensive techniques such as gas and water injection are employed to enhance oil recovery from the reservoir. It is therefore challenging to maintain a high performance of the overall system over time, while optimising the oil and gas production.

Svalheim and King [109] stressed the large power demand of the gas compression and water injection processes over the lifespan of the oilfield. To the knowledge of the authors, it is the only study in the open literature that investigates the life of field variations of the energy demand of oil and gas facilities. The variations are due to changes in field pressure, water-to-oil and gas-to-oil ratios over the lifetime of the field. Their studies also emphasised the benefits that resulted from applying best practices in energy management (e.g. gas turbine operation near design load, reduction of flaring and venting practices, and integration of waste heat recovery).

Similarly, Kloster [46, 47] argued that these measures could and did contribute to significant energy savings and a reduction of the CO_2-emissions of the Norwegian oil and gas installations. A mapping of the thermodynamic inefficiencies is useful, as it indicates room for improvements in a rational manner. Such information can be obtained by carrying out an exergetic analysis, which is based on both the 1st and 2nd laws of thermodynamics. The exergy of a system is defined as the maximum theoretical ability to do work when it interacts with the environment, and is, unlike energy, not conserved in real processes [50]. An exergy accounting reveals the locations and extents of thermodynamic irreversibilities present in a given system, and these irreversibilities account for a greater fuel use throughout successive processes [13].

Oliveira and Van Hombeeck [22] conducted an exergy analysis of a Brazilian oil platform which included the separation, compression and pumping modules but not the production manifolds. Their work showed that the least exergy-efficient subsystem was the oil and gas separation, while the most exergy-consuming ones were the petroleum heating and the gas compression processes. Voldsund et al. [126] carried out an exergy analysis of a Norwegian oil platform and considered the production manifold, the separation and recompression processes, the fuel gas subsystem and the oil pumping and gas reinjection trains. Their study demonstrated that the largest exergy destruction took place in the production manifold and in the gas reinjection systems. There were no considerable petroleum heating operations on this platform, since the feed temperature was high enough for separation of the specific oil by pressure reduction only, and thus there was no exergy destruction due to heating operations. Nguyen et al. [71] conducted a generic analysis of Norwegian oil and gas facilities. Their work suggested that the production manifold and gas compression trains were generally the most exergy-destructive parts, followed by the recompression and separation modules. It was also shown that these results were particularly sensitive to the compressor and pump efficiencies, as well as to the petroleum composition.

The similitude and discrepancies in the results of these studies suggest that differences in the design setup and in the field conditions may affect the locations and extents of the thermodynamic irreversibilities of the overall system. The literature appears to contain no systematic comparison of the sources of exergy destruction for oil and gas platforms. Therefore, in this work, the platform analysed by Voldsund et al. [126] is compared with three other North Sea offshore platforms, which have not been studied in this manner before. The variations of the reservoir fluid composition over the life cycle of each field are not investigated, but it is worth emphasising that the four platforms operate at a different production period of an oilfield (peak and end-life). The work was carried out in three main steps:

- simulation and investigation of the platforms;
- exergy accounting;

- comparison of the four platforms, based on the outcomes from the two previous steps.

The present paper is part of two projects dealing with modelling and analysis of oil and gas producing platforms. It builds on previous works conducted by the same authors and is structured as follows: Section 4.2 describes the followed methodology, with a strong emphasis on the system description and on the similarities and differences between the four cases. Section 4.3 presents a comparison of the results obtained for each platform. The results are discussed in Section 4.4 and are followed by concluding remarks in Section 4.5.

4.2 Methodology

4.2.1 System description

The purpose of an offshore platform is to extract, process and export petroleum. A typical offshore platform consists of a processing plant, utilities, drilling modules, and a living quarter. The focus of this study is the processing of oil and gas, which takes place in the processing plant. All power and heat that are needed in the processing plant are delivered by power turbines and heat recovery systems that are part of the utilities, normally by combustion of the natural gas produced at the platform. A flare gas system, which is also a part of the utilities, handles gas released during unplanned over-pressuring of plant equipment and small volumes of waste gas that cannot be easily captured and returned to the system for processing.

The structural designs of the processing plants on the four platforms are similar. Meanwhile, different reservoir fluid characteristics and reservoir properties, as well as different requirements for the products, have resulted in dissimilar temperatures, pressures and flow rates throughout the process, and different demands for compression, heating, cooling and treatment.

Below we give a generalised overview of the oil and gas processing plant for the studied platforms, present key information on the platforms, to indicate the main differences between them, and list process data that are important to explain the different results for the platforms.

A generalised overview of the processing plant

An overview of the processing plants on the four platforms, with subsystems and material streams, is shown schematically in Fig. 4.1. This figure shows the common overall set-up of the processing plants. The detailed process set-ups are illustrated in Figs. 4.7–4.10. Well fluids from several producing wells (1) enter one or more

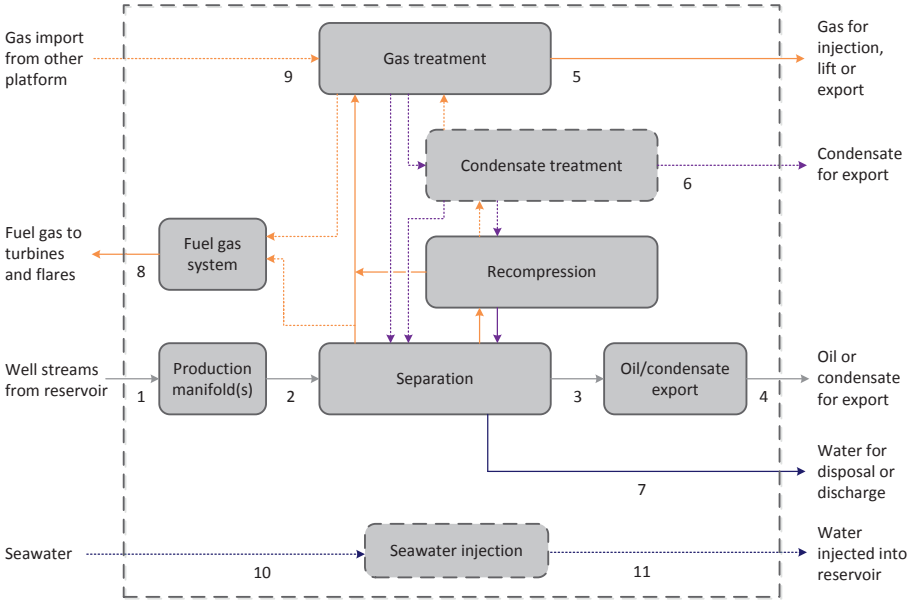

Figure 4.1: A generalised overview of the processing plant on the four North Sea platforms. The arrows represent one or several mass streams while the blocks represent subsystems. Dotted arrows and blocks are not present at all four platforms. Flared and vented gases come from several sections of the processing plant and are not shown in the figure for readability.

production manifolds where pressure is reduced and streams from the different wells are mixed. The mixed streams (2) are sent to a separation train where oil, gas and water are separated in several stages by reducing pressure in each step, and where heating may be required.

Oil or condensate (3) is sent to the main oil/condensate treatment section where it is pumped for further export (4). Produced gas is compressed in a recompression train to match the pressure of the stream entering the separation train (2). This compression is done in several stages, each stage with a cooler, a scrubber and a compressor. Condensate from the recompression train is sent back to the separation train, while compressed gas is sent to the gas treatment section.

The produced gas is treated differently on the four platforms, with different demands for compression and dehydration, depending on the properties of the gas and on whether the product (5) is to be exported or used for enhanced oil recovery. This can be performed either with gas injection, where gas is injected into the reservoir in order to maintain a high pressure, or gas lift, where gas is injected in the wells in order to reduce the density of the well-streams. On one of the platforms additional gas is imported (9) and compressed in this section. Condensate from the

gas treatment is either recycled to the separation train or pumped, dehydrated and exported (6) in a separate condensate treatment section. Fuel gas is taken from one of the streams with produced gas, treated in a fuel gas system and sent (8) to the power turbines, and for two of the platforms also to the flares for pilot flames.

From each of the subsystems shown in Fig. 4.1, except from the seawater injection system, some gas may be sent to the flares, in urgency cases and/or in order to maintain a stable production. The amount of flared gas is normally negligible compared to the main hydrocarbon flows, representing less than 2% of the total exergy of the crude oil and gas flows. In special cases large amounts of gas may be flared to avoid emergencies.

Produced water (7) is treated and either discharged to the sea or injected into another reservoir. Seawater (10) may be compressed for injection into the producing reservoir for enhanced recovery (11).

Key information on the studied platforms

The studied platforms are labelled Platform A, B, C and D, and their main characteristics are given below:

- Platform A has been in production for approximately 20 years and is characterised by a high gas-to-oil ratio. Oil is pumped to a nearby platform while gas is injected into the reservoir for pressure maintenance. Water injection is also used as a recovery technique, but the injection water is produced at another platform, and is therefore not taken into consideration in this analysis. Produced water is discharged to the sea. Platform A was investigated in previous works of the same authors and more details of the analysis can be found in [126].
- Platform B has been in production for approximately 10 years. It has high reservoir temperature, pressure and gas-to-oil ratio and produces gas and condensate through pressure depletion. The exported gas is not dehydrated. Produced water is injected into another reservoir for disposal. Power consumption is small because of a relatively low compression demand. There is some heat integration between process streams with cooling- and heating demand.
- Platform C has also been in production for approximately 10 years. It produces oil with high viscosity, and heating is required to ease the crude oil-water separation. The heating demand is met by waste heat recovery from the exhaust gases exiting the gas turbines, and by heat integration with other process streams. Gas lift and gas injection are used as recovery strategies: however, the gas-to-oil ratio of this field is small and gas is therefore imported. Produced water is discharged to the sea. A flare gas recovery system

is installed. An exergetic assessment of this platform was also presented by Jøssang [43].

- Platform D has been in production for approximately 20 years, and gas, oil and condensate are exported. The treatment of condensate is due to a high propane content in the reservoir fluid and is done to prevent recirculation of medium-weight alkanes in the separation and recompression trains. Both gas and condensate are dehydrated. Condensate and gas are mixed at the outlet of the condensate treatment section and are exported in the same pipeline network. Heating is required to enhance separation of oil, gas and water, for regenerating the glycol used for dehydration, and for fractionating condensate. Gas lift and water injection are used to enhance oil recovery. A thermodynamic analysis of this platform with focus on production of an end-life oil field is presented by Nguyen et al. [69].

The gas-to-oil ratios and product flow rates for each of the studied platforms are given in Table 4.1. Volume flows are estimated at a temperature of 15 °C and a pressure of 1.013 bar. These conditions are denoted *standard* and are used as a norm by e.g. the Norwegian Petroleum Directorate. It should be noted that the choice of these conditions only impacts the values of the volume flows, and is not related to the choice of the reference conditions for the energy and exergy analyses.

Table 4.1: Gas-to-oil ratios and product flow rates for the studied oil and gas platforms. Gas-to-oil ratio is given on a standard volume basis.

	Platform A	Platform B	Platform C	Platform D
Gas-to-oil ratio, -	2800	3200	360	230
Exported oil/condensate, Sm^3/h	133	239	1105	271
Exported gas, 10^3 Sm^3/h	-	761	-	7.9
Injected gas, 10^3 Sm^3/h	369	-	363	-
Lift gas, 10^3 Sm^3/h	-	-	22	49.4
Produced water, Sm^3/h	67	12	250	1110
Injected seawater, Sm^3/h	-	-	-	890

Process details

Temperatures and pressures for key streams are given in Tables 4.2 and 4.3. The values given as range (e.g. 64–111 for Platform B, Table 4.2) mean that the reservoir fluids are extracted through different wells, which are located at different depths and are thus operated at different temperatures. The following points are essential for a better understanding of the outcome of the analysis:

- Pressure is reduced in the production manifold and the separation train. Well stream pressures, p_1, and pressures into the separation train, p_2, vary between the platforms, while pressure out of the separation train, p_3, ranges between

1.7 and 2.8 bar for all platforms, due to vapor pressure requirements for the oil/condensate export.

- Temperatures at the outlet of the production manifold, T_2, are higher for Platforms A and B than for Platforms C and D. No heating is required in order to separate the well streams of the first two platforms, while the low temperature together with the petroleum characteristics make heating necessary for the latter two. Export pipelines are subject to practical constraints such as limitations on the operating temperatures, and low temperatures at the inlets of the pumps and compressors are preferred for efficient operation. Thus, the well stream temperatures have effect on the heating demands, and also to a certain extent on the cooling demands of the platforms.

- In the export pumping section the pressure of the produced oil or condensate is increased from p_3 to p_4. The magnitude of p_4 depends on the export requirements.

- The gas treatment section differs across the platforms, depending on the conditions of the incoming gas, and the planned use of it. On Platforms A, C and D the pressure is increased from p_2 to p_5, since the produced gas is to be injected, used for gas lifting or exported at a pressure higher than p_2. On Platform B the gas is not compressed. Since the well-stream pressure is high, the operators can allow a pressure at the outlet of the production manifold higher than the pressure required for export, so p_5 is lower than p_2. For a detailed overview of the structural design of this section in each of the platforms, we refer to Figs. 4.7–4.10.

- The imported gas on Platform C is compressed from p_9 to p_5 in the gas treatment section.

- On Platform D seawater is pressurised from p_{10} to p_{11} and injected.

Since flow rates throughout the process change over the field lifetime, some parts are run at lower flow rates than the process equipment was designed for. To avoid compressor surging in this situation, gas is recycled around the compression stages, to keep a minimum flow rate through the compressor. The recycled gas is also sent through the cooler and the scrubber of the compression stage (see Figs.4.7–4.10 for the exact process set-up), to keep a low temperature and remove the liquid resulting from the cooling. Gas recycling only takes place within a given sub-system (e.g. recompression or compression). The gas recycling rates around compressor stages in the various compression sections of the four platforms are given in Table 4.4. There is anti-surge recycling in the recompression trains of all platforms, while in the gas treatment section there is recycling of the imported gas in Platform B and of the produced gas in Platform D.

Table 4.2: Pressures (bar) in key streams throughout the processes. Stream numbers refer to Fig. 4.1.

Stream number (type)	Platform A	Platform B	Platform C	Platform D
1 (reservoir fluids)	88–165	123–155	13–111	15–187
2 (reservoir fluids)	70	120	46[a], 7[b], 13[c]	7.8[d], 7.9[e], 8[c]
3 (oil/condensate)	2.8	2.4	2.7	1.7
4 (oil/condensate)	32	107	99	19
5 (treated gas)	236	118	184	179
6 (condensate)	-	-	-	179
7 (produced water)	9	61	7.2	1.3
8 (fuel gas)	18	37	39	21
9 (gas import)	-	-	110	-
10 (inlet seawater)	-	-	-	8.5
11 (injection seawater)	-	-	-	127[f], 147[g]

[a]From high pressure manifold.
[b]From low pressure manifold.
[c]From test manifold.
[d]From platform manifold.
[e]From subsea manifold.
[f]Pressure level 1.
[g]Pressure level 2.

Table 4.3: Temperatures (°C) in key streams throughout the processes. Stream numbers refer to Fig. 4.1.

Stream number (type)	Platform A	Platform B	Platform C	Platform D
1 (reservoir fluids)	80–87	64–111	51–72	49–74
2 (reservoir fluids)	74	106	62[a], 69[b], 65[c]	59[d], 64[e], 63[c]
3 (oil/condensate)	55	62	97	63
4 (oil/condensate)	50	56	76	45
5 (treated gas)	78	35	75	81
6 (condensate)	-	-	-	68
7 (produced water)	73	78	72	55
8 (fuel gas)	54	50	61	59
9 (gas import)	-	-	4.4	-
10 (inlet seawater)	-	-	-	19
11 (injection seawater)	-	-	-	57

[a]From high pressure manifold.
[b]From low pressure manifold.
[c]From test manifold.
[d]From platform manifold.
[e]From subsea manifold.

Table 4.4: Anti-surge recycle rates in the various compression sections of the studied oil and gas platforms, given as percentage (%) of the flow through the compressors.

	Platform A	Platform B	Platform C	Platform D
Recompression train	69–92	4–34	32–44	65–75
Gas treatment, produced gas	0	-	0	5–35
Gas treatment, import gas	-	-	22	-

4.2.2 Process simulation

One typical production day was simulated for each platform. The simulations were built on measured values and on values assumed or found in documentation of equipment. The measured values used for Platforms A, B and D are mean values for the simulated day, while the values for Platform C are measured at 12:00. The simulated production days were days with stable conditions, meaning that the standard deviations for the flow rates throughout the day for exported oil or condensate were either lower than 10 Sm^3/h or 3% and the standard deviation of produced gas was lower than 2% (Table 4.5). The basic data used in the simulations is available in the literature [126] for Platform A, in the supplementary information of this paper (Appendix 4.B) for Platforms B and C, and it is confidential for Platform D.

Table 4.5: Standard deviation in measured flow rates of produced oil, condensate and gas for Platforms A, B and D for the simulated days. The values given for Platform C (marked with *) are maximum deviation through the day from the value measured at 12:00.

	Platform A	Platform B	Platform C	Platform D
Exported oil, Sm^3/h	9	7	8*	2.2
Exported oil, %	7	3	0.7*	0.80
Lift-, injected or exported gas, Sm^3/h	$\leq 0.8{\cdot}10^3$	$8{\cdot}10^3$	$6{\cdot}10^3$*	$55{\cdot}10^3$
Lift-, injected or exported gas, %	≤ 0.2	1.1	1.7*	0.7

Platforms A, C and D process oil and gas, and the Peng-Robinson equation of state (EOS) [77] was selected. Platform B mainly processes gas and light liquid hydrocarbons, and the Soave-Redlich-Kwong EOS [97] was used. The process simulations of Platforms A and C were carried out with Aspen HYSYS [7] version 7.3. Platform D was simulated with Aspen Plus [6] version 7.2 using the Peng-Robinson EOS and the Non-Random Two Liquid model [81], with the exception of the glycol dehydration system that was simulated using the glycol property package of Aspen HYSYS.

The test manifold was merged together with the 1st stage separator in the simulations of Platforms A and B, while it was included as an independent separator in the simulations of Platforms C and D. Crude oil mixtures contain a large variety of chemical compounds, from hydrocarbons such as light alkanes and heavy aromat-

ics, to impurities such as nickel and vanadium. Detailed compositional analyses of these mixtures are rarely carried out, and crude oils are thus modelled as mixtures of known and unknown, named hypothetical components. Light- and medium-weight hydrocarbons are represented by known components such as light alkanes and alkenes. On the contrary, the components forming the heavy fractions of the crude oil are not modelled individually, but are lumped into the fictive groups of components. A given hypothetical component corresponds therefore to several real components, and displays the thermophysical and chemical properties of a given fraction of the crude oil. In this work, the hypothetical properties were obtained from the operators for the Platforms A, B and C, while they were derived from crude oil assays and measurements for Platform D. The numerical tolerance limits of the process models were set so that the relative deviations between in and out flows of the systems were smaller than $2{\cdot}10^{-5}$ both for mass and energy for all four platforms.

4.2.3 Exergy analysis

Exergy accounting

An exergy accounting was performed to identify the sources of thermodynamic inefficiencies in the four cases investigated. The exergy of a stream of matter is defined as the maximum theoretical work obtainable when the stream of matter interacts with the environment to reach equilibrium. This maximum theoretical work is obtained when all processes involved are reversible.Internal irreversibilities, that take place in all real processes, are responsible for exergy destruction in the oil and gas processing units. The exergy destruction can be calculated from an exergy balance [50, 13]. For an open control volume in steady-state conditions, the exergy *destruction* rate, $\dot{E}_{\mathrm{d}}$, is defined as the difference between the rates of exergy entering and leaving a system:

$$\dot{E}_{\mathrm{d}} = \dot{E}_Q + \dot{E}_W + \sum \dot{m}_{\mathrm{in}} e_{\mathrm{in}} - \sum \dot{m}_{\mathrm{out}} e_{\mathrm{out}}, \tag{4.1}$$

where $\dot{E}_W$ and $\dot{E}_Q$ are the rates of exergy accompanying work and heat entering the system. For simplicity we name these variables power and heat exergy in the rest of this study. The symbols $\dot{m}$ and e represent the mass flow rate and the specific exergy of the stream of matter. Out of the exergy streams leaving the system, some streams are not useful, and is therefore discharged to the environment. Such streams can be identified as exergy *losses*.

Exergy transfer

The exergy transported with a material stream, e, can be expressed as the sum of its kinetic, e^{kin}, potential, e^{pot}, physical, e^{ph}, and chemical components, e^{ch} [50]:

$$e = e^{\mathrm{kin}} + e^{\mathrm{pot}} + e^{\mathrm{ph}} + e^{\mathrm{ch}}. \tag{4.2}$$

The specific physical exergy accounts for differences in temperature and pressure with the ambient temperature and pressure (T_0, p_0) without changes in chemical composition. It is defined as:

$$e^{\mathrm{ph}} = (h - h_0) - T_0(s - s_0), \tag{4.3}$$

where h and s are the specific enthalpy and entropy calculated at the stream conditions and h_0 and s_0 at ambient temperature, T_0, and pressure, p_0. The specific chemical exergy accounts for differences in chemical composition with a reference environment and can be expressed as:

$$e^{\mathrm{ch}}_{\mathrm{mix}} = \underbrace{\sum_i x_i e^{\mathrm{ch}}_i}_{\mathrm{I}} + \underbrace{h_0 - \sum_i x_i h_{i,0} - T_0 \left(s_0 - \sum_i x_i s_{i,0} \right)}_{\mathrm{II}} = \underbrace{\sum_i x_i e^{\mathrm{ch}}_{i,\mathrm{mix}}}_{\mathrm{III}}, \tag{4.4}$$

where term I represents the chemical exergy of the pure components, with x_i the mass fraction and e^{ch}_i the specific chemical exergy. Term II corresponds to the decrease of chemical exergy due to mixing effects, with $h_{i,0}$ the enthalpy of pure component i at ambient conditions, and $s_{i,0}$ the corresponding entropy. Term III denotes the chemical exergy of the components in the mixture, with $e^{\mathrm{ch}}_{i,\mathrm{mix}}$ the specific chemical exergy of component i in the mixture. The specific potential and kinetic exergies are equal to the potential and kinetic energies, respectively.

Exergy transferred as work (e.g. electric or mechanical work) is equal to the amount of work:

$$\dot{E}_W = \dot{W}, \tag{4.5}$$

and exergy transferred as heat is determined by the Carnot efficiency, and is for temperatures above the ambient given by:

$$\dot{E}_Q = \left(1 - \frac{T_0}{T} \right) \dot{Q}. \tag{4.6}$$

The symbol $\dot{W}$ denotes work transfer and $\dot{Q}$ denotes transfer of thermal energy.

Calculation details

The ambient pressure and temperature used in the calculation of physical exergy were 1 atm and 8 °C, which is the average air temperature for the North Sea [73]. The chemical exergy of the pure components were taken as presented by Szargut [114] for the real chemical components. They are calculated following the method and correlations of Rivero [85] for the hypothetical components. Potential and kinetic exergy were assumed negligible in comparison with chemical and physical exergy in the present cases.

The control volume chosen for the exergy analysis on the four platforms includes the process modules shown in Fig. 4.1, with the components presented in Figs. 4.7–4.10. The exergy destruction taking place in the heaters in Platforms B and C is assigned to the separation sub-systems, as the heating demand results from the temperature requirements in that section. The following sub-systems are not considered in this work, as they are not part of the processing plant as such, or contribute only to a minor extent to the total exergy destruction of the plant.

- The seawater lift, which includes the pumps required to lift the seawater onsite and to bring it to the pressure of the cooling water distribution system;
- The cooling medium system;
- The pilot flares and flare headers, where the unusable gas, released by pressure relief valves in several parts of the plant (e.g. separation and fuel gas subsystems), is burnt off with air and rejected to the atmosphere;
- The produced water treatment, where chemicals such as biocides are mixed with produced water to ease separation with impurities;
- The gas lift, where the pressure of the gas streams is decreased to match the wellhead pressure and ease petroleum production.

In the present work, the term *exergy destruction* refers to the irreversibilities taking place within the control volume under study (*internal irreversibilities*). The term *exergy losses* refers to the irreversibilities outside this control volume, i.e. the ones taking place when waste exergy streams are dissipated to the environment.

For instance, the flare headers are considered as a part of the utility plant of an oil and gas platform. They are therefore not included in the control volume and all the chemical exergy in flared gas is counted as a loss. In the case of the coolers, the irreversibilities caused by the pressure drops on the gas and water side, as well as with heat transfer, are accounted as exergy destruction. The increase in temperature-based exergy on the cooling medium side is accounted as an exergy loss.

4.3 Results

The exergy input of the oil and gas processing plants, as well as the useful and lost exergy outputs, are given in Table 4.6. The exergy input consists of the exergy flowing with the well streams, the imported gas, and the heat and power exergies. The useful exergy output includes the exergy flowing with the export streams, gas for injection and lift, and fuel gas. The useful exergy output corresponds to 99.5%–99.8% of the exergy input. Such values are often referred to as the total exergy efficiencies. The exergy flows associated with the heat and power inputs to the processing plants are 0.05%–1.8% of the magnitude of the exported exergy flows.

The fuel gas is counted as useful output, even though it is not an exported product, because the focus of this study is the processing plants, and not the overall platforms. The fuel gas exergy represents 0.3%–8% of the exported exergy. The fuel gas is consumed to produce power for the drilling modules (where the loads vary significantly from day to day) and for the living quarter, as well as heat and power for the processing plants.

The main sources of exergy losses on the four studied platforms include the discharge of produced water, the release of flared and vented gases to the atmosphere, and the rejection of cooling water to the sea. The exact amount of exergy losses with flared and vented gases varies from day to day, as gas flaring is not practiced continuously and is subject to significant variations over days. For the days we study, the chemical exergy of the flared gases are significant at Platforms A and D, while exergy losses with produced water are significant in the cases of Platforms C and D.

The power and heat exergy, which are consumed in each subsystem for the four platforms, are presented in absolute numbers and per oil equivalent (o.e.) in Figs. 4.2 and 4.3, respectively. The unit *oil equivalent* is used by oil and gas companies as a way to present into a single measure the production of oil, gas and condensate. It is considered that 1 unit of volume of oil has roughly the same energy content as 1 unit of volume of condensate, or as 1000 units of volume of gas. The production manifolds are not included in Figs. 4.2 and 4.3, because no heat or power exergy is consumed there on any of the platforms, since the only processes taking place in the manifolds are mixing and throttling. For the remaining subsystems it is shown that:

- Power is mainly used for compression in the recompression sections, gas treatment sections and oil/condensate sections.
- On Platform D a significant amount of power is also used for increasing the seawater pressure for further injection.
- No power is required in the gas treatment section on Platform B, at the difference of the three other platforms, because the feed pressure (p_1) at

Table 4.6: Exergy flows (MW) on the studied platforms. Stream numbers refer to Fig. 4.1.

	Stream number	Platform A	Platform B	Platform C	Platform D
Input flows					
Well streams, total exergy	1	$5.8{\cdot}10^3$	$11{\cdot}10^3$	$15{\cdot}10^3$	$3.8{\cdot}10^3$
Gas import, total exergy	9	-	-	$1.8{\cdot}10^3$	-
Power exergy input	-	25	5.5	30	17
Heat exergy input[a]	-	-	0.28	6.9	1.8
Output flows, useful					
Exported oil/condensate, total exergy	4+6	$1.4{\cdot}10^3$	$2.4{\cdot}10^3$	$13{\cdot}10^3$	$2.8{\cdot}10^3$
Exported gas, total exergy	5	-	$8.6{\cdot}10^3$	-	$0.2{\cdot}10^3$
Gas injection and lift, total exergy	5	$4.3{\cdot}10^3$	-	$4.3{\cdot}10^3$	$0.8{\cdot}10^3$
Fuel gas, total exergy	8	110	30	110	90
Output flows, lost					
Produced water, chemical exergy	7	0.94	0.17	3.6	16
Produced water, physical exergy	7	0.54	0.14	2.0	6.1
Flared gas, chemical exergy	-	5.0	1.3	0	4.7
Flared gas, physical exergy	-	≤ 0.03	≤ 0.01	0	≤ 0.2
Exergy leaving with cooling medium[b]	-	3.2	4.5	1.8	0.7

[a]Both heat from the utilities and from heat integration between process streams.
[b]The temperature-based exergy received by the cooling medium.

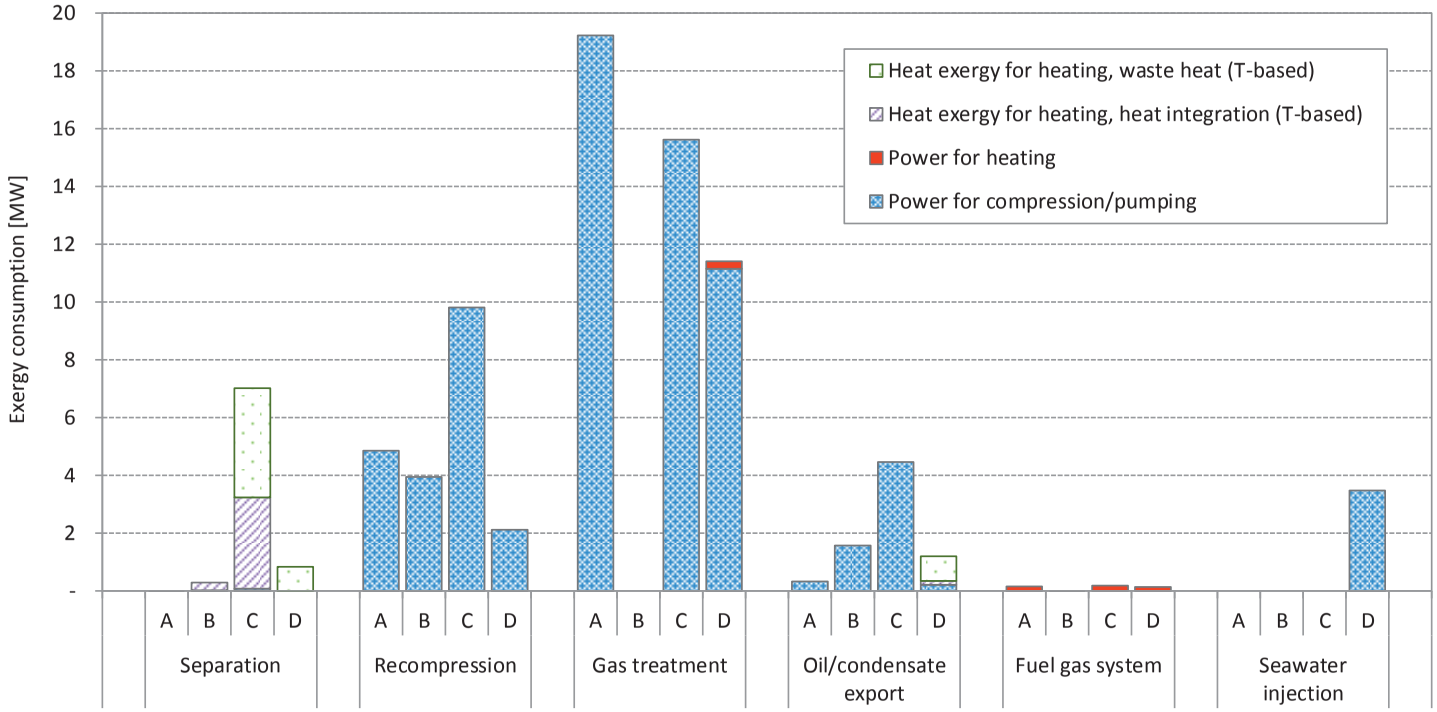

Figure 4.2: Power and heat exergy consumed in each subsystem for the studied platforms (Platforms A–D). The production manifolds are not included, since no power and heat exergy is consumed there. The thermal energy labelled 'waste heat' is from a heating medium that is heated with waste heat from the power turbines. The thermal energy labelled 'heat integration' is from heat integration with other process streams.

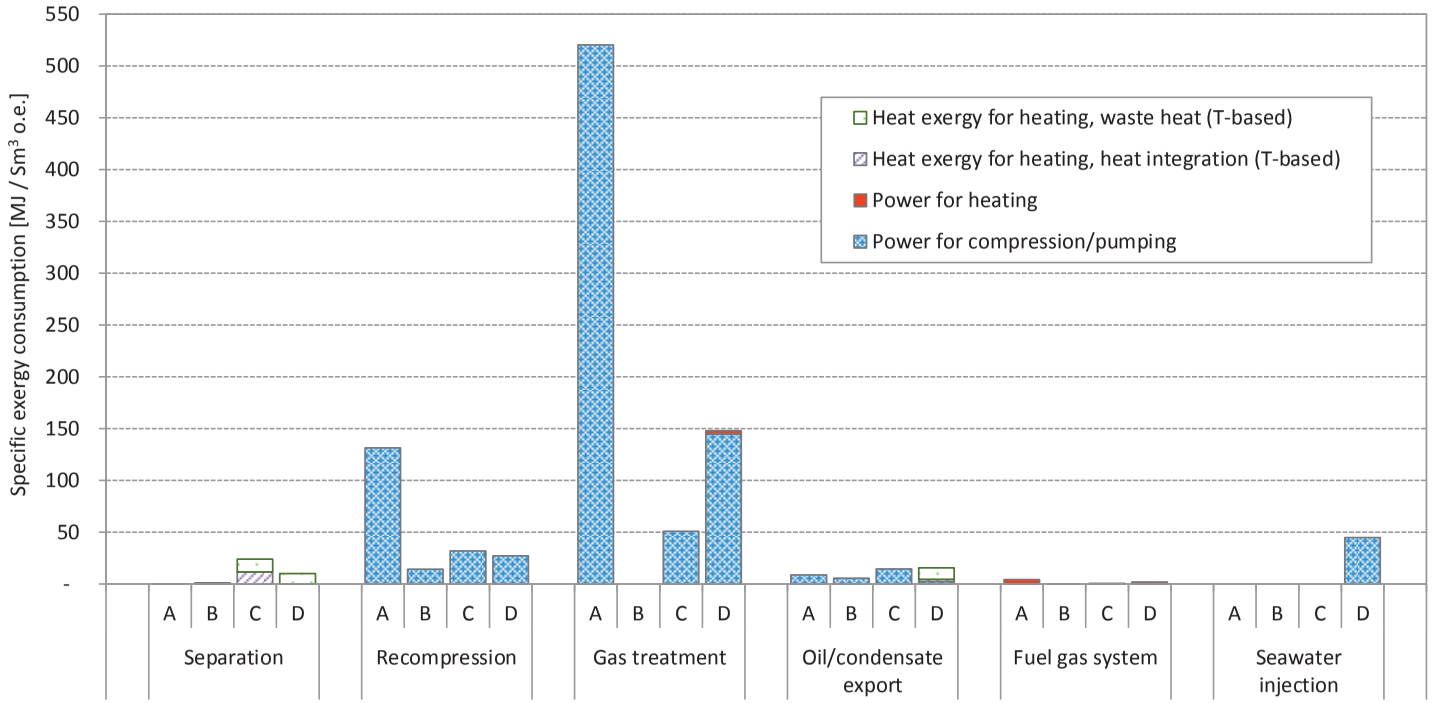

Figure 4.3: Power and heat exergy consumed per exported oil equivalent (o.e.) in each subsystem for the studied platforms (Platforms A–D). The production manifolds are not included, since no power and heat exergy is consumed there. The heat exergy labelled 'waste heat' is from a heating medium that is heated with waste heat from the power turbines. The thermal energy labelled 'heat integration' is from heat integration with other process streams.

the inlet of the separation subsystem is high enough to meet the export specifications (p_5).

- In the separation section on Platform C, approximately half of the exergy used for crude oil heating comes from heat integration with other product streams, while the other half comes from waste heat from the power turbines.
- The heating demand of the gas treatment and oil/condensate treatment sections on Platform D (in the dehydration processes) is met by recovering waste heat from the power turbines, electrical heating, and to a minor extent by heat integration.
- Power used for heating in the fuel gas systems is less than 1% of the total power consumption for each of the platforms.
- Power and heat exergy consumed per oil equivalent is highest for Platform A, followed by Platform D, while it is relatively small for Platforms B and C.
- The power exergy consumed per oil equivalent is particularly high in the gas treatment section on Platform A with 520 MJ/o.e.

In Fig. 4.4 exergy destruction in each subsystem for each of the platforms are given and in Fig. 4.5 the same values are given as percentage for each platform. In general, the highest contributions to exergy destruction are due to:

- throttling in production manifolds and separation trains;
- irreversibilities in coolers;
- inefficiencies in compressors and anti-surge recycling.

A more detailed investigation of Fig. 4.5 shows the following about the locations and sources of exergy destruction on the four platforms:

- Exergy destruction in production manifolds represents 10–24% of the total exergy destruction at the four platforms.
- Exergy destruction due to throttling in separation trains accounts for 2–12%.
- Exergy destroyed in compressors amounts to 28–40%, with the exception of Platform B where it amounts to only 13%.
- On Platform B, 33% is due to cooling in the gas treatment section.
- Exergy destruction due to pressure loss in recycled streams amounts to 4–15% for the four platforms.
- Exergy destruction in the crude oil heater makes up approximately 6% and 5% respectively for Platforms C and D.

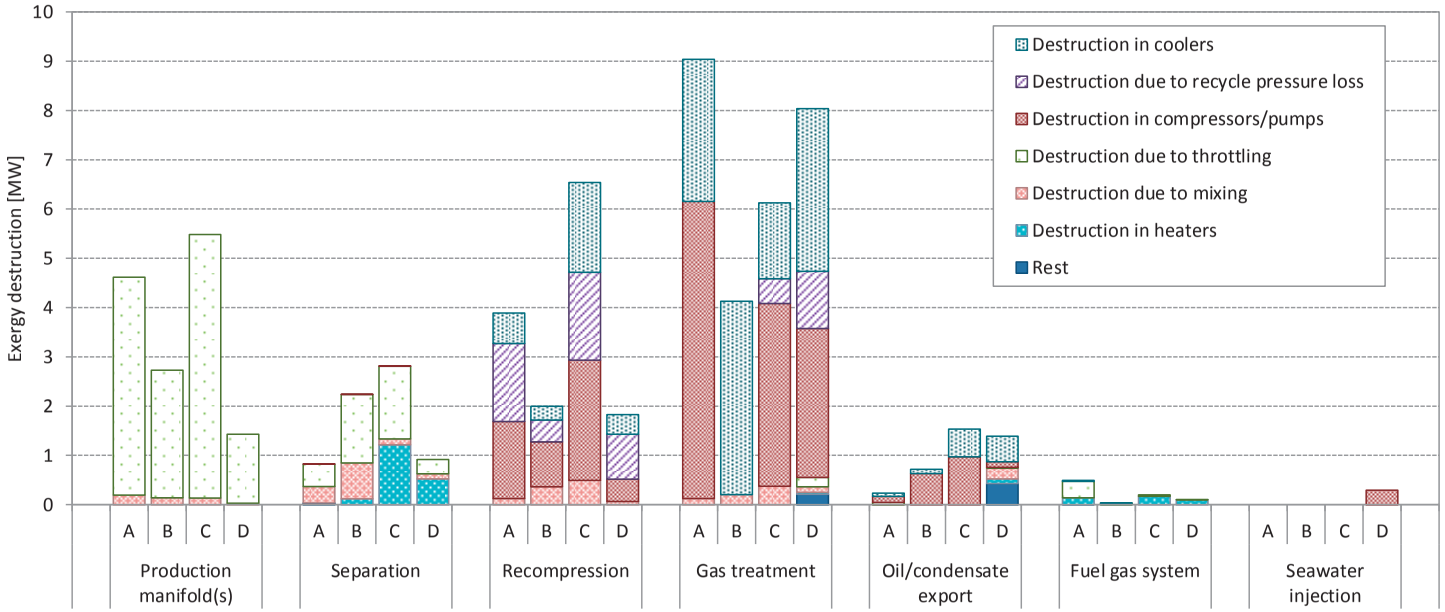

Figure 4.4: Exergy destruction in each subsystem for the studied platforms (Platforms A–D). The main sources of exergy destruction/loss in each subsystem are indicated with different colours, and smaller sources are lumped into 'rest'. The term 'rest' corresponds to minor contributions to the exergy destruction such as pressure drops in pipelines, distillation and regeneration columns.

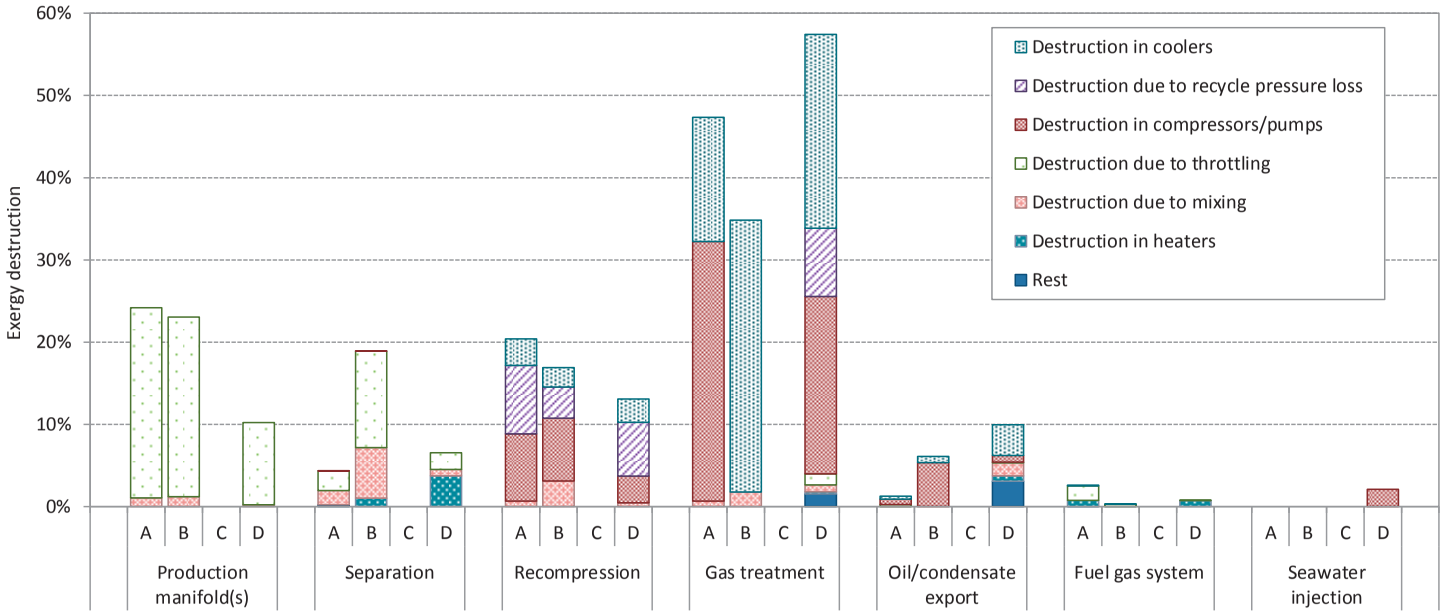

Figure 4.5: Percentage of exergy destruction in each subsystem for the studied platforms (Platforms A–D). The main sources of exergy destruction/loss in each subsystem are indicated with different colours, and smaller sources are lumped into 'rest'. The term 'rest' corresponds to minor contributions to the exergy destruction such as pressure drops in pipelines, distillation and regeneration columns.

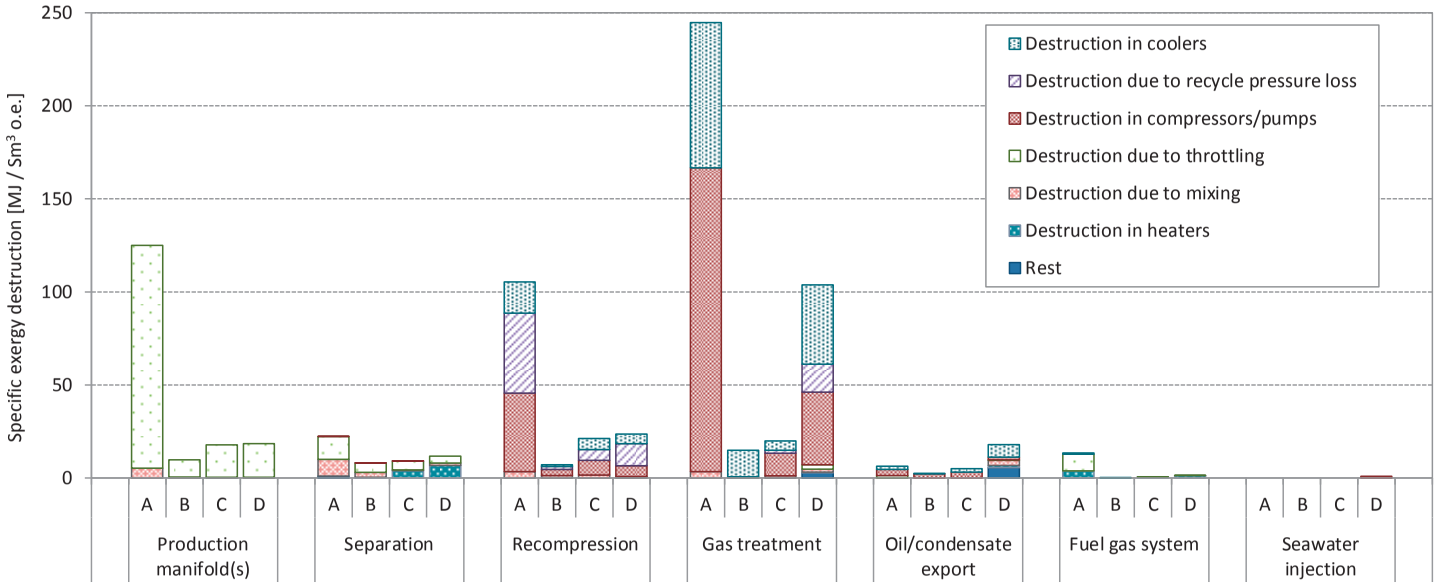

Figure 4.6: Exergy destruction per exported oil equivalent (o.e.) in each subsystem for the studied platforms (Platforms A–D). The main sources of exergy destruction/loss in each subsystem are indicated with different colours, and smaller sources are lumped into 'rest'. The term 'rest' corresponds to minor contributions to the exergy destruction such as pressure drops in pipelines, distillation and regeneration columns.

- The exergy destruction in the oil/condensate export system of Platform A accounts for 1%, while for Platforms B–D it accounts for 6–10%.
- Exergy destruction in the fuel gas, produced water handling and seawater injection systems are of minor importance compared to the other studied systems.

The exergy destroyed per exported oil equivalent in each subsystem for the four platforms are shown in Fig. 4.6. Platforms A and D have clearly more inefficiencies per oil equivalent than Platforms B and C. They are older than the other two platforms and have export flow rates that are low compared to their peak production. Platform A has a high gas-to-oil ratio (2800), injects gas and exports only oil. The injection of gas makes a high oil recovery from the reservoir possible but is responsible for considerable power consumption and exergy destruction:

- The large amount of gas that is not exported gives high exergy destruction per exported oil equivalent in the production manifold (125 MJ/o.e.).
- In the recompression train, recycling of gas to prevent compressor surging has led to almost constant flow rates, and thus exergy destruction, even if the amount of oil in the separation train has decreased.
- The high exergy destruction per exported oil equivalent in the gas treatment section (245 MJ/o.e.) is because here a significant amount of compression work is done to produce gas that is not exported but used for enhanced oil recovery.

Platform D has a low gas-to-oil ratio (230), uses gas and seawater for lift and injection, and exports oil, gas and condensate. The high exergy destruction per exported oil equivalent (178 MJ/o.e.) results from the large amount of power required to compress the gas.

4.4 Discussion

4.4.1 Accuracy

The main results of this study are estimates for heat and power exergy consumption, exergy destruction and exergy losses. The accuracy of these results, i.e. the closeness to the true values, depends on the accuracy of the simulations and on the energy and exergy calculations. The following points may affect the accuracy: (i) the variations of the process variables throughout the day, (ii) measurement uncertainties, (iii) accuracy of the equations of state, (iv) accuracy of correlations used

in calculation of chemical exergy and (v) selection of standard state for chemical exergy calculations.

There are natural variations in the feed compositions, temperatures, pressures and flow rates, which lead to variations also in other process variables throughout the system. However, steady-state conditions were assumed in the calculations. As described in Section 4.2.2, the measured values considered in the simulations for Platforms A, B and D were day-averaged, and this results in a levelling of inconsistencies due to lag effects of the system. In the case of Platform C, the measured values were taken at a specific point of time so for this platform there is a higher possibility for inconsistent data. All four platforms are simulated on days with stable conditions, and this both limits lag effects and gives small standard deviations over the day.

An overview of measurement uncertainties is given in Table 4.7. The authorities have set requirements for the uncertainties of fiscal measurements, e.g. export flow rates and fuel gas consumption. The measurement uncertainties for such variables were assumed to be equal to the limits set in the requirements. The values for the measurement uncertainties for other process variables were assumed based on guidelines set by the oil company, discussions with the operators and the authors' own experiences. In most cases, the measurement uncertainties were larger than the standard deviations of the variables over the day, so the latter were therefore not taken into consideration in this study.

The Peng-Robinson [77] and the Soave-Redlich-Kwong [97] equations of state (EOS) were used to calculate the enthalpies and entropies of each stream. Both were conceived to estimate the vapour-liquid equilibrium properties and fugacities of hydrocarbon mixtures, and they are widely used for modelling petroleum processes. The Soave-Redlich-Kwong EOS was initially designed to describe the behaviour of small and non-polar molecules in vapour phase, making it particularly suitable for modelling gas processes. However, it was inaccurate for calculations of hydrocarbon properties in liquid phase. This was improved in the Peng-Robinson EOS [123, 98]. The Soave-Redlich-Kwong EOS was chosen for the simulations of Platform C, which mostly processes gas, and the Peng-Robinson EOS for the simulations of Platforms A, B and D.

For the calculation of heat and power exergy consumption and exergy losses, uncertainty originating from measurements and from the equation of state are most relevant. A detailed analysis of the impact of these points were performed for Platform A [126]. Uncertainty originating from the equation of state was evaluated by comparing values obtained for methane from the equation of state used in the simulation, with values obtained from a presumably more accurate equation of state. The total uncertainties originating from these two error sources were lower than 10% for the power consumption and exergy destruction in the production manifolds, recompression and gas treatment sections. The uncertainties for the separation and export sections were higher (Table 4.8). For all four platforms, the processes are similar, the measurements are of the same type, and the same

or similar equations of state were used as for Platform A. These points suggest that the uncertainties of the calculated heat and power consumption and exergy destruction for Platforms B–D are of the same magnitude as for Platform A.

Table 4.7: Measurement uncertainty assumed at 95% confidence level for process variables.

Process variable	Uncertainty
Pressure	1.0%
Temperature	1.0 °C
Electric power	2%
Oil/condensate export flow rate	0.3%
Gas export flow rate	1.0%
Fuel gas flow rate	1.8%
Flare gas flow rate	5%
Other flow rates	10%

Table 4.8: Uncertainty of total power consumption and total exergy destruction for Platform A [126], expressed in %.

	Power	Exergy destruction
Production manifold	-	9
Separation	15	25
Export section	47	40[a]
Recompression	0.6	5
Gas treatment	1	5
Fuel gas system	1	1

[a]Misprint in [126]. For exergy destruction in export section, the uncertainty should be 100 kW.

The method of Rivero [85] was used to calculate the chemical exergy of hypothetical components, based on the lower heating value and on the elemental composition of each crude oil fraction. Szargut presented a similar expression, which takes fewer elements into account and this equation is claimed to have a mean accuracy of 0.5% [114]. The petroleum correlations used to estimate the lower heating value have an accuracy of 1% [102]. The correlations are based on the elemental composition and the specific gravity of each crude oil fraction, and these properties are not exactly known. Petroleum assays for blends containing the specific crude oils were used instead, and this gives additional error to the exergy of the hypothetical components.

The reference environment of Szargut [114] was used in this study. It is worth noticing that the model of Kotas [50], which is based on a previous model of Szargut, predicts a standard chemical exergy three times larger for water, but displays similar values for hydrocarbon compounds. However, the model of Kotas has a reference atmosphere with a relative humidity of 28%, while the relative humidity is 70% in the model of Szargut. Since the platforms are located offshore, the model of Szargut is considered to be most realistic.

The accuracy of the calculated exergy of waste streams (exergy losses), as well as the exergy of feed and export streams, do mainly depend on the calculation of chemical exergy of the hypothetical components, and on the uncertainty of the exported flow rates. The exergy losses associated with produced water does in addition have a strong dependency on the choice of reference environment.

4.4.2 Suggestion of process improvements

The four platforms compared within this study are of the North Sea platform type. They illustrate the diversity among these facilities, with production of heavy and viscous oil to condensate and gas, and with different product specifications, reservoir conditions, and operating strategies. The mapping of the thermodynamic irreversibilities shows where exergy is destroyed in the system and hints therefore to process route improvements.

Production manifold

Significant quantities of exergy are destroyed in the production manifold in any case. It is therefore expected that most North Sea platforms present this behaviour, and this is supported by the findings of the generic analysis conducted by Nguyen et al. [71]. The two platforms where this exergy destruction is the lowest (Platforms B and D) are characterised by a small difference between the inlet pressures of the choke valves and of the 1st stage separators. The first one has the highest gas-to-oil ratio (3200), and condensate-gas separation can be started at a relatively high pressure (120 bar). On the opposite, the second one has the lowest gas-to-oil ratio (230), but the highest water production (1110 Sm^3/h). It is run at the end-life of the production field, and the pressure at the inlet of the production manifold has therefore decreased.

A first possibility for improving these systems is to design the production manifolds at several pressure levels, as done on some platforms. Gas can be recovered at higher pressures, meaning that a smaller amount of exergy is destroyed by throttling, and lower compression power is required. It would also limit mixing of well-streams with different compositions, and ease phase separation. As the reservoir pressure decreases with time, inflowing streams can be rerouted to another manifold when their pressure becomes lower. However, the selection of the number of manifolds, and of the pressure levels, is a compromise between the supplementary equipment cost (capital cost), the operating costs (smaller power demand and larger gas export) and the oil production (smaller liquid production).

Other possibilities are to integrate multiphase expanders, which would reduce the exergy destruction taking place in the expansion process and generate additional power, or multiphase ejectors that can use exergy in high pressure wells to increase production in depleted ones. However, the design of such equipment is

a challenging task because the well-streams contain sand, hydrogen sulphides and other impurities, and this could cause corrosion and reduce the lifetime of these components.

The overall benefits of measures on production manifolds are linked to the development of the feed composition over time. High pressure gas contains more pressure-based exergy than high pressure liquid.

Gas treatment

The present comparison suggests that the gas treatment process often is the major exergy-destroying sub-system. It results from combined effects of the inefficiencies of the turbomachinery components, and of the temperature gap between the cooling water and hot gas streams. These trends were observed for all platforms where there was a need for gas compression, both with and without anti-surge recycling. This illustrates that designing and operating a highly efficient gas compression process is critical for reaching a high performance of the overall processing plant. However, it is challenging to maintain a high performance because the gas flow rates decrease with time, resulting in compressors run in off-design conditions. Svalheim [109, 110] and Bothamley [14] proposed various measures, such as re-wheeling the compressors when large amounts of gas must be recycled to prevent surge. The integration of several but parallel trains would also result in higher energy savings, since varying flow rates can be handled by closing or opening parallel trains, and the compressors will be run for a longer period near their nominal point.

The exergy destruction taking place in the coolers placed before the compressors is partly caused by the anti-surge recycling, as larger gas flow rates need to be cooled before being recompressed. Smaller amounts of exergy may be destroyed with a better match of the water and gas flow rates and temperatures. The exergy discharged from the gas streams may be recovered, although it may be difficult to recover heat at these temperature levels (30 to 150 °C). Further integration with the heating systems present on the facilities may be investigated.

Process–utility integration

The interactions between the utility system and the processing plant should be investigated in further details. A comparison with the Brazilian platform investigated by Oliveira and Van Hombeeck [22] shows the differences across platforms located in different oil regions. On the four North Sea platforms studied in this work, the heating demand was limited, and waste heat from the exhaust gases was enough to cover it. The gas turbines were designed to provide the required electrical power, but a large amount of excess heat is discharged into the environment, as it is recovered only to a moderate extent. On the opposite, on the Brazilian platform, the oil separation process has a significant heating demand, and recovering waste heat

from the gas turbines was not sufficient. A furnace was therefore complementing the heat recovery system.

The heating demand depends, among other factors, on (i) the initial feed temperature, which is lower in the Brazilian Gulf than in the North Sea, (ii) the viscosity of the crude oil (iii) the content of medium-weight hydrocarbons, which is much higher for the oil extracted on Platform D than conventional light oil, (iv) the integration of processes such as CO_2-capture by chemical absorption, glycol dehydration and condensate fractionation. These energy efficiency measures are discussed in the works of Kloster [46, 47] and of Nguyen et al. [71]. Replacing conventional combustion technologies to combined cycles may be one of the most significant measures for improving the efficiency of oil and gas platforms. Cogeneration technologies together with a high level of process integration, may be relevant for platforms with a high heat demand. The integration of bottoming cycles would improve the efficiency of the complete system, at the expense of higher capital costs due to higher space requirements. Such solutions are already in use on other North Sea installations [4].

Flaring, cooling water and produced water

Losses with flaring vary from day to day, but for some platforms the total amount of exergy dissipated with these gas losses can be significant throughout the year. Such losses can be reduced with the use of gas recovery systems, as already done on Platform C.

Little can be done to recover exergy from the produced and cooling water flows, since their chemical exergy is hardly usable, and their temperature is relatively low (50–75 °C). Kloster [46] suggested to use the produced water extracted along with oil and gas instead of treated seawater or to re-use the cooling water for enhanced oil recovery water injection, as done on some platforms, to reduce the pumping and water demands. However, the hydrocarbon content of the wastewater may be problematic, as it could cause plugging, and re-using the produced water for injection is only possible for platforms operated on fields with a high water-to-oil ratio.

4.4.3 Significance and limitations

We have mapped the exergy destruction and losses in the oil and gas processing plants of four oil and gas platforms. The present findings are in accordance with the results of Svalheim and King [110], who stated that the gas compression step is the most energy-demanding steps. They can also be compared to the previous findings of Bothamley [14] who focused on the variety of offshore processing options in different oil regions. The findings of this paper may be used for estimating qualitatively the locations and extents of thermodynamic irreversibilities on North

Sea oil and gas platforms, although caution should be exercised when other design setups are considered, or if the compositions of the well-streams differ strongly.

Moreover, the four platforms present significant differences among each other: the well-fluid composition differs from one facility to another, different products are exported and gas is sometimes used for lift or injection, and processes such as condensate treatment and gas dehydration are not always installed. A direct comparison is therefore made difficult. However, it should be noted that, although significant differences can be found between the four platforms, general trends can be observed. Significant exergy destruction takes place in the compressors and coolers in any case, and the gas recirculation to prevent surge has a significant impact for platforms with decreasing oil and gas production. The results depend on factors such as (i) the efficiency and the control strategies of the turbo-machinery components (ii) the integration of additional subsystems and (iii) the outlet specifications of the processing plant.

The integration of gas dehydration has little impact on the total exergy destruction of the platform. The irreversibilities taking place in the glycol absorber and in the regenerator are small in comparison to the ones taking place in the compressors and coolers, because of the small flow rate of tri-ethylene glycol. The integration of an additional condensate treatment section results in a smaller power consumption, compared to the case where no separate section is integrated [53].

Finally, the differences between the platforms analysed in this study and the Brazilian case shows that caution should be exercised when extending the present conclusions to platforms in other regions of the world. This suggests that each oil platform should be assessed individually, to pinpoint major sources of exergy destruction on that specific facility.

4.5 Conclusion

Exergy analyses were performed on the oil and gas processing plants on four North Sea oil and gas platforms, which differ by their operating conditions and strategies. The comparison of the sources to exergy destruction and exergy losses illustrated the large exergy destruction associated with the gas treatment and production manifold systems, ranging above 27% and 10%, respectively. The fuel gas and seawater injection processes represent less than 3% each in every case. For two of the platforms the exergy losses due to flaring were significant.

However, the contributions of the recompression, separation and oil export sections vary across the different platforms. Although the precise values of the exergy destruction rates differ from one platform to another, the results indicate that the largest rooms for improvement lie in (i) gas compression systems, (ii) production manifolds, and (iii) flared gas recovery.

Nomenclature

e	specific exergy, J/kg
h	specific enthalpy, J/kg
$\dot{m}$	mass flow rate, kg/s
p	pressure, Pa
s	specific entropy, J/kgK
x	mass fraction, -
$\dot{E}$	exergy rate, W
Q	thermal energy, kJ
T	temperature, K
W	work, kJ

Abbreviations

EOS	Equation of state

Superscripts

ch	chemical
kin	kinetic
mix	mixture
ph	physical
pot	potential
Q	thermal energy
W	work

Subscripts

d	destruction
i	component
in	inlet
l	loss
out	outlet
0	dead state

Acknowledgements

The motivation from Statoil's new-idea project of reducing CO_2 emissions from offshore oil and gas platforms is essential to this study. The Faculty of Natural Sciences and Technology at the Norwegian University of Science and Technology is acknowledged for financial support, as well as the funding from the Norwegian Research Council through the Petromaks programme, within the project 2034/E30 led by Teknova.

4.A Process Flowsheets

The process flowsheets of each of the platforms are shown in Figs. 4.7 – 4.10.

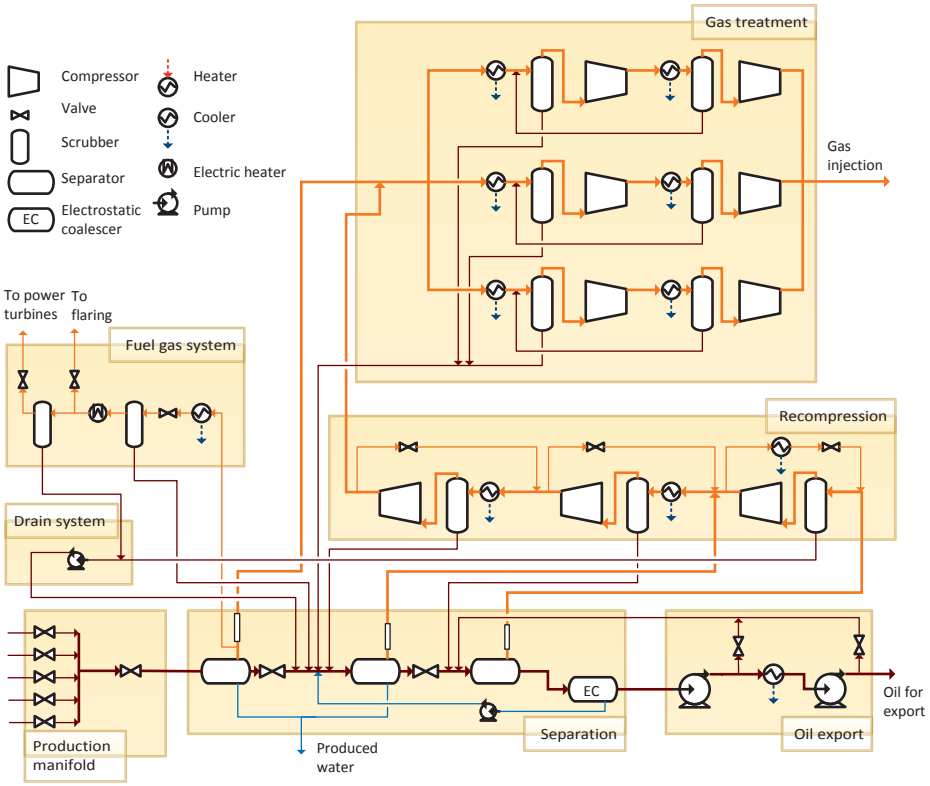

Figure 4.7: Process flow diagram of the processing plant of Platform A. Gas streams are shown with orange arrows, water streams with blue arrows, and oil, condensate and mixed streams are shown with brown arrows.

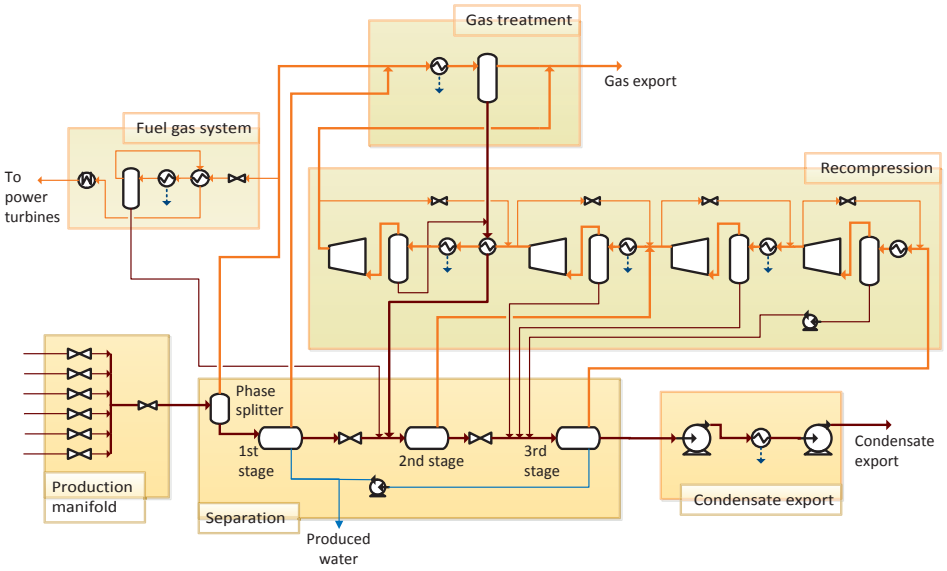

Figure 4.8: Process flow diagram of the processing plant of Platform B. Gas streams are shown with orange arrows, water streams with blue arrows, and oil, condensate and mixed streams are shown with brown arrows. Symbol explanations can be found in Fig. 4.7

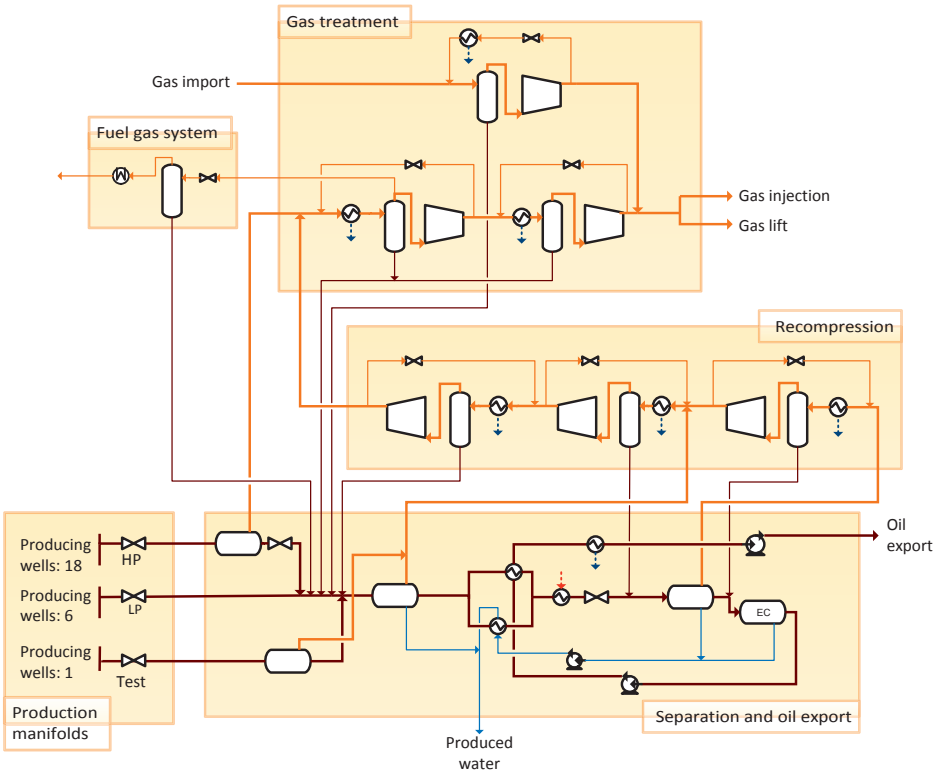

Figure 4.9: Process flow diagram of the processing plant of Platform C. Gas streams are shown with orange arrows, water streams with blue arrows, and oil, condensate and mixed streams are shown with brown arrows. Symbol explanations can be found in Fig. 4.7

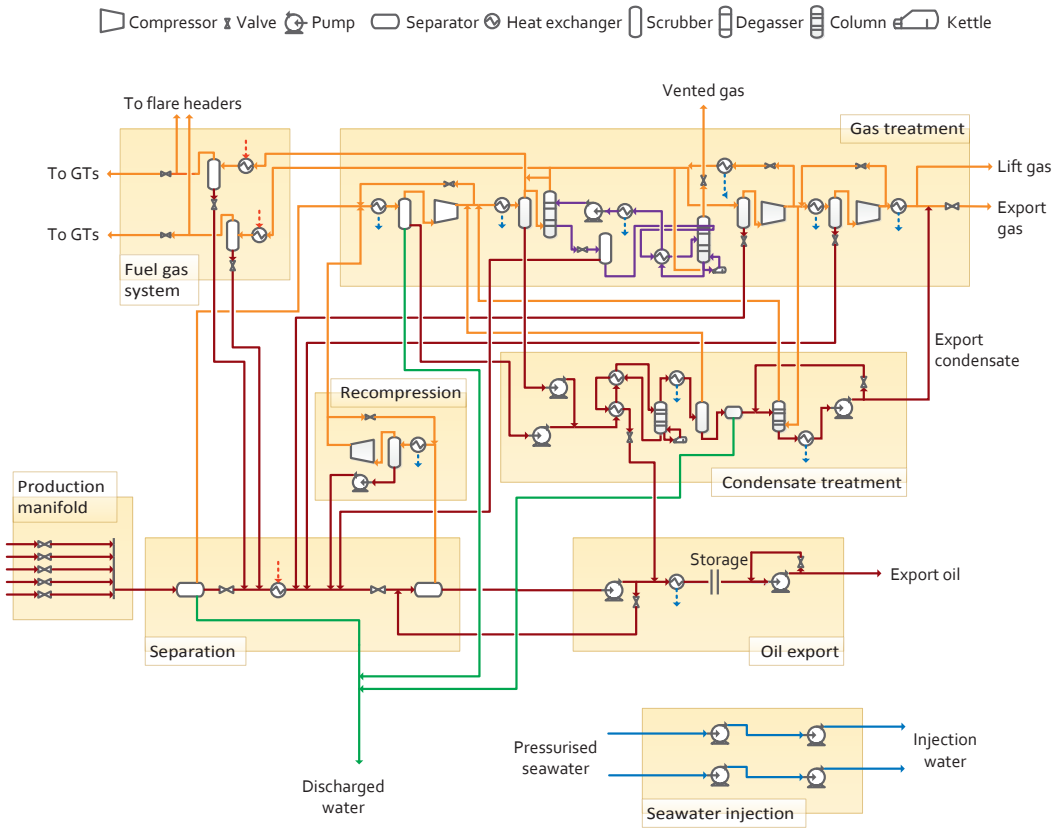

Figure 4.10: Process flow diagram of the processing plant of Platform D. Gas streams are shown with orange arrows, water streams with blue arrows, glycol is shown with purple arrows, and oil, condensate and mixed streams are shown with brown arrows.

4.B Supplementary information: Process modelling

4.B.1 Platform A

All details on process data, except for the cooling water system, for Platform A can be found in Ref [126]. The process flowsheet is given in Fig. 4.7 in Appendix 4.A. Details for the cooling water system are found in Table 4.9.

Table 4.9: Pressure, p, pressure drop, ΔP, temperatures, T, and mass fractions, x, from the oil company's documentation of the cooling system set in the simulation of the cooling water system of Platform A.

Process unit	Variable	Value
Cooling medium to coolers	p, bar	7.8
Pressure drop on cold side in coolers	Δp, bar	0.5
Cooling medium to coolers	T, °C	17
Cooling medium from all coolers mixed	T, °C	37.7
Cooling medium, TEG weight fraction	x_{TEG}, -	0.3
Cooling medium, water weight fraction	x_{water}, -	0.7
Seawater to export cooler	T, °C	8.0

4.B.2 Platform B

The process at Platform B was simulated for a real production day with stable and typical process conditions. The process flowsheet of Platform B is given in Fig. 4.8 in Appendix 4.A.

Composition data was available for (i) the reservoir fluids at the start of the field lifetime and (ii) the export gas from a few months before the simulated production day. To simulate the well streams, the composition of the reservoir fluids was used, but to get the correct water-to-oil ratio, water was mixed in, while to get the correct gas-to-oil ratio, gas with the composition of the export gas was removed. The compositions of the three fluids used to simulate the well streams are given in Table 4.10. Hypothetical components (developed by the oil company) were used to describe the heavy fractions of the reservoir fluids, and the properties set for these hypothetical components are given in Table 4.11. Calculated flow rates of the gas, condensate and water phases in each well stream are given in Table 4.12. Calculated flow rates are flow rates for each phase in the three-phase well streams estimated by the oil company. Measured flow rates of exported gas, exported condensate and produced water are given in Table 4.13. The well stream flow rates of each phase were set such that the flow rates of the simulated product streams of the process fitted with the measured product streams in Table 4.13 after all other input data in the simulation was set. The more uncertain calculated flow rates of the well

streams in Table 4.12 were used to set the ratio of flow from the different wells for each of the phases.

Table 4.10: Composition of fluids used for simulation of feed streams of Platform B. The composition of gas is a measured composition of the exported gas a few months before the simulated production day. The composition of reservoir fluids is the composition of the reservoir at start the start of the field lifetime.

Component	Gas	Reservoir fluids	Water
Nitrogen	$1.89{\cdot}10^{-3}$	$1.80{\cdot}10^{-3}$	0
CO_2	$3.78{\cdot}10^{-2}$	$3.53{\cdot}10^{-2}$	0
Water	0	0	1
Methane	0.831	0.801	0
Ethane	$6.98{\cdot}10^{-2}$	$7.00{\cdot}10^{-2}$	0
Propane	$3.02{\cdot}10^{-2}$	$3.09{\cdot}10^{-2}$	0
i-Butane	$4.56{\cdot}10^{-3}$	$4.80{\cdot}10^{-3}$	0
n-Butane	$9.04{\cdot}10^{-3}$	$1.01{\cdot}10^{-2}$	0
i-Pentane	$2.71{\cdot}10^{-3}$	$3.50{\cdot}10^{-3}$	0
n-Pentane	$2.91{\cdot}10^{-3}$	$4.00{\cdot}10^{-3}$	0
HypoB-1	$1.03{\cdot}10^{-2}$	$5.10{\cdot}10^{-3}$	0
HypoB-2	0	$7.90{\cdot}10^{-3}$	0
HypoB-3	0	$8.50{\cdot}10^{-3}$	0
HypoB-4	0	$4.90{\cdot}10^{-3}$	0
HypoB-5	0	$4.50{\cdot}10^{-3}$	0
HypoB-6	0	$3.10{\cdot}10^{-3}$	0
HypoB-7	0	$2.00{\cdot}10^{-3}$	0
HypoB-8	0	$1.20{\cdot}10^{-3}$	0
HypoB-9	0	$8.00{\cdot}10^{-4}$	0
HypoB-10	0	$6.00{\cdot}10^{-4}$	0
HypoB-11	0	$3.00{\cdot}10^{-4}$	0
HypoB-12	0	$1.00{\cdot}10^{-4}$	0

Measured temperatures, pressures and flow rates set within the process are given in Table 4.14, while values set based on assumptions and information from documentation of the equipment are given in Table 4.15. The following simplifications were done in the simulation:

- In the real process there is an additional test separator in the 1st separation stage. This separator was merged into the main 1st stage separator.
- All identical parallel coolers, pumps and scrubbers were merged into one.
- The individual delivery and return temperatures of the cooling medium from each of the coolers was set to the measured delivery temperature and the temperature of the mixed cooling medium from all coolers (Table 4.14), unless this gave a temperature difference betweem inlet gas and outlet cooling medium lower than 10 °C. In the latter case the temperature was set to give a difference of 10 °C.

Table 4.11: Molecular weight, M, normal boiling point, T_b, ideal liquid density, $\rho_{id.liq.}$, critical temperature, T_c, critical pressure, p_c, critical volume, V_c, and acentric factor, ω, for the hypothetical components used to describe the heavy oil fractions of Platform B.

Component	M, g/mol	T_b, °C	$\rho_{id.liq.}$, kg/m^3	T_c, °C	p_c, bar	V_c, m^3/kmol	ω, -
HypoB-1	85.65	68.75	664.5	234.2	29.69	0.37	0.296
HypoB-2	91.13	91.95	741	255	34.49	0.3938	0.454
HypoB-3	104.3	116.7	765.5	279.3	30.35	0.4153	0.492
HypoB-4	118.9	142.2	778	302.2	26.38	0.4571	0.534
HypoB-5	140.1	176.3	790.7	331.6	22.35	0.5269	0.594
HypoB-6	167.5	217.6	805.5	365.2	19.12	0.6203	0.669
HypoB-7	197.5	255.9	818	397.8	16.87	0.7285	0.747
HypoB-8	229	291.1	828.9	429	15.3	0.8467	0.825
HypoB-9	256.6	318.6	838.6	454.5	14.38	0.952	0.89
HypoB-10	289	349.8	849.1	483	13.61	1.081	0.963
HypoB-11	336	390.1	861.8	521.5	12.81	1.271	1.059
HypoB-12	403.6	439	876.9	573.2	12.09	1.555	1.177

Table 4.12: Calculated flow rates of the gas (10^3 Sm^3/h), oil (Sm^3/h) and water (Sm^3/h) phases in each well stream entering the production manifold at Platform B. These flow rates are estimated by the oil company, based on measurements, and they have a high uncertainty.

Well	Gas	Condensate	Water
5	153.9	73.61	1.72
6	88	41.9	0.76
11	136	65.1	1.53
12	10.6	5.09	0.11
13	42.1	22.64	0.37
14	180.3	85.94	1.85

Table 4.13: Measured flow rates, F, in process steams leaving Platform B.

Produced fluid	Variable	Value
Exported condensate	F, Sm^3/h	238.9
Exported gas	F, 10^3 Sm^3/h	761
Produced water	F, m^3/h	12.6

- The gas fraction in the oil from the phase splitter was modified by splitting a part of the gas outlet stream and adding it to the oil stream.
- Pressure drops in tubes and separators and heat losses from tubes were neglected. Pressure drops in heat exchangers, where this was not a function of measured pressures (Table 4.14) were set to 1.0 bar.

Measured process variables are compared with simulated process variables in Table 4.16. The following points can be noted:

- The simulated temperature of the 1st stage separator is within the uncertainty of 1°C (Table 4.7) of the measured value, while the simulated temperatures of the 2nd and 3rd stage separators deviated with 7.5 and 5.1 °C from the measured temperatures. These temperatures are strongly dependent on the amount of condensate from the wet gas scrubber, and given that the temperature measurements are correct, the reason for the deviation is assumed to be too high condensate flow from the wet gas scrubber, which indicate that the feed composition is not correct. Decreasing the flow rate of condensate with 2/5 gives the measured temperatures in the separators. Decreasing the liquid flow rate at the outlet of the wet gas cooler with 2/5 gave less than 1% change in the exergy destruction in this unit, while changing the temperatures in the separators to the measured ones, resulted in increased exergy destruction in the coolers in the recompression train with 20% and decreased exergy destruction the compressors in the recompression train with 3.6%. Other changes were less than 1%.
- All simulated flow rates were within the uncertainty of 10% (Table 4.7) of the measured values.
- Simulated pressure of water and oil entering the water and 1st oil pumps, are 2.4 bar, while the measured values are 3.75 and 3.86 bar, respectively. These deviations are found because height differences are not taken into consideration in the simulation. As discussed for Platform A [126], this has little impact on the overall results.

Table 4.14: Measured values for pressure, p, temperature, T, and flow rate, F, set in the simulated process flowsheet of Platform B.

Process stream	Variable	Value	Process stream	Variable	Value
Production manifold			*Recompression*		
Well 5, valve, in	p, bar	131.2	1st compressor, in	p, bar	2.26
Well 6, valve, in	p, bar	155.2	1st compressor, out	p, bar	9.35
Well 11, valve, in	p, bar	127.4	2nd compressor, in	p, bar	8.90
Well 12, valve, in	p, bar	123.2	2nd compressor, out	p, bar	27.88
Well 13, valve, in	p, bar	124.4	3rd compressor, in	p, bar	27.15
Well 14, valve, in	p, bar	145.9	3rd compressor, out	p, bar	62.87
Well 5, valve, out	p, bar	122	4th compressor, in	p, bar	61.87
Well 6, valve, out	p, bar	121.3	4th compressor, out	p, bar	118.4
Well 11, valve, out	p, bar	122.4	Condensate pump, out	p, bar	5.7
Well 12, valve, out	p, bar	121.1	1st cooler, out	T, °C	29.4
Well 13, valve, out	p, bar	121.7	1st compressor, out	T, °C	101.3
Well 14, valve, out	p, bar	121.6	2nd cooler, out	T, °C	31.6
Well 5, valve, in	T, °C	109.6	2nd compressor, out	T, °C	115.1
Well 6, valve, in	T, °C	107	3rd cooler, out	T, °C	30.0[a]
Well 11, valve, in	T, °C	110.1	3rd compressor, out	T, °C	95.5
Well 12, valve, in	T, °C	63.9	4th cooler, out	T, °C	35.0[a]
Well 13, valve, in	T, °C	101	4th compressor, out	T, °C	88.4
Well 14, valve, in	T, °C	110.5	1st compressor, in	F, m^3/h	7200
Separation			2nd compressor, in	F, m^3/h	1200
1st separator	p, bar	119.6	3rd compressor, in	F, m^3/h	1410
2nd separator	p, bar	27.8	4th compressor, in	F, m^3/h	650
3rd separator	p, bar	2.4	*Flare system*		
Phase splitter, gas out	F, Sm^3/h	74,000	To flare	F, m^3/h	94.3
Water pump, out	p, bar	61.06	*Condensate export*		
Fuel gas system			2nd pump, in	p, bar	18.78
After inlet valve	p, bar	39	2nd pump, out	p, bar	106.7
Fuel gas cooler, out	T, °C	29.8	Condensate cooler, out	T, °C	49.4
Fuel gas heater, out	T, °C	49.8	2nd pump, out	T, °C	56.4
To power turbines	F, Sm^3/h	2300	*Cooling system*		
Gas treatment			Cooling medium, delivery	p, bar	12.9
Wet gas scrubber	p, bar	118.2	Cooling medium, delivery	T, °C	24.5
Wet gas cooler, out	T, °C	32	Cooling medium, return[b]	T, °C	55

[a]Set point for cooler.
[b]Mixed return cooling medium from all coolers.

Table 4.15: Values for efficiency, η, overall heat transfer coefficient, U, heat transfer surface area, A, temperature, T, Pressure, p, mass fraction, x, and electric work, W_{el}, assumed or from documentation from process equipment for Platform B.

Process unit	Variable	Value	Source
Separation			
Water pump	η, %	75	Assumed
Recompression			
Cross heat exchanger	Overall UA, kJ/°C-h	580,000	Assumed, operators
Condensate export			
1st pump	η, %	55	Pump performance curves
Cooling system			
Cooling medium	x_{MEG}, -	0.35	Documentation of cooling system
Cooling medium	x_{water}, -	0.65	Documentation of cooling system
Fuel gas system			
Fuel gas heater	W_{el}, kW	0	Assumed, system description

Table 4.16: Measured values for temperature, T, Pressure, p, and flow, F, compared with simulated values for Platform B.

Process stream	Variable	Measured value	Simulated value
Separation			
1st separator	T, °C	105.5	105.8
2nd separator	T, °C	86.9	79.4
3rd separator	T, °C	67.3	62.2
1st separator, water out	F, m^3/h	4.8	4.3
3rd separator, water out	F, m^3/h	7.8	8.3
Water pump, in	p, bar	3.75	2.4
Gas treatment			
Wet gas scrubber, out	F, 10^3 Sm^3/h	690	720
Condensate export			
1st pump, in	p, bar	3.86	2.4
1st pump, out	F, m^3/h	250	250
2nd pump, out	F, m^3/h	250	250

4.B.3 Platform C

The process at Platform C was simulated for a real production day with stable conditions, and the measured data given for this process is measured at 12.00 for this day. The day was a typical day with the exception that the produced water injection system was not in operation, so the water was discharged to the sea. The process flowsheet of Platform C is given in Fig. 4.9 in Appendix 4.A.

Composition data was available for (i) the reservoir fluids at the start of the field lifetime and (ii) typical composition of the imported gas (which is injected into the reservoir for pressure maintenance). These two fluids plus water was mixed to produce well streams giving realistic water-to-oil and gas-to-oil ratios. The compositions of these three fluids are given in Table 4.17. Properties of hypothetical components (developed by the oil company) used to describe the heavy fractions are given in Table 4.18. Calculated flow rates for each well stream are given in Table 4.19. Calculated flow rates are flow rates for each phase in the three-phase well streams estimated by the oil company. Measured flow rates for product streams are given in Table 4.20. The oil and gas flow rates in each well were set to make the simulated product streams fit with the measured product streams (Table 4.20) after all other input data in the simulation was set. The more uncertain calculated flow rates in the well streams (Table 4.19) were used to set the ratio of gas flow rates from each well and the ratio of oil flow rate from each well. Since the produced water was discharged to the sea, and not injected as usual, the flow rate of the produced water was not measured. The water flow rates in each well was therefore set equal to the calculated flow rate (Table 4.19).

Measured temperatures, pressures and flow rates set in the simulation are given in Tables 4.21 and 4.22, while values set based on assumptions and information

Table 4.17: Composition of fluids (molar fraction) used for simulation of feed streams of Platform C. The composition of 'gas' is the typical composition of the imported gas. The composition of 'reservoir fluids' is the composition of the reservoir at start the start of the field lifetime.

Component	Gas	Reservoir fluids	Water
Nitrogen	$8.2{\cdot}10^{-3}$	$2.7{\cdot}10^{-3}$	0
CO_2	$1.4{\cdot}10^{-2}$	$6.0{\cdot}10^{-4}$	0
Water	$1.0{\cdot}10^{-6}$	0	1
Methane	$8.6{\cdot}10^{-1}$	$1.6{\cdot}10^{-1}$	0
Ethane	$7.8{\cdot}10^{-2}$	$1.1{\cdot}10^{-2}$	0
Propane	$3.1{\cdot}10^{-2}$	$2.8{\cdot}10^{-3}$	0
i-Butane	$2.6{\cdot}10^{-3}$	$5.8{\cdot}10^{-3}$	0
n-Butane	$4.0{\cdot}10^{-3}$	$1.6{\cdot}10^{-3}$	0
i-Pentane	$4.7{\cdot}10^{-4}$	$3.7{\cdot}10^{-3}$	0
n-Pentane	$4.3{\cdot}10^{-4}$	$1.0{\cdot}10^{-3}$	0
HypoA-1	$2.4{\cdot}10^{-4}$	0	0
HypoC-1	0	$5.5{\cdot}10^{-2}$	0
HypoC-2	0	$8.3{\cdot}10^{-2}$	0
HypoC-3	0	$1.4{\cdot}10^{-1}$	0
HypoC-4	0	$2.4{\cdot}10^{-1}$	0
HypoC-5	0	$2.0{\cdot}10^{-1}$	0
HypoC-6	0	$9.5{\cdot}10^{-2}$	0

Table 4.18: Molecular weight, M, normal boiling point, T_b, ideal liquid density, $\rho_\mathrm{id.liq.}$, critical temperature, T_c, and critical pressure, p_c, for the hypothetical components used to describe the heavy oil fractions of Platform C.

Component	M, g/mol	T_b, °C	$\rho_\mathrm{id.liq.}$, kg/m^3	T_c, °C	p_c, bar
HypoA-1	81.00	73.00	721.2	247.9	33.46
HypoC-1	98.78	85.76	754.3	269.3	35.50
HypoC-2	141.2	173.9	816.6	365.7	27.19
HypoC-3	185.8	240.5	861.0	434.1	22.71
HypoC-4	241.1	314.5	902.5	505.2	18.54
HypoC-5	404.5	487.1	955.3	647.0	10.45
HypoC-6	907.0	552.8	1007	710.0	9.610

Table 4.19: Calculated flow rates of the gas (10^3 Sm^3/h), oil (Sm^3/h) and water (Sm^3/h) phases for each well stream entering the production manifolds at Platform C.

Well	Gas	Oil	Water
High pressure production manifold			
2	18.06	43.69	9.59
6	6.84	17.49	4.10
8	7.29	17.56	0.54
9	3.97	11.49	0.01
10	7.35	20.03	0.83
15	30.52	133.09	18.15
16	30.51	106.90	5.63
17	3.88	7.41	0.01
18	6.85	13.49	0.01
19	7.22	33.02	0.33
21	2.72	7.81	0.00
25	4.43	22.91	3.42
26	6.59	20.60	0.42
27	3.71	14.40	0.45
28	15.51	41.93	2.21
30	6.15	19.17	4.21
35	18.62	48.19	3.08
40	6.40	27.01	1.42
Low pressure production manifold			
3	2.88	183.26	29.83
12	9.14	24.28	2.40
13	1.65	105.37	89.76
22	0.39	14.28	0.60
34	0.21	14.15	0.44
39	0.68	43.17	54.94
Test manifold			
1	22.08	91.81	27.42

Table 4.20: Measured flow rates, F, in process steams leaving Platform C.

Produced fluid	Variable	Value
Oil	F, m^3/h	1147
Injected gas	F, 10^3 Sm^3/h	360
Gas lift	F, 10^3 Sm^3/h	22

from documentation of the equipment are given in Table 4.23. The following simplifications were done in the simulation:

- All identical parallel coolers, pumps and scrubbers were merged into one.
- The delivery and return temperatures of the cooling medium in each of the coolers were set to the values for delivery and return temperature given in the documentation of the seawater system (Table 4.23).
- Pressure drops and heat losses in tubes and separators were neglected.
- For heat exchangers where values for pressure drops were not direct functions of measured pressures (Tables 4.21 and 4.22), pressure drops were set equal to values found in datasheets (Table 4.23) or to 1.0 bar.
- A dummy pump was included to increase the pressure of the condensate from 1st scrubber in the recompression train, to avoid inconsistencies in the flowsheet. The pressure out of the pump was set to the pressure out from the 2nd stage separator. In reality the pressure is increased due to height differences.

Simulated values are compared with measured values in Table 4.24. The following points can be noted:

- Most simulated temperatures (21 out of 28) are within the uncertainty of 1°C (Table 4.7) of the measured temperatures. The maximum deviation between measured and simulated temperature is 3.7 °C, and this is either due to measurements with higher errors than the assumed uncertainty, or due to inaccuracies in the equation of state. Since deviations higher than 1 °C only take place in a few of the wells, the effect of this is assumed to be negligible compared to the error sources mentioned in Section 4.4.
- Simulated pressure of water and oil entering the water and 1st oil pumps, are 2.75 bar, while the measured values are 4.20 and 3.96 bar, respectively. These deviations are found because height differences are not taken into consideration in the simulation. As discussed for Platform A [126], this has little impact on the overall results.
- Simulated flow rates in the oil export and gas treatment sections are within an uncertainty of the measured values of 10% (Table 4.7).

Table 4.21: Measured values for pressure, p, temperature, T, and flow rate, F, set in the simulated process flowsheet of Platform C. Part I.

Process stream	Variable	Value	Process stream	Variable	Value
High pressure production manifold			Well 21, valve, in	T, °C	50.5
Well 2, valve, in	p, bar	85.8	Well 25, valve, in	T, °C	58.5
Well 6, valve, in	p, bar	95.9	Well 26, valve, in	T, °C	60.9
Well 8, valve, in	p, bar	93.9	Well 27, valve, in	T, °C	57.0
Well 9, valve, in	p, bar	92.1	Well 28, valve, in	T, °C	60.9
Well 10, valve, in	p, bar	95.6	Well 30, valve, in	T, °C	64.2
Well 15, valve, in	p, bar	65.4	Well 35, valve, in	T, °C	67.8
Well 16, valve, in	p, bar	77.0	Well 40, valve, in	T, °C	64.4
Well 17, valve, in	p, bar	110.5	*Low pressure production manifold*		
Well 18, valve, in	p, bar	105.4	Well 3, valve, in	p, bar	14.61
Well 19, valve, in	p, bar	83.7	Well 12, valve, in	p, bar	90.2
Well 21, valve, in	p, bar	96.5	Well 13, valve, in	p, bar	13.04
Well 25, valve, in	p, bar	87.4	Well 22, valve, in	p, bar	70.2
Well 26, valve, in	p, bar	94.1	Well 34, valve, in	p, bar	48.4
Well 27, valve, in	p, bar	80.8	Well 39, valve, in	p, bar	22.5
Well 28, valve, in	p, bar	94.5	Well 3, valve, out	p, bar	9.20
Well 30, valve, in	p, bar	94.0	Well 12, valve, out	p, bar	8.08
Well 35, valve, in	p, bar	96.6	Well 13, valve, out	p, bar	9.36
Well 40, valve, in	p, bar	88.5	Well 22, valve, out	p, bar	7.85
Well 2, valve, out	p, bar	47.1	Well 34, valve, out	p, bar	8.05
Well 6, valve, out	p, bar	47.0	Well 39, valve, out	p, bar	8.22
Well 8, valve, out	p, bar	47.0	Well 3, valve, in	T, °C	71.1
Well 9, valve, out	p, bar	47.0	Well 12, valve, in	T, °C	61.7
Well 10, valve, out	p, bar	47.1	Well 13, valve, in	T, °C	70.9
Well 15, valve, out	p, bar	47.8	Well 22, valve, in	T, °C	56.0
Well 16, valve, out	p, bar	47.4	Well 34, valve, in	T, °C	57.2
Well 17, valve, out	p, bar	47.2	Well 39, valve, in	T, °C	71.8
Well 18, valve, out	p, bar	47.0	*Test manifold*		
Well 19, valve, out	p, bar	46.9	Well 1, valve, in	p, bar	60.4
Well 21, valve, out	p, bar	46.9	Well 1, valve, out	p, bar	14.76
Well 25, valve, out	p, bar	46.9	Well 1, valve, in	T, °C	68.4
Well 26, valve, out	p, bar	46.9	*Recompression*		
Well 27, valve, out	p, bar	46.8	1st compressor, in	p, bar	1.24
Well 28, valve, out	p, bar	47.0	1st compressor, out	p, bar	7.14
Well 30, valve, out	p, bar	47.2	2nd compressor, in	p, bar	5.84
Well 35, valve, out	p, bar	47.1	2nd compressor, out	p, bar	17.5
Well 40, valve, out	p, bar	47.0	3rd compressor, in	p, bar	16.8
Well 2, valve, in	T, °C	64.5	3rd compressor, out	p, bar	45.7
Well 6, valve, in	T, °C	66.1	1st cooler, out	T, °C	30.5
Well 8, valve, in	T, °C	58.0	1st compressor, out	T, °C	164.7
Well 9, valve, in	T, °C	60.6	2nd cooler, out	T, °C	28.3
Well 10, valve, in	T, °C	62.4	2nd compressor, out	T, °C	123.0
Well 15, valve, in	T, °C	71.8	3rd cooler, out	T, °C	26.5
Well 16, valve, in	T, °C	66.8	3rd compressor, out	T, °C	125.1
Well 17, valve, in	T, °C	51.7	1st compressor, in	F, 10^3 Sm^3/h	6.3
Well 18, valve, in	T, °C	57.9	2nd compressor, in	F, 10^3 Sm^3/h	101
Well 19, valve, in	T, °C	61.9	3rd compressor, in	F, 10^3 Sm^3/h	87

Table 4.22: Measured values for pressure, p, temperature, T, and flow rate, F, set in the simulated process flowsheet of Platform C. Part II.

Process stream	Variable	Value	Process stream	Variable	Value
Separation and oil export			Import compressor, out	p, bar	184.3
HP degasser	p, bar	46.0	1st cooler, out	T, °C	27.0
Test separator	p, bar	12.9	1st compressor, out	T, °C	91.9
1st stage separator	p, bar	7.22	2nd cooler, out	T, °C	30.0
2nd stage separator	p, bar	2.75	2nd compressor, out	T, °C	91.6
Water pump, out	p, bar	13.48	Imported gas	T, °C	4.4
1st oil pump, out	p, bar	12.48	Import cooler, out	T, °C	29.0
2nd oil pump, in	p, bar	9.46	Import compressor, in	T, °C	9.0
2nd oil pump, out	p, bar	99.1	Import compressor, out	T, °C	52.5
Oil heater, out	T, °C	98.0	Imported gas	F, 10^3 Sm^3/h	159
Export cooler, in	T, °C	80.8	For gas lift, HP	F, 10^3 Sm^3/h	0
Export cooler, out	T, °C	74.0	For gas lift, LP	F, 10^3 Sm^3/h	22
Gas treatment			For injection	F, 10^3 Sm^3/h	360
1st compressor, in	p, bar	44.4	*Fuel gas system*		
1st compressor, out	p, bar	94.3	Scrubber, in	p, bar	39.0
2nd compressor, in	p, bar	93.1	Heater, out	T, °C	60.9
2nd compressor, out	p, bar	184.9	To flare	F, Sm^3/h	0
Imported gas	p, bar	110.2	To turbines	F, Sm^3/h	9650
Import compressor, in	p, bar	108.7			

Table 4.23: Split flow ratios, values for split flow ratios, r, overall heat transfer coefficient, U, heat transfer surface area, A, pressure drop, Δp, efficiency, η, mass fraction, x, pressure, p and temperature, T, assumed or from documentation from process equipment for Platform C.

Process unit	Variable	Value	Source
Separation and oil export			
Flow splitter	r, -	0.5	Separation system manual
Oil-water heat exchanger, UA	UA, kJ/C-h	$1.85 \cdot 10^6$	Assumed, operators
Electrostatic coalescer, water in oil	%	0.5	Product flow specification
Oil-oil heat exchanger, hot side	Δp, bar	1.5	Datasheet
Oil-oil heat exchanger, cold side	Δp, bar	1.5	Datasheet
Oil-water heat exchanger, hot side	Δp, bar	1.5	Datasheet
Oil-water heat exchanger, cold side	Δp, bar	1.5	Datasheet
Oil heater, hot side	Δp, bar	1.0	Datasheet
Oil heater, cold side	Δp, bar	1.5	Datasheet
Water pump	η, %	75	Assumed
1st oil pump	η, %	76	Pump performance curves
2nd oil pump	η, %	74	Pump performance curves
Gas treatment			
1st flow splitter, recirculation	r, -	0	Assumed, operators
2nd flow splitter, recirculation	r, -	0	Assumed, operators
Hot water system			
Heating medium	x_{water}, -	1.00	Hot water system manual
Delivery pressure	p, bar	25.9	Hot water system manual
Delivery temperature	T, °C	170	Hot water system manual
Return temperature	T, °C	120	Hot water system manual
Cooling system			
Cooling medium	x_{water}, -	1.00	Assumed
Delivery pressure	p, bar	11.4	Seawater system manual
Delivery temperature	T, °C	10	Seawater system manual
Return temperature	T, °C	45	Seawater system manual

Table 4.24: Measured values for temperature, T, pressure, p, and flow, F, compared with simulated values for Platform C.

Process stream	Variable	Measured value	Simulated value
High pressure production manifold			
Well 2, valve, out	T, °C	61.5	61.6
Well 6, valve, out	T, °C	62.7	62.9
Well 8, valve, out	T, °C	53.9	53.2
Well 9, valve, out	T, °C	58.6	56.5
Well 10, valve, out	T, °C	58.5	58.2
Well 15, valve, out	T, °C	70.7	70.9
Well 16, valve, out	T, °C	64.7	64.7
Well 17, valve, out	T, °C	43.4	43.6
Well 18, valve, out	T, °C	51.6	50.7
Well 19, valve, out	T, °C	59.9	59.8
Well 21, valve, out	T, °C	47.0	45.9
Well 25, valve, out	T, °C	56.7	57.1
Well 26, valve, out	T, °C	57.8	57.1
Well 27, valve, out	T, °C	55.5	54.7
Well 28, valve, out	T, °C	57.1	56.8
Well 30, valve, out	T, °C	61.5	61.6
Well 35, valve, out	T, °C	63.7	63.6
Well 40, valve, out	T, °C	62.1	62.1
Low pressure production manifold			
Well 3, valve, out	T, °C	70.5	71.0
Well 12, valve, out	T, °C	53.0	51.3
Well 13, valve, out	T, °C	70.6	70.9
Well 22, valve, out	T, °C	52.0	55.7
Well 34, valve, out	T, °C	54.9	57.4
Well 39, valve, out	T, °C	70.8	71.9
Test manifold			
Well 1, valve, out	T, °C	64.9	65.0
Separation and oil export			
Water pump, in	p, bar	4.20	2.75
1st oil pump, in	p, bar	3.96	2.75
1st separator, in	T, °C	65.1	65.5
2nd separator, in	T, °C	96.6	97.2
2nd oil pump, out	F, Sm^3/h	1000	1100
Gas treatment			
1st compressor, in	F, Sm^3/h	240,000	230,000
2nd compressor, in	F, Sm^3/h	260,000	230,000
Fuel gas system			
Heater, in	T, °C	23.1	24.2

Chapter 5

Thermodynamic performance indicators for offshore oil and gas processing: Application to four North Sea facilities

Mari Voldsund[1], Tuong-Van Nguyen[2], Brian Elmegaard[2], Ivar Ståle Ertesvåg[3] and Signe Kjelstrup[1]

1. Department of Chemistry,
Norwegian University of Science and Technology,
NO-7491 Trondheim, Norway

2. Department of Mechanical Engineering,
Technical University of Denmark,
DK-2800 Kongens Lyngby, Denmark

3. Department of Energy and Process Engineering,
Norwegian University of Science and Technology,
NO-7491 Trondheim, Norway

This chapter is submitted to
Oil and gas facilities

Is not included due to copyright

Chapter 6

On the definition of exergy efficiency for petroleum systems: Application to offshore oil and gas processing

Tuong-Van Nguyen[1], Mari Voldsund[2], Brian Elmegaard[1], Ivar Ståle Ertesvåg[3] and Signe Kjelstrup[2]

1. Department of Mechanical Engineering,
Technical University of Denmark,
DK-2800 Kongens Lyngby, Denmark

2. Department of Chemistry,
Norwegian University of Science and Technology,
NO-7491 Trondheim, Norway

3. Department of Energy and Process Engineering,
Norwegian University of Science and Technology,
NO-7491 Trondheim, Norway

This chapter is submitted to
Energy - The International Journal

Abstract

Exergy-based efficiencies are measures of the thermodynamic perfection of systems and processes. A meaningful formulation of these performance criteria for petroleum separation systems is difficult because of (i) the high chemical exergy of hydrocarbons, (ii) a large variety of chemical components, and (iii) differences in operating conditions between facilities. We focus on application to offshore oil and gas processing plants. Different formulations are applied to four offshore platforms which differ by their working conditions and designs. Several approaches from the scientific literature for similar processes are presented and applied to the four cases. These formulations could not successfully be used to evaluate our systems. They showed low sensitivity to performance improvements, gave inconsistent results, or favoured platforms operating under certain conditions. We suggest an alternative formulation called the *component-by-component* exergy efficiency, which is applicable to all petroleum separation systems. The *component-by-component* efficiency is sensitive to process improvements and gives consistent results. It evaluates successfully the theoretical improvement potential and allows a sound comparison of the thermodynamic perfection. In order to evaluate the technical achievable improvement potential considerations about avoidable/unavoidable exergy destruction can be taken into account. The *component-by-component* efficiency ranges between 1.7 and 30% for our four cases.

6.1 Introduction

Conventional indicators for evaluating the performance of oil and gas platforms, such as the specific power consumption, the specific CO_2 emissions, or the energy efficiency, present inherent limitations. The specific power consumption is defined as the power consumed per oil equivalent exported, the specific CO_2 emissions as the amount of carbon dioxide emitted per unit of oil equivalent exported, and the energy efficiency as the ratio of the energy exported with the oil and gas sent onshore to the energy entering the system with the feed streams. Each oil field has different natural characteristics (e.g. gas-to-oil ratio, well-fluid composition, field size) and comparing different facilities with these metrics could be misleading. They provide useful information on the energy use of the onsite processes, but they cannot be used alone to compare the performance of different facilities [109, 110].

Exergy analysis is a quantitative assessment method that is based on both the First and Second Laws of Thermodynamics. This thermodynamic method presents advantages over a conventional energy analysis: it pinpoints the locations and types of the irreversibilities taking place within a given system. As emphasised by Rivero [83], the application of the exergy concept in the petroleum industry would provide more detailed and consistent information on the performance of petrochemical systems. The exergy concept was introduced in the literature along with the con-

cept of exergy efficiency, which aims at measuring the degree of thermodynamic perfection of the process under investigation.

Formulations of exergy-based criteria of performance have been proposed from the middle of the 20th century, with amongst others the contributions of Nesselmann [67] and Fratzscher [29, 30]. Both works reported the definition of the exergy efficiency of a given system as the ratio of its total exergy output to its total exergy input and discussed the advantages and drawbacks of such formulation. Grassmann [31] and Nesselmann [68] suggested to define the exergy efficiency as the ratio of the part of the exergy transfers that contribute to the transformations taking place, i.e. *consumed* exergy, to the part of the exergy transfers that are generated within the system, i.e. *produced* exergy. Baehr [10, 11] worked further on this concept, and stressed the difficulties of providing a non-ambiguous definition of an exergy efficiency, as different views on *consumed* and *produced* exergies may apply.

Further advances within this field include the studies of Brodyansky [16], Szargut [114, 64, 113], Kotas [50] and Tsatsaronis [118, 120]. Brodyansky [16] suggested a systematic procedure for calculating the *produced* and *consumed* exergies, without regarding whether they are useful to the owner of the system. His work was based on the concept of *transit exergy* introduced by Kostenko (cf. Brodyansky [16]) and discussed also by Sorin et al. [100]. Szargut [114, 64, 113], Kotas [50] and Tsatsaronis [118, 120] proposed to consider only the exergy transfers representing the *desired* exergetic output and the *driving* exergetic input of the system, leading to the concept of *product* and *fuel* exergies. Such considerations must be consistent with the purpose of owning and operating the system of investigation [48, 49, 13, 62], both from an economic and a thermodynamic prospect. Lazzaretto and Tsatsaronis [51, 52] suggested a systematic procedure for defining the exergy efficiency at a process component level. However, at a process level, a unique formulation may not be available and several expressions may be appropriate [118].

Various expressions of exergy efficiency for separation systems have been presented in the literature [16, 50, 118, 101]. Cornelissen [19] investigated three formulations for an air separation unit and a crude distillation plant. Different results were obtained, illustrating the variations and lack of uniformity across the exergy efficiency definitions [10, 11, 55]. Oliveira and Van Hombeeck [22] presented an exergy analysis of a Brazilian offshore platform, with another formulation of the exergy efficiency. This formulation was also used by Voldsund et al. [127, 128, 126] for a Norwegian offshore platform. Rian and Ertesvåg [82] studied a liquefied natural gas (LNG) plant using an exergy efficiency formulated particulary for LNG plants.

The literature seems to contain little, if nothing, on a uniform performance parameter for petroleum processes. In this paper we present a formulation of exergy efficiency that can be used on all types of such processes. The work was carried out in three main steps:

- literature review of formulations of exergy efficiency for various petroleum

processes;

- application of such formulations to the processing plants on four different offshore platforms;
- derivation and application of a new formulation based on the experience from the two first steps.

This paper is structured as follows: Section 6.2 presents the four oil and gas platforms used as case studies in this work. Section 6.3 describes the theoretical background, and Section 6.4 presents definitions of exergy efficiencies found in the literature and their applicability to the four platforms. In Section 6.5 the derivation of a new exergy efficiency suitable for petroleum separation processes is described, together with the application of this efficiency to the four platforms. The outcomes are discussed in Section 6.6 and concluding remarks are outlined in Section 6.7.

6.2 System description

6.2.1 General overview

Offshore platforms are large structures with facilities to extract and process petroleum from subsea reservoirs. Petroleum is processed in a processing plant using power (and often also heat) that is produced in a utility plant. The power is produced by gas turbines fuelled with a fraction of the produced gas, or alternatively heavy oil or diesel. A heating demand is either met by using fuel gas burners, electric heaters or by waste heat recovery from the utility plant. A schematic overview of the processing and utility plants are given in Fig. 6.1. The focus in this work is on the processing plant.

Petroleum is a complex multiphase mixture: it contains a large spectrum of chemical components, from light hydrocarbons in gaseous form (e.g. methane) to heavy ones in liquid phase (e.g. naphtenes and cycloalkanes) and is extracted along with subsurface water. The aim of the processing plant is to separate efficiently the different phases to satisfy the different process and export constraints, and to maximise the hydrocarbon production. Crude oil consists mostly of medium- to heavy hydrocarbons in liquid form, while natural gas mostly consists of light-weight alkanes. Differences across offshore platforms can be summarised as follows [14, 21, 74, 42, 57, 78, 1, 125]:

- reservoir characteristics (e.g. initial temperature and pressure);
- fluid properties (e.g. chemical composition, gas- and water-to-oil (GOR and WOR) ratios);

- product requirements (e.g. export pressure and temperature, chemical purity);
- operating strategies (e.g. oil and gas recovery, gas treatment, condensate export).

These differences induce variations in temperatures, pressures and flow rates throughout the system as well as in demands for compression, heating, cooling, dehydration, desalting and sweetening. The structural design of the processing plant stays nevertheless similar.

In the processing plant oil, gas and water enter one or several production manifolds in which the well-fluid streams are mixed and the pressure reduced to ease separation between the liquid and gaseous phases. The well-fluid streams are fed into a separation system where oil, gas and water are separated by gravity in one or more stages, with throttling in between. Crude oil leaving the separation train enters a treatment and export pumping section. Gas leaving the separation and oil pumping steps enters the recompression train. It is cooled, sent to a scrubber where condensate and water droplets are removed, and recompressed to the pressure of the previous separation stage. It is then sent to the gas treatment train, where it is purified and possibly dehydrated by triethylene glycol (TEG). Gas may be compressed for export to the shore, lift or injection.

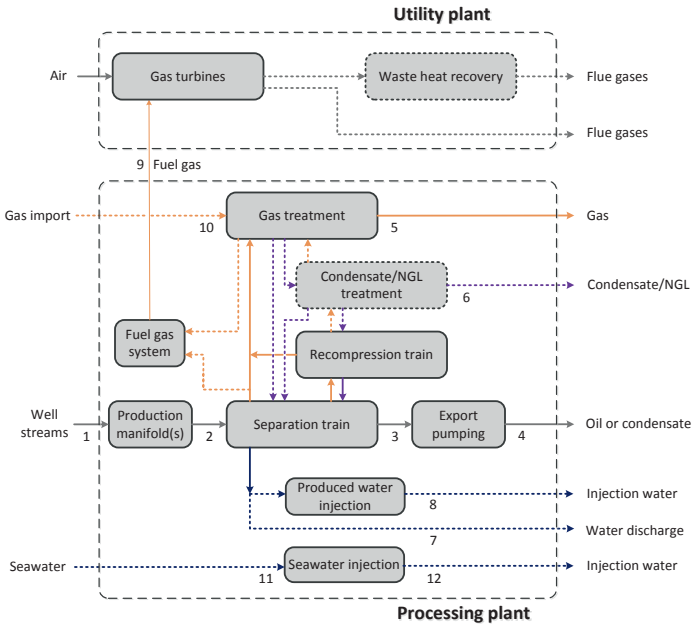

Figure 6.1: General overview of the processing and power plants.

Condensate removed from the recompression and gas treatment trains is (i) either sent back to the separation train and mixed with crude oil or (ii) processed in a condensate treatment section. Produced water enters a wastewater handling train, in which suspended particulates and dissolved hydrocarbons are removed. It is then discharged into the sea or enters an injection train where it is further cleaned and pumped to a high pressure level. In parallel, seawater may be processed on-site for further injection into the reservoir for enhanced oil recovery.

The cooling demand is satisfied by using a direct cooling medium, e.g. seawater or air, or an indirect one, e.g. a glycol/water mixture. Heat exchanger networks between the different streams flowing through the system may also be integrated to promote heat integration.

Processes such as condensate treatment and natural gas liquid recovery are uncommon offshore, with only a few applications worldwide. Oil and gas treatment is generally limited to gas dehydration in the North Sea, whereas it also includes oil desalting and gas sweetening in the Gulf of Mexico. Further details on oil and gas processing are given in [56] and more specific information on North Sea platforms are given in [14, 71].

6.2.2 Case studies

The four oil and gas platforms (Platforms A–D) investigated within this study are located in the North Sea region and present specific design characteristics (Table 6.1). Flowsheets of the processes plants on each of the platforms and temperature and pressure levels of the most important process streams are given in the appendix.

These four platforms, although similar in terms of structural design, present significant differences in well-fluid processing and in operating conditions:

- The gas-to-oil ratio is either increasing (Platforms A, B and C), meaning that the gas treatment train is run at full-design conditions, or decreasing (Platform D), meaning that this subsystem is run in off-design conditions, and that anti-surge recycling is practiced to protect the compressors.
- Platforms processing heavy and viscous crude oil (e.g. platform C) or with a high propane content (e.g. platform D) require heating in the separation train to enhance vapour-liquid separation and to meet the export specifications.
- The pressure at the final stage of the separation train (p_3) is constrained by the maximum allowable vapour pressure of the crude oil/condensate in the pipelines and shuttle tankers, and is below 3 bar for all platforms.
- The pressure of the produced oil/condensate at the outlet of the pumping section (p_4) is either higher (e.g. platform C) or lower (e.g. platforms A, B and D) than at the outlet of the production manifold (p_2).

- The pressure at the outlet of the gas treatment section (p_5) is either higher (e.g. platforms A, C and D) or lower (e.g. platform B) than at the inlet of the separation system (p_2). There is a need for gas compression in three of the four platforms.

For more details about the processes taking place on each of these platforms, the reader is referred to two previous works conducted by the same authors [126, 129].

Table 6.1: Comparison of the four offshore facilities discussed in this study. n means not-included and y means included.

Platform	A	B	C	D
System characteristics				
Age, years	20	10	10	20
Gas-to-oil ratio (Sm^3 basis)	2800	3200	360	230
Gas-to-oil ratio trend	↗	↗	↗	↘
System products				
Oil	export	none	export	export
Gas	fuel injection	fuel export	fuel injection import lift	fuel export
Condensate	export (mixed with oil)	export	export (mixed with oil)	export (mixed with gas)
Produced water	discharge	injection	discharge	discharge
Seawater	cooling	cooling	cooling	cooling injection
Additional processes				
Dehydration	n	n	n	y
Condensate treatment	n	n	n	y
Water injection	n	n	n	y

6.2.3 Modelling and simulation

The process simulations were carried out with Aspen HYSYS® [7] and Aspen Plus® version 7.2 [6], with the exception of the glycol dehydration system. Simulations of the production manifolds, petroleum separation, oil pumping, gas recompression and flaring were based on the Peng-Robinson and Soave-Redlich-Kwong equations of state [77, 97]. The water purification and injection processes were simulated based on the Non-Random Two Liquid (NRTL) model [81] and the dehydration process on the Schwartzentruber-Renon equation of state [90, 91].

6.3 Theoretical background

6.3.1 Exergy analysis

Exergy is defined as the maximum theoretical useful work as the system is brought into complete thermodynamic equilibrium with the thermodynamic environment while the system interacts with this environment only [114]. In this work, the discussions on exergy efficiencies focus exclusively on the exergy associated with mass and energy transfers.

Unlike energy, exergy is not conserved in real processes – some is destroyed due to internal irreversibilities. On a time rate form and for a control volume with in- and outgoing flows, the exergy balance is expressed as:

$$\begin{aligned}\dot{E}_\mathrm{d} &= \sum \dot{E}_\mathrm{in} - \sum \dot{E}_\mathrm{out} \\ &= \sum \left(1 - \frac{T_0}{T_k}\right) \dot{Q}_k - \dot{W} + \sum \dot{m}_\mathrm{in} e_\mathrm{in} - \sum \dot{m}_\mathrm{out} e_\mathrm{out},\end{aligned} \tag{6.1}$$

where $\dot{E}_\mathrm{d}$ is the exergy destroyed inside the control volume, $\dot{E}_\mathrm{in}$ is *all* exergy entering the system and $\dot{E}_\mathrm{out}$ is *all* exergy leaving it. The symbol $\dot{m}$ denotes the mass flow rate of a stream of matter, $\dot{Q}_k$ and $\dot{W}$ the time rates of energy transfer by heat and work ($\dot{Q} \geq 0$ indicates heat transfer to the system, $\dot{W} \geq 0$ work done by the system) and e the specific exergy of a stream of matter. The symbols T_0 and T_k denote the environmental temperature and the local temperature where heat transfer takes place. The subscripts in and out denote the inlet and outlet of the system and k the boundary of the component. The exergy destruction rate can also be calculated from the Gouy-Stodola theorem, which is expressed as:

$$\dot{E}_\mathrm{d} = T_0 \dot{S}_\mathrm{gen}, \tag{6.2}$$

where $\dot{S}_\mathrm{gen}$ is the entropy generation rate inside the control volume.

Exergy destruction is also called *internal exergy losses*, since this is exergy that is lost related to the irreversibilities taking place *inside* the control volume under study. Exergy discharged to the environment without any practical use (e.g. exergy content of exhaust gases from a gas turbine – exergy transferred to the cooling water) is referred to as *external exergy losses* or just *exergy losses* [13, 119]. This waste exergy is destroyed when mixed irreversibly with the environment.

6.3.2 Flow exergy

In the absence of nuclear, magnetic and electrical interactions, the exergy associated with a stream of matter is a function of its physical e^ph, chemical e^ch, kinetic e^kin

and potential e^{pot} components [13]. The molar exergy of a material stream is expressed as:

$$e = e^{\text{ph}} + e^{\text{ch}} + e^{\text{kin}} + e^{\text{pot}}. \tag{6.3}$$

In this work, kinetic and potential contributions on the flow exergies are assumed to be negligible compared to physical and chemical exergies.

Physical exergy accounts for temperature and pressure differences from the environmental state and is defined as:

$$\begin{aligned} e^{\text{ph}} &= (h - h_0) - T_0(s - s_0) \\ &= \underbrace{h - h(T_0, p) - T_0\left(s - s(T_0, p)\right)}_{\text{I}} + \underbrace{h(T_0, p) - h_0 - T_0\left(s(T_0, p) - s_0\right)}_{\text{II}}, \end{aligned} \tag{6.4}$$

where h and s are the specific enthalpy and entropy of a stream of matter, respectively. Terms I and II refer to the the temperature-based and pressure-based components of the physical exergy [50], respectively, and are also named thermal and mechanical exergies [118].

Chemical exergy accounts for deviations in chemical composition from reference substances present in the environment. In this work, chemical exergy is calculated using the reference environment defined in Szargut [114, 112, 65]. The specific chemical exergy of a given mixture $e^{\text{ch}}_{\text{mix}}$ is expressed as [88]:

$$\begin{aligned} e^{\text{ch}}_{\text{mix}} &= \underbrace{\sum_i x_i e^{\text{ch}}_{i,\text{mix}}}_{\text{I}} \\ &= \underbrace{\sum_i x_i e^{\text{ch}}_{i,0}}_{\text{II}} + \underbrace{\left(\sum_i x_i \left(h_{i,\text{mix}} - h_{i,0}\right)\right) - T_0 \left(\sum_i x_i \left(s_{i,\text{mix}} - s_{i,0}\right)\right)}_{\text{III}}, \end{aligned} \tag{6.5}$$

where the mass fraction, the chemical component and the mixture are denoted by x, i and mix, respectively. The specific exergy of a given chemical component is written $e^{\text{ch}}_{i,\text{mix}}$ when it is in the mixture and $e^{\text{ch}}_{i,0}$ when it is in a pure component state. The term I illustrates the chemical exergy of each individual chemical component in the mixture, the term II the chemical exergy of these components in an unmixed form and the term III the reduction in chemical exergy due to mixing effects.

If no chemical transformations are taking place within a separation system, the terms related to the chemical exergy of pure components cancel and the change in chemical exergy is equal to the exergy used to perform the separation work [50].

The specific chemical exergy of hypothetical components e^{ch}_{h} is determined with the heuristic correlations of Rivero [85]:

$$e^{\text{ch}}_{\text{h}} = \beta NHV_{\text{h}} + \sum x_{\text{mt}} e^{\text{ch}}_{\text{mt}}, \tag{6.6}$$

where NHV stands for Net Heating Value, x_{mt} for the mass fraction of metal impurities, $e^{\text{ch}}_{\text{mt}}$ for the corresponding chemical exergy and β for the chemical exergy correction factor.

6.3.3 Exergy efficiency

The definitions of exergy efficiency, as presented and discussed in the open literature, can be divided into two main groups, as suggested by Lior and Zhang [55]:

- the *total*, *overall*, *input-output* or *universal* exergy efficiency, which is defined as the ratio of all outgoing to ingoing exergy flows;
- the *task*, *utilitarian*, *consumed-produced*, *rational* or *functional* exergy efficiency, which is defined as the ratio of the exergy terms associated with the products generated within the system, i.e. the *produced exergy*, to the exergy terms associated with the resources expended to achieve these outputs, i.e. the *consumed exergy*.

Total exergy efficiency

For a given open thermodynamic system at steady-state, the exergy balance can be expressed as:

$$\sum \dot{E}_{\text{in}} = \sum \dot{E}_{\text{out}} + \dot{E}_{\text{d}} = \sum \dot{E}_{\text{out,u}} + \sum \dot{E}_{\text{out,l}} + \dot{E}_{\text{d}}, \tag{6.7}$$

where $\dot{E}_{\text{in}}$ and $\dot{E}_{\text{out}}$ are the exergy inputs and outputs to and from the system, associated with streams of matter and of energy, and $\dot{E}_{\text{d}}$ the exergy destruction. The exergy output consists of useful exergy output $\dot{E}_{\text{out,u}}$, and exergy that is lost $\dot{E}_{\text{out,l}}$ (i.e. the exergy of waste products that is not taken into use, but discharged to the environment).

The *total* exergy efficiency ε_I is defined as the ratio of all exergy outflows to inflows [19, 55, 131]:

$$\varepsilon_{I-1} \equiv \frac{\sum \dot{E}_{\text{out}}}{\sum \dot{E}_{\text{in}}} = 1 - \frac{\dot{E}_{\text{d}}}{\sum \dot{E}_{\text{in}}}, \tag{6.8}$$

where some authors exclude the exergy associated with waste products [30, 131]:

$$\varepsilon_{I-2} \equiv \frac{\sum \dot{E}_{\text{out,u}}}{\sum \dot{E}_{\text{in}}} = 1 - \frac{\dot{E}_{\text{out,l}} + \dot{E}_{\text{d}}}{\sum \dot{E}_{\text{in}}}. \tag{6.9}$$

The *total* exergy efficiency is claimed to be adequate when (i) the ingoing and outgoing exergy flows are converted to other forms of exergy [19] or (ii) a major part of the out-flowing exergy can be considered as useful, as it is the case of power plants [55] or (iii) for dissipative processes and devices [61, 50].

Task exergy efficiency

The concept of *total* exergy efficiency has been criticised as it takes into account all the exergetic flows entering and exiting a system, without considering whether they are utilised in the thermodynamic conversions. The *task* exergy efficiency, on the opposite, differentiates the exergy flows undergoing transformations from the exergy flows that are not affected, i.e. neither used nor produced. Grassmann [31] proposed a general formulation for an exergy efficiency: he suggested the ratio of the intended increase to the used decrease in ability to do work. In exergy terms, this means that the exergy efficiency should be defined as the ratio of the production of exergy that is desired to the reduction of exergy that is utilised. It was emphasised that this performance criterion always has a value between 0 and 1, as the increased ability to do work always is smaller than the decreased ability.

Baehr [11] proposed a variant of this formulation, considering *all* the exergy increases in the numerator and *all* the exergy decreases in the denominator. At the difference of the expression proposed by Grassmann [31], the total production and expenditure of exergy are considered, whether they are actually desired or utilised within the system. It was pointed out that (i) exergy efficiencies based on exergy differences are more sensitive to changes in the system than the total exergy efficiency and are therefore more suitable and (ii) different numerical values could be obtained with the formulation of exergy efficiency proposed by Grassmann [31], as it depends on whether an exergy difference is considered as *useful*, *used* or none of those.

Szargut [111, 114, 113], and Kotas [49, 50] argued that the exergy efficiency should be defined as the ratio of (i) the *desired output* or *useful exergetic effect* and (ii) the *necessary input* or *driving exergy expense*. Other authors name the same terms *exergetic product* $\dot{E}_\mathrm{p}$ and *exergetic fuel* $\dot{E}_\mathrm{f}$ [119, 13]. The exergetic balance (Eq. 6.1) can be rewritten:

$$\dot{E}_\mathrm{p} = \dot{E}_\mathrm{f} - \dot{E}_\mathrm{l} - \dot{E}_\mathrm{d}. \tag{6.10}$$

Hence, the task exergy efficiency can be written:

$$\varepsilon \equiv \frac{\dot{E}_\mathrm{p}}{\dot{E}_\mathrm{f}} = 1 - \frac{\dot{E}_\mathrm{l} + \dot{E}_\mathrm{d}}{\dot{E}_\mathrm{f}}. \tag{6.11}$$

Brodyansky [16] and Sorin [100] proposed to define the exergy efficiency as the ratio of the total exergy output to the total exergy input, minus the *transit exergy* $\dot{E}_\mathrm{tr}$ in both numerator and denominator:

$$\varepsilon \equiv \frac{\sum \dot{E}_\mathrm{out} - \sum \dot{E}_\mathrm{tr}}{\sum \dot{E}_\mathrm{in} - \sum \dot{E}_\mathrm{tr}}. \tag{6.12}$$

The concept of *transit exergy* was introduced by Kostenko (cf. Brodyansky [16]), and it was further developed by Brodyansky [16]. The transit exergy is the part of

the exergy supplied to a system that flows through the system without undergoing any physical or chemical transformation. The concept of transiting exergy is also mentioned by Cornelissen [19], who applied this method to an air separation unit and a crude oil distillation plant. The lack of ambiguity and the complexity of the calculations were underlined, as this method requires a precise decoupling of the exergy flows into their components. This efficiency can also be regarded as a variant of the *total* exergy efficiency.

6.4 Exergy efficiencies for petroleum processes

In this section we conduct a literature survey of the derivations of exergy efficiencies for petroleum processing systems in general, apply them to our four offshore processing plants and discuss their relevance. An overview of the relevant definitions are given in Section 6.4.1, while each of them are derived for offshore processing plants and discussed in detail in Sections 6.4.2–6.4.5. The exergy efficiencies for the utility plant, which consists of gas turbines, and some times also of a waste heat recovery system, are not in the scope of this work, as they are well-established definitions that can be found in the literature (see e.g. [50]).

6.4.1 Overview of definitions

Several approaches for the exergy efficiencies of petroleum processing systems can be found in the literature [50, 22, 19, 127, 128, 126, 82, 120, 121]. In addition to the *total* exergy efficiency, three different *task* exergy efficiencies are found. The concepts of the *task* exergy efficiency formulations are summarised in Table 6.2. For the types of *task* efficiencies where it is possible both to include waste streams as product or as loss, we have chosen to systematically regard the exergy associated with them as lost exergy.

Table 6.2: The concepts of three *task* exergy efficiencies found in the literature for petroleum systems.

System	Fuel	Product
General separation [50] Offshore platform [22, 126]	Added heat and work	Physical and chemical exergy changes
LNG plant [82] Crude oil distillation [19]	Added heat and work + input physical exergy	Chemical exergy increase + output physical exergy
Distillation [121]	Added heat and work + physical exergy decrease	Chemical exergy increase + physical exergy increase

Fig. 6.2 shows schematically the exergy streams entering and leaving the processing plant, as well as the utility plant, and clarifies the notation used in the following sections.

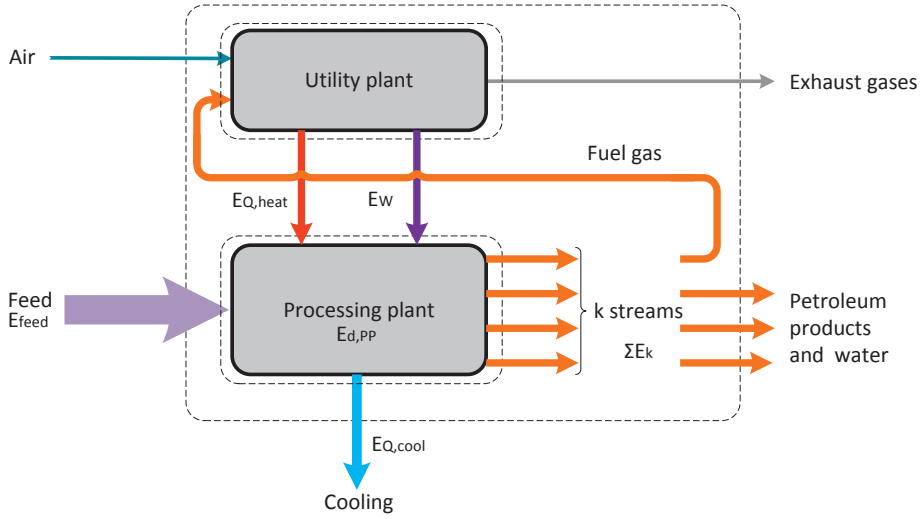

Figure 6.2: Schematic overview of exergy streams entering and exiting the processing and utility plants.

6.4.2 Total exergy efficiency

The exergy balance for the processing plant of the oil and gas facility can be expressed as:

$$\underbrace{\dot{E}_{\text{feed}} + \dot{E}^{\text{Q}}_{\text{heat}} + \dot{E}^{\text{W}}}_{\dot{E}_{\text{in}}} = \underbrace{\sum_{k,\text{u}} \dot{E}_{k,\text{u}}}_{\dot{E}_{\text{out,u}}} + \underbrace{\sum_{k,\text{w}} \dot{E}_{k,\text{w}} + \dot{E}^{\text{Q}}_{\text{cool}}}_{\dot{E}_{\text{out,l}}} + \underbrace{\dot{E}_{\text{d,PP}}}_{\dot{E}_{\text{d}}} . \tag{6.13}$$

The left-hand side terms consist of the exergy associated with the feed entering the processing plant $\dot{E}_{\text{feed}}$ (i.e. reservoir fluid) and the heat exergy $\dot{E}^{\text{Q}}_{\text{heat}}$ and power exergy $\dot{E}^{\text{W}}$ delivered by the utility plant. The right-hand side terms consist of the exergy of the useful outlet material streams of the processing plant $\sum_k \dot{E}_{k,\text{u}}$ (i.e. oil, gas, condensate, fuel gas), the wasted outlet material streams $\sum_k \dot{E}_{k,\text{w}}$ (i.e. flared gas, produced water), the exergy lost in the cooling system $\dot{E}^{\text{Q}}_{\text{cool}}$ and the destroyed exergy $\dot{E}_{\text{d,PP}}$. All the left-hand side terms comprise the input exergy E_{in} while the useful outlet material streams on the right-hand side are counted as useful output exergy $E_{\text{out,u}}$. The produced water that is extracted along with oil and gas is normally considered as waste, since it is discharged to the surroundings

without being used. The exception to this rule is if the produced water is injected back for enhanced oil recovery, which is a future plan for Platform D.

The *total* exergy efficiency without differentiating the *useful* from the *waste* streams [67] is:

$$\varepsilon_{I-1} = \frac{\sum_{k,\mathrm{u}} \dot{E}_{k,\mathrm{u}} + \sum_{k,\mathrm{w}} \dot{E}_{k,\mathrm{w}} + \dot{E}^{\mathrm{Q}}_{\mathrm{cool}}}{\dot{E}_{\mathrm{feed}} + \dot{E}^{\mathrm{Q}}_{\mathrm{heat}} + \dot{E}^{\mathrm{W}}}, \tag{6.14}$$

while the *total* exergy efficiency considering only the *useful* streams is:

$$\varepsilon_{I-2} = \frac{\sum_{k,\mathrm{u}} \dot{E}_{k,\mathrm{u}}}{\dot{E}_{\mathrm{feed}} + \dot{E}^{\mathrm{Q}}_{\mathrm{heat}} + \dot{E}^{\mathrm{W}}}. \tag{6.15}$$

The total exergy efficiencies of all four processing plants (Table 6.3) range between 99% – 100% when waste streams are considered as a part of the product and between 98% – 100% when waste streams are considered lost (Fig. 6.3). The facility that presents the highest efficiency is Platform B, as gas is not compressed before export and little power is required on-site.

Table 6.3: *Total* exergy efficiencies (%) without differentiating between waste useful streams and waste streams ε_{I-1} and with waste streams regarded as lost ε_{I-2}.

	Platform A	Platform B	Platform C	Platform D
ε_{I-1}	99.7	99.9	99.9	99.6
ε_{I-2}	99.5	99.8	99.8	98.0

The high numbers are caused by the inclusion of the chemical exergy of hydrocarbons in the formulation of these exergy efficiencies, and the total efficiencies are therefore always high. They can hardly be used to compare the performance of oil and gas facilities, since (i) they give the impression that all platforms are similar in terms of efficiency and (ii) they are poorly sensitive to improvement efforts.

Kotas [50] and Tsatsaronis [118] support this view in their works. They argue that the total exergy efficiencies do not show the potential for reducing the system inefficiencies, and that conclusions based on them would be misleading. Another critique on the total exergy efficiencies is that they do not reflect the *purposes* of operating these facilities, which are to separate the petroleum from the water, and to export the oil and gas to the shore.

The same reasoning can be drawn for the energy efficiency that is used for evaluation of some oil and gas platforms. On Platform D this parameter has varied between 92% and 94% these last years, although the flows of exported oil and gas have changed from day-to-day, and that flaring and venting was significantly reduced. This indicator provides limited information when the performance of an oil and gas system is analysed over time.

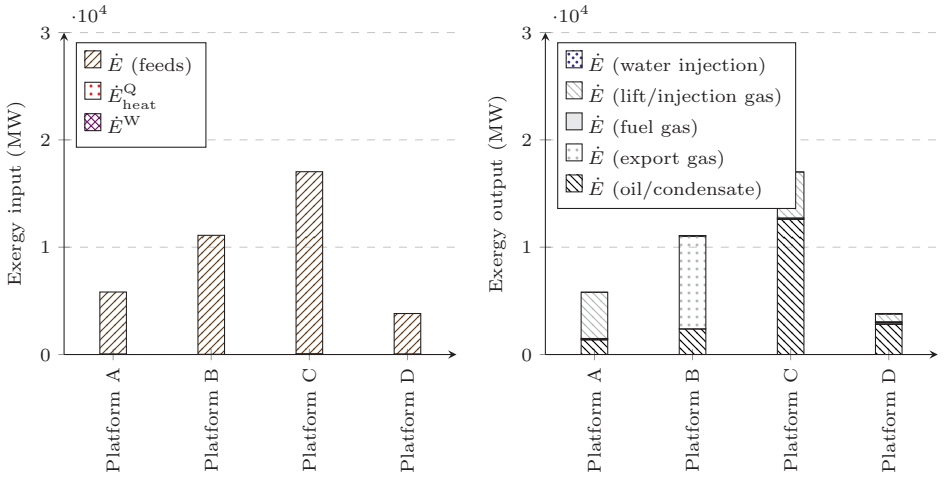

Figure 6.3: Exergy input and useful output flows.

6.4.3 Task exergy efficiency: Kotas for general separation systems, Oliveira for offshore platform

The exergy balance for the processing plant, Eq. 6.13, can be rewritten:

$$\underbrace{\dot{E}^{\mathrm{Q}}_{\mathrm{heat}} + \dot{E}^{\mathrm{W}}}_{\dot{E}_{\mathrm{f}}} = \underbrace{\left(\sum_k \dot{E}_k - \dot{E}_{\mathrm{feed}}\right)}_{\dot{E}_{\mathrm{p}}} + \underbrace{\dot{E}^{\mathrm{Q}}_{\mathrm{cool}}}_{\dot{E}_{\mathrm{l}}} + \underbrace{\dot{E}_{\mathrm{d,PP}}}_{\dot{E}_{\mathrm{d}}} . \tag{6.16}$$

The left-hand side terms can be identified as the resources required to drive the processing plant, i.e. the exergetic fuel $\dot{E}_{\mathrm{f}}$, while the difference of exergy between the inlet and outlet material streams can be considered as the exergetic product $\dot{E}_{\mathrm{p}}$. This approach is similar to the one suggested by Kotas [50] and used by Oliveira and Van Hombeeck [22] for petroleum separation processes on a Brazilian offshore platform, and used for the processing plant of an North Sea oil platform by Voldsund et al. [127, 128, 126].

This approach considers that the desired effect of the offshore platforms is the difference of exergy between the inlet and outlet streams, i.e. the exergy increase due to separation, and possibly the exergy increase with physical processes such as compression. The resources required to drive the processing plant and to separate the three phases correspond to the power and heat required on-site. The losses are identified as the exergy lost with the cooling water $\dot{E}_{\mathrm{l}}$ and the rest is the destroyed exergy $\dot{E}_{\mathrm{d}}$.

The expression for the exergy efficiency, denoted ε_{II-1}, is then given by:

$$\varepsilon_{II-1} = \frac{\sum_k \dot{E}_k - \dot{E}_{\text{feed}}}{\dot{E}^{\text{Q}}_{\text{heat}} + \dot{E}^{\text{W}}} = 1 - \frac{\dot{E}^{\text{Q}}_{\text{cool}} + \dot{E}_{\text{d,PP}}}{\dot{E}^{\text{Q}}_{\text{heat}} + \dot{E}^{\text{W}}}, \tag{6.17}$$

which is similar to the expression of the rational efficiency for a generalised separation plant [50].

Calculating the exergy efficiency with Eq. 6.17 (Table 6.4), it can be seen that most exergy (>85%) consumed in the processing plant corresponds to the power produced in the gas turbines (Fig. 6.4). This power consumption is related to the compression and pumping demands on-site. The consumption of thermal exergy is negligible in two cases, since heating is only required in the fuel gas system, where power is used to drive electric heaters.

The exergy efficiencies as defined in Eq. 6.17 for the processing plants of Platforms A, C and D are relatively low ($\simeq$ 13-24%). This is in accordance with the findings of Kotas [50], who suggested that the rational efficiency of separation processes is often low, because of the large compression ratios of the gas streams.

Table 6.4: Task exergy efficiencies (%) based on the approach of Kotas [50] and Oliveira and Van Hombeeck [22] for generic separation systems.

	Platform A	Platform B	Platform C	Platform D
ε_{II-1}	12.7	-215	20.6	23.6

Platform B presents a negative efficiency, since the exergy of the output streams is smaller than the exergy of the feeds. The pressures and temperatures of the oil and gas are lower than those of the feed since there is no need for gas compression before export. The reductions of physical exergy ($\simeq$ 12,200 kW) are thus higher than the increases of chemical exergy ($\simeq$ 300 kW), leading to the negative value. The same has been seen when this definition of the exergy efficiency has been applied at the level of the separation module for another platform [127].

This case illustrates the limitations of applying this approach for evaluation of our four different processing plants, and suggests that the differences of physical and chemical exergy between the input and output streams should be considered apart. The reduction of pressure throughout the platform results in a higher vapour fraction of the streams and drives the separation. The expense of physical exergy may therefore be accounted as a part of the resources spent to drive the processing plant.

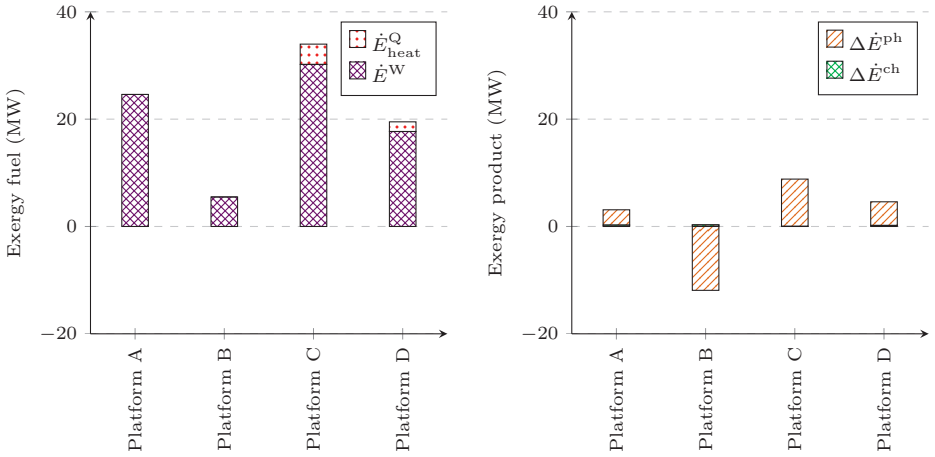

Figure 6.4: Exergy fuels and products, based on the approach of Kotas [50] and Oliveira and Van Hombeeck [22] for generic separation systems.

6.4.4 Task exergy efficiency: Cornelissen for crude oil distillation, Rian and Ertesvåg for LNG plant

Kotas [50] suggested an alternative to Eq. 6.17 for air distillation plants, where the physical and chemical exergy in the material streams are treated separately:

$$\begin{aligned}\underbrace{\dot{E}^{\mathrm{ph}}_{\mathrm{feed}} + \dot{E}^{\mathrm{Q}}_{\mathrm{heat}} + \dot{E}^{\mathrm{W}}}_{\dot{E}_{\mathrm{f}}} &= \sum_k \dot{E}^{\mathrm{ch}}_k - \dot{E}^{\mathrm{ch}}_{\mathrm{feed}} + \sum_k \dot{E}^{\mathrm{ph}}_{k,\mathrm{u}} + \sum_k \dot{E}^{\mathrm{ph}}_{k,\mathrm{w}} + \dot{E}^{\mathrm{Q}}_{\mathrm{cool}} + \dot{E}_{\mathrm{d,PP}} \\ &= \underbrace{\Delta E^{\mathrm{ch}} + \sum_{k,\mathrm{u}} \dot{E}^{\mathrm{ph}}_{k,\mathrm{u}}}_{\dot{E}_{\mathrm{p}}} + \underbrace{\sum_{k,\mathrm{w}} \dot{E}^{\mathrm{ph}}_{k,\mathrm{w}} + \dot{E}^{\mathrm{Q}}_{\mathrm{cool}}}_{\dot{E}_{\mathrm{l}}} + \underbrace{\dot{E}_{\mathrm{d,PP}}}_{\dot{E}_{\mathrm{d}}}.\end{aligned} \tag{6.18}$$

The exergetic fuel is now taken to be the sum of the exergy transferred as heat and power and the physical exergy of the feed. Similarly, the exergetic product is now taken as the difference of chemical exergies between the inlet and outlets of the processing plant as well as the physical exergy of the useful output streams.

This approach is similar to the one applied by Cornelissen [19] for a crude oil distillation plant and by Rian and Ertesvåg [82] for an LNG plant, where it is suggested that all physical exergy of the feed streams is consumed along with exergy associated with heat and power. The desired result is taken as the physical exergy of the outlet streams, as well as the increased chemical exergy due to separation.

The expression for the exergy efficiency of the system (ε_{II-2}) is then given by:

$$\varepsilon_{II-2} = \frac{\Delta E^{\mathrm{ch}} + \sum_{k,\mathrm{u}} \dot{E}^{\mathrm{ph}}_{k,\mathrm{u}}}{\dot{E}^{\mathrm{ph}}_{\mathrm{feed}} + \dot{E}^{\mathrm{Q}}_{\mathrm{heat}} + \dot{E}^{\mathrm{W}}} = 1 - \frac{\sum_{k,\mathrm{w}} \dot{E}^{\mathrm{ph}}_{k,\mathrm{w}} + \dot{E}^{\mathrm{Q}}_{\mathrm{cool}} + \dot{E}_{\mathrm{d,PP}}}{\dot{E}^{\mathrm{ph}}_{\mathrm{feed}} + \dot{E}^{\mathrm{Q}}_{\mathrm{heat}} + \dot{E}^{\mathrm{W}}}. \tag{6.19}$$

When applying this approach (Table 6.5, Fig. 6.5), the exergetic fuel amounts from 33 MW (Platform D) to 110 MW (Platform B). The major contributions to the fuel are the physical exergy of the feeds and the power consuption. In any case, it can be seen that most exergy consumed on the plant is used to produce high-pressure gas, and that the separation effect is negligible in comparison.

Table 6.5: Task exergy efficiencies (%) based on the approach of Cornelissen [19] and Rian and Ertesvåg [82] for crude oil distillation and LNG plants.

	Platform A	Platform B	Platform C	Platform D
ε_{II-2}	70.9	84.2	71.0	33.2

The platform that presents the highest exergy efficiency, as defined in Eq. 6.19, is Platform B ($\simeq$ 84%), followed by Platforms A ($\simeq$ 71%), C ($\simeq$ 71%) and D ($\simeq$ 33%). The higher performance of Platform B can be explained by the high rate of physical exergy transiting throughout the plant with the produced gas. Gas is exported at nearly the same conditions as it enters, and its physical exergy dominates transformations taking place on-site. On the opposite side, Platform D presents a smaller exergy efficiency, because the lift and export pressures ($\simeq$ 175–180 bar) are much higher than the feed pressures ($\simeq$ 11–45 bar) and the separation pressures ($\simeq$ 1.7–8 bar). Significant amount of power is required to increase the gas pressure, which results in high irreversibilities in the gas compression section. Moreover, the water cut of the feeds is much higher ($\simeq$ 85–95% on a mole basis), and the produced water is currently discharged to the sea at high temperatures, and thus high physical exergies ($\simeq$ 6.1 MW), without being further used.

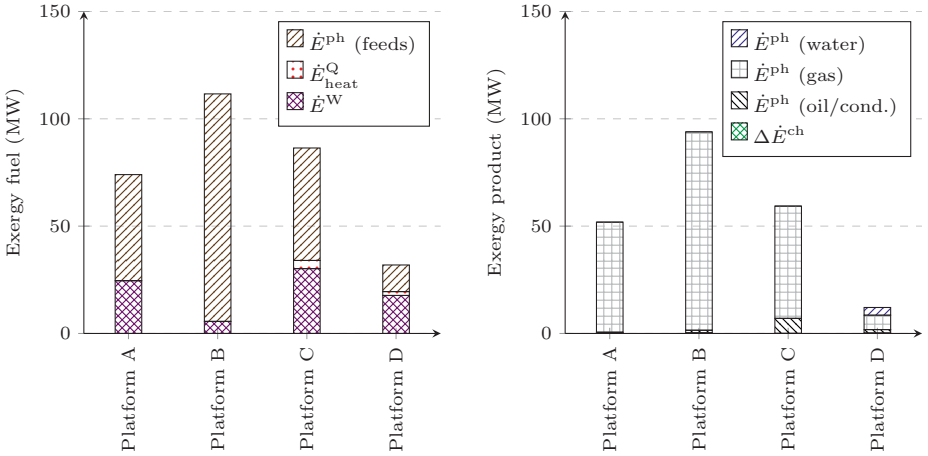

Figure 6.5: Exergy fuels and products, based on the approach of Cornelissen [19] and Rian and Ertesvåg [82] for crude oil distillation and LNG plants.

When this approach was used for an LNG plant, most physical exergy entering

the system was pressure-based, and most leaving the system was temperature-based. This is different in the present cases, where most physical exergy that enters and exits is pressure based, and has not necessarily undergone exergy transformations within the process.

6.4.5 Task exergy efficiency: Tsatsaronis and Cziesla for distillation columns

In the third alternative formulation of the *task* exergy efficiency, the fuel exergy is defined as the sum of the physical exergy decreases between the inflowing feed and the separated streams with a lower specific physical exergy (k^-) and the exergy associated with heating and power. The product exergy is defined as the sum of the physical exergy increases between the inflowing feed and the separated useful products with a higher specific physical exergy (k^+) and the chemical exergy increases between the feed and products. By separating between product streams with increased and decreased specific physical exergy, Eq. 6.13 can be rewritten:

$$\underbrace{\sum_{k^-} \dot{m}_{k^-} \cdot (e^{\mathrm{ph}}_{\mathrm{feed}} - e^{\mathrm{ph}}_{k^-}) + \dot{E}^{\mathrm{Q}}_{\mathrm{heat}} + \dot{E}^{\mathrm{W}}}_{\dot{E}_{\mathrm{f}}} =$$

$$\underbrace{\Delta E^{\mathrm{ch}} + \sum_{k^+,\mathrm{u}} \dot{m}_{k^+,\mathrm{u}} \cdot (e^{\mathrm{ph}}_{k^+,\mathrm{u}} - e^{\mathrm{ph}}_{\mathrm{feed}})}_{\dot{E}_{\mathrm{p}}} + \underbrace{\sum_{k^+,\mathrm{w}} \dot{m}_{k^+,\mathrm{w}} \cdot (e^{\mathrm{ph}}_{k^+,\mathrm{w}} - e^{\mathrm{ph}}_{\mathrm{feed}}) + \dot{E}^{\mathrm{Q}}_{\mathrm{cool}}}_{\dot{E}_{\mathrm{l}}} + \underbrace{\dot{E}_{\mathrm{d,PP}}}_{\dot{E}_{\mathrm{d}}}. \tag{6.20}$$

The expression for the exergy efficiency of this system (ε_{II-3}) is then given by:

$$\begin{aligned} \varepsilon_{II-3} &= \frac{\Delta E^{\mathrm{ch}} + \sum_{k^+,\mathrm{u}} \dot{m}_{k^+,\mathrm{u}} \cdot (e^{\mathrm{ph}}_{k^+,\mathrm{u}} - e^{\mathrm{ph}}_{\mathrm{feed}})}{\sum_{k^-} \dot{m}_{k^-} \cdot (e^{\mathrm{ph}}_{\mathrm{feed}} - e^{\mathrm{ph}}_{k^-}) + \dot{E}^{\mathrm{Q}}_{\mathrm{heat}} + \dot{E}^{\mathrm{W}}} \\ &= 1 - \frac{\sum_{k^+,\mathrm{w}} \dot{m}_{k^+,\mathrm{w}} \cdot (e^{\mathrm{ph}}_{k^+,\mathrm{w}} - e^{\mathrm{ph}}_{\mathrm{feed}}) + \dot{E}^{\mathrm{Q}}_{\mathrm{cool}} + \dot{E}_{\mathrm{d,PP}}}{\sum_{k^-} \dot{m}_{k^-} \cdot (e^{\mathrm{ph}}_{\mathrm{feed}} - e^{\mathrm{ph}}_{k^-}) + \dot{E}^{\mathrm{Q}}_{\mathrm{heat}} + \dot{E}^{\mathrm{W}}}. \end{aligned} \tag{6.21}$$

which is similar to the expression of the exergy efficiency for a generalised distillation column, as discussed by Tsatsaronis and Cziesla [120].

The approach of Tsatsaronis and Cziesla considers the physical exergy decreases as part of the exergetic fuel, and the increases as part of the exergetic product, which is in accordance with the SPECO method proposed by Lazzaretto and Tastsaronis [51, 52] and the previous works of Baehr [11] and Grassmann [31]. They define physical exergy decreases and increases by comparing the specific physical exergies of the outlet and inlet streams on a mass basis.

Calculating this efficiency on a mass basis (Table 6.6), suggests that Platform C presents the highest performance ($\simeq 54\%$), followed by Platforms A ($\simeq 48\%$), B ($\simeq 39\%$) and D ($\simeq 39\%$).

Table 6.6: Task exergy efficiencies (%) based on the approach of Tsatsaronis and Cziesla for distillation columns.

	Platform A	Platform B	Platform C	Platform D
$\varepsilon_{II-3,\text{mass}}$	48.1	39.0	53.9	38.8
$\varepsilon_{II-3,\text{molar}}$	38.2	1.7	49.3	39.3

The exergetic fuel includes two major contributions (Fig. 6.6), which are the reduction in physical exergy and the power consumption. With the exception of Platform B, most exergetic fuel consists of the power input ($\geq 55\%$). The physical exergy reduction is mainly caused by the decrease of pressure of the produced water (Platform D) and of the exported oil (Platforms A, B and C) compared to the feed pressure.

The exergetic product mainly includes an exergy increase of the gas flows, either for injection (Platforms A and C) or for export (Platform B), with the exception of Platform D, where nearly 40% of the exergetic product consists of the exergy increase of the seawater pumped for injection. Such conclusions may be expected, as the gas products mostly have significantly higher pressures than the feed streams. An exception is the exported gas from Platform B, which presents both lower pressure and temperature than the feed streams, but still displays a higher specific physical exergy than the feed streams.

Applying the same expression on a molar basis, returns different numerical values and conclusions (Table 6.6, Fig. 6.7). Furthermore, the exergetic fuels and products differ slightly for Platforms A, C and D, and significantly for Platform B. The inconsistencies are due to the different compositions of the feed and product streams that are compared. For Platforms A, C and D a calculation on molar basis lead to a somewhat higher or lower value for each exergy increase or decrease. For Platform B, this results in a change from an exergy increase to an exergy decrease, and thus in different calculations of the product and fuel exergies for the gas export stream. Specific and molar physical exergy of the inlet and outlet streams for Platform B are shown in Fig. 6.8. It can be seen that the specific physical exergy of the export gas is higher than the specific physical exergy of the well streams, while the molar physical exergy is lower.

Effects from this inconsistency may be small for distillation columns that separate similar components, while for our application to oil and gas platforms, which process highly different chemical components, the effect is considerable.

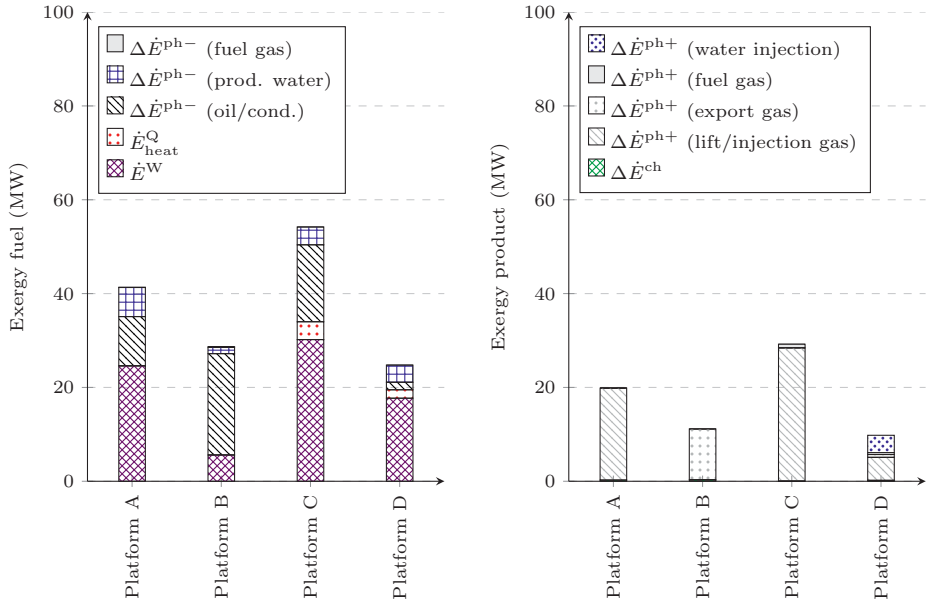

Figure 6.6: Exergy fuels and products, based on the approach of Tsatsaronis and Cziesla for distillation columns, calculated on a mass basis.

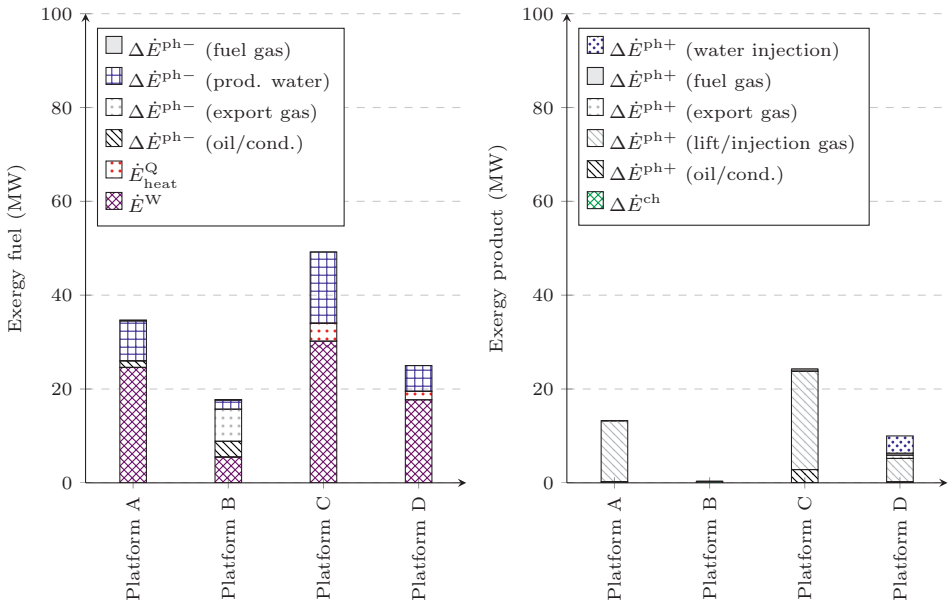

Figure 6.7: Exergy fuels and products, based on the approach of Tsatsaronis and Cziesla for distillation columns, calculated on a molar basis.

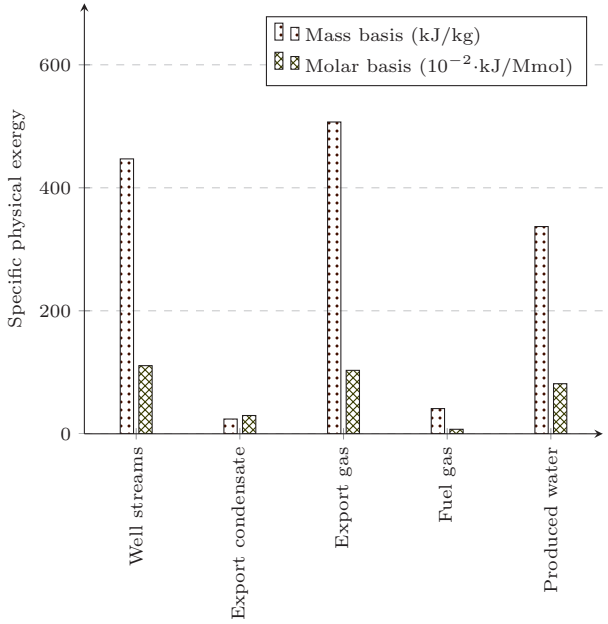

Figure 6.8: Specific physical exergy of the inlet and outlet streams for Platform B, expressed on a mass and molar basis.

6.4.6 Applicability to offshore processing plants

The calculations of exergy efficiencies with definitions found in the literature, and applied to our four offshore processing plants, raise several points of importance. The expressions were derived for either similar systems (e.g. the approach of Kotas [50] and Oliveira [22]) or systems which present common features to petroleum separation systems (e.g. the approach of Rian and Ertesvåg [82]). In consequence, they may not be fully applicable to the systems investigated in this work.

The *total* exergy efficiencies can unambiguously be calculated, but they can hardly be used for suggesting system improvements, as they do not assess the thermodynamic transformations taking place on-site. The *task* efficiencies reflect the tasks of the systems they are used for. The formulations presented so far show a few drawbacks and may favour or penalise platforms of a special type, or operating under certain conditions. The exergy efficiency as defined by Kotas [50], which was derived for oil and gas separation systems, fails for systems where the physical exergy outputs are smaller than the inputs (Platform B). The one suggested by Rian and Ertesvåg [82] is not directly applicable to oil and gas separation systems, as they investigate a gas facility where natural gas is cooled and liquefied. This refrigeration task is not found on any of the petroleum separation systems studied in this work. The literal formulation of an exergy efficiency as proposed by Tsatsaronis and Cziesla [118] has limitations, since the numerical values differ with the choice of

a molar or mass basis. This approach may be applied at the level of each chemical component, to quantify precisely the exergy transfers taking place, rather than at the level of each material stream.

6.5 Component-by-component exergy efficiency

6.5.1 Concept

As seen in the previous section the formulation of an exergy efficiency for oil and gas platforms is not straightforward, because of (i) the high transit chemical (and sometimes also physical) exergy of hydrocarbon components, (ii) the large variety of chemical components and (iii) the differences in process conditions and product specifications among these facilities. In order to fully evaluate the performance of a petroleum system and of separation processes, we propose the following definition of efficiency. It builds on the same reasoning as presented in the work of Tsatsaronis and Cziesla [121]. The increase of chemical exergy between all input and output streams is taken as the first contribution to the exergetic product. The second contribution is related to increases in physical exergy of useful product streams. However, the specific physical exergies of the *entire* streams are not compared with the specific physical exergies of the feed streams. For each feed stream, different parts may end up in different products. Therefore, the physical exergy of each such part in the feeds are compared with the physical exergy of the corresponding parts in the products. The exergy that is spent in the system is taken as the power and heat exergy consumed onsite, as well as the decrease of physical exergy of fractions that lose physical exergy on the way from feed to product. This is the same concept as that of the exergy efficiency that consider transit exergy [16], but carried out on the chemical component level.

A schematic overview of the component flows for a system with two components, two feeds and two products is shown in Fig. 6.9. The physical exergy of each part at the outlet $\dot{E}^{\mathrm{ph}}_{j,k,\mathrm{out}}$, will either have increased or decreased compared to the physical exergy of the same part at the inlet $\dot{E}^{\mathrm{ph}}_{j,k,\mathrm{in}}$. Since the exergetic fuel and the exergetic product are evaluated at the chemical component level, this efficiency is called the *component-by-component* efficiency.

6.5.2 Derivation

The physical exergies of the *part* of a stream coming from feed j, $\dot{E}^{\mathrm{ph}}_{j,k,\mathrm{in}}$, and ending up in product k, $\dot{E}^{\mathrm{ph}}_{j,k,\mathrm{out}}$, are calculated using the following equations:

$$\dot{E}^{\mathrm{ph}}_{j,k,\mathrm{in}} = \sum_{i} \dot{n}_{i,j,k} \hat{e}^{\mathrm{ph}}_{i,j} \tag{6.22}$$

$$\dot{E}^{\mathrm{ph}}_{j,k,\mathrm{out}} = \sum_i \dot{n}_{i,j,k} \hat{e}^{\mathrm{ph}}_{i,k}. \tag{6.23}$$

The symbol $\hat{e}^{\mathrm{ph}}_{i,j}$ denotes the partial molar physical exergy of component i in feed stream j, $\hat{e}^{\mathrm{ph}}_{i,k}$ denotes partial molar physical exergy of component i in product stream k and $n_{i,j,k}$ denotes the molar flow of component i from feed j to product k.

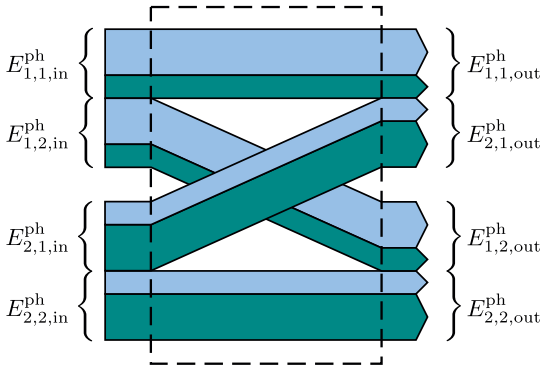

Figure 6.9: Schematic overview of component flows in and out of a control volume for a system with two components marked with different colors, two feeds at the left and two product streams at the right.

For each component in each feed stream, it is assumed that the fraction of the component ending up in each product stream is the same as the fraction of the total amount of this component entering as feeds ending up in each product stream. For instance, for methane in feed 1, it is assumed that the fraction of this methane ending up in product 1 is the same as the fraction of the total amount of methane ending up in product 1.

Physical exergy increases of parts of streams can be expressed mathematically:

$$\left(\Delta \dot{E}^{\mathrm{ph}}_{j,k}\right)^{+} = \begin{cases} \dot{E}^{\mathrm{ph}}_{j,k,\mathrm{out}} - \dot{E}^{\mathrm{ph}}_{j,k,\mathrm{in}} & \text{if } \dot{E}^{\mathrm{ph}}_{j,k,\mathrm{out}} > \dot{E}^{\mathrm{ph}}_{j,k,\mathrm{in}} \\ 0 & \text{if } \dot{E}^{\mathrm{ph}}_{j,k,\mathrm{out}} < \dot{E}^{\mathrm{ph}}_{j,k,\mathrm{in}} \end{cases} \tag{6.24}$$

Oppositely, physical exergy decreases of parts of streams can be expressed:

$$\left(\Delta \dot{E}^{\mathrm{ph}}_{j,k}\right)^{-} = \begin{cases} 0 & \text{if } \dot{E}^{\mathrm{ph}}_{j,k,\mathrm{out}} > \dot{E}^{\mathrm{ph}}_{j,k,\mathrm{in}} \\ \dot{E}^{\mathrm{ph}}_{j,k,\mathrm{in}} - \dot{E}^{\mathrm{ph}}_{j,k,\mathrm{out}} & \text{if } \dot{E}^{\mathrm{ph}}_{j,k,\mathrm{out}} < \dot{E}^{\mathrm{ph}}_{j,k,\mathrm{in}} \end{cases} \tag{6.25}$$

The exergy balance, Eq. 6.13, can thus be rewritten:

$$\underbrace{\sum_j \sum_k \left(\Delta \dot{E}^{\mathrm{ph}}_{j,k}\right)^- + \dot{E}^{\mathrm{Q}}_{\mathrm{heat}} + \dot{E}^{\mathrm{W}}}_{\dot{E}_{\mathrm{f}}} =$$

$$\underbrace{\Delta \dot{E}^{\mathrm{ch}} + \sum_j \sum_{k,\mathrm{u}} \left(\Delta \dot{E}^{\mathrm{ph}}_{j,k}\right)^+_{\mathrm{u}}}_{\dot{E}_{\mathrm{p}}} + \underbrace{\sum_j \sum_{k,\mathrm{w}} \left(\Delta \dot{E}^{\mathrm{ph}}_{j,k}\right)^+_{\mathrm{w}} + \dot{E}^{\mathrm{Q}}_{\mathrm{cool}}}_{\dot{E}_{\mathrm{l}}} + \underbrace{\dot{E}_{\mathrm{d,PP}}}_{\dot{E}_{\mathrm{d}}}. \tag{6.26}$$

This result in the following expression for the exergy efficiency (ε_{II-4}):

$$\begin{aligned} \varepsilon_{II-4} &= \frac{\sum_j \sum_k \left(\Delta \dot{E}^{\mathrm{ph}}_{j,k}\right)^+_{\mathrm{u}} + \Delta \dot{E}^{\mathrm{ch}}}{\sum_j \sum_k \left(\Delta \dot{E}^{\mathrm{ph}}_{j,k}\right)^- + \dot{E}^{\mathrm{Q}}_{\mathrm{heat}} + \dot{E}^{\mathrm{W}}} \\ &= 1 - \frac{\sum_j \sum_k \left(\Delta \dot{E}^{\mathrm{ph}}_{j,k}\right)^+_{\mathrm{w}} + \dot{E}^{\mathrm{Q}}_{\mathrm{cool}} + \dot{E}_{\mathrm{d,PP}}}{\sum_j \sum_k \left(\Delta \dot{E}^{\mathrm{ph}}_{j,k}\right)^- + \dot{E}^{\mathrm{Q}}_{\mathrm{heat}} + \dot{E}^{\mathrm{W}}}. \end{aligned} \tag{6.27}$$

This approach, at the chemical component level, takes into account the fact that in separation processes the feed and product streams display the same chemical components, but in different quantities. Gas mostly contains light-hydrocarbons, which have much lower molecular weight than the chemical components of oil. As different types of chemical components do not have the same thermodynamic properties (enthalpy and entropy) at the same environmental conditions (temperature and pressure), this implies that different components carry different quantities of physical exergy. Decomposing the physical exergy of a stream into the physical exergy per chemical component allows therefore a more accurate calculation of the exergy fuels and products. This formulation of exergy efficiency is not valid only for oil and gas offshore platforms, but can be generalised to separation processes.

6.5.3 Results

The calculations of the exergy efficiency as given in Eq. 6.27, suggest that Platforms D and C present the highest thermodynamic performances, while Platform B presents the poorest performance (Table 6.7). With the exception of Platform B, the major exergy fuel consists of the power consumed on-site to perform the pumping and compression operations (Fig. 6.10).

Table 6.7: *Task* exergy efficiencies (%) based on the *component-by-component* approach.

	Platform A	Platform B	Platform C	Platform D
ε_{II-4}	17.9	1.7	26.8	29.6

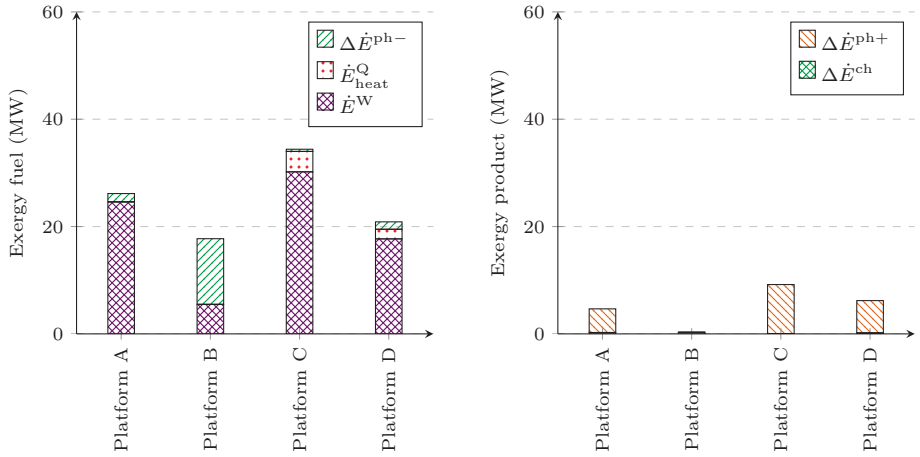

Figure 6.10: Exergy fuels and products, based on the *component-by-component* approach.

Oil and gas platforms perform separation, pumping and compression work, but in different magnitudes, and this explains some the large differences in terms of efficiencies between the four facilities:

- Platform A processes oil, gas and water: the three phases are separated, oil is pumped to another platform, gas is compressed to more than 200 bar for further injection, and water is discharged to the sea at low pressures. The *separation* work is small in comparison to the pumping work, and negligible towards the compression one.

- Platform B processes condensate, gas and water: gas and oil exported at a pressure lower than the feed pressure, and the separation work is mostly driven by the decreases in physical exergy.

- Platform C processes oil, gas and water: oil is exported at a much higher pressure than the feed pressure, and the pumping work on this platform is significantly higher than on Platforms A and B.

- Platform D processes oil, gas, and significant quantities of produced water. Seawater is also pumped for further injection, and small quantities of gas are compressed and exported or injected compared to Platform A.

6.6 Discussion

6.6.1 Sensitivity

The problems rising from the use of the total exergy efficiencies when evaluating petroleum separation processes stem from the fact that these expressions include the chemical exergy of hydrocarbons. The interest of these expressions of exergy efficiencies is limited, because these indicators return similar numerical values for all cases. They will indeed have so little sensitivity to changes in the system that they cannot be used for assessing the improvement potentials of oil and gas systems, or to analyse the different trade-off. All the *task* exergy efficiencies showed a clear difference between the four facilities, and are also expected to be sensitive to system improvements.

6.6.2 Feasibility and simplicity

The approaches found in the scientific literature presented all drawbacks compared to the *component-by-component* efficiency, stemming from the fact that they were derived for systems with partly different tasks. However, some of them require significantly less calculation efforts. The use of the exergy efficiencies as defined in the approaches of Kotas [50] and Oliveira [22], and of Cornelissen [19] and Rian and Ertesvåg [82], requires flow, temperature and pressure measurements, which are often already conducted, as well as crude oil and gas assays to estimate the composition. The *component-by-component* efficiency requires significantly more calculational efforts than the other definitions, since the calculations are done on a component level, and the partial molar physical exergy of each component has to be calculated.

6.6.3 Transparency

The expressions and numerical values of the exergy efficiencies are dependent on the choice of:

- environmental state: the environmental temperature has a direct impact on physical and chemical exergy, and the environmental pressure has an impact on the physical exergy;
- system boundaries: the inclusion of the import and export pipelines and of the gas lift system would impact the numerical values of the mechanical exergy increases.

The choice of the environmental state and the system boundaries should be made clear to allow a sound comparison of different facilities.

6.6.4 Temperature-based and pressure-based exergy

The exergy balances and interpretation of product in the *component-by-component* efficiency can be improved by decomposing the physical exergy term into its temperature-based and pressure-based components. For example, one of the desired outcomes of the processing plant is the export of gas at high pressure, which is equivalent, from a thermodynamic viewpoint, to the production of pressure-based exergy. The temperature-based exergy of gas streams is a result of the turbomachinery component inefficiencies, and is dissipated to a large extent in the export pipelines. Pressure-based exergy increases should therefore be accounted as a part of the exergetic product (desired outcome of the system), while the temperature-based exergy increases should be considered as a part of the exergetic losses. These considerations were also emphasised in the studies of Kotas [50], Cornelissen [19] for oil and gas distillation systems, and Marmolejo-Correa and Gundersen [59] for LNG processes.

Such decompositions would further increase the required computational efforts [51, 52]. In the present cases it is expected that the decomposition would only very slightly affect the numerical results, as the pressure-based exergy of gas generally dominates the temperature-based exergy (96% against 4% in the work of Voldsund et al. [126] for Platform A). The benefit of such an improvement in the efficiency should be evaluated against the larger required computational efforts.

6.6.5 Theoretical versus practical improvement potential

Exergy efficiencies should give hints for setting meaningful benchmarks, and evaluate unambiguously the performance of the system under study. They should provide a measure of the resources that are required to drive the processing plant and platform, and of the desired outcome of these systems. One may argue that these targets are not realistic, as there are practical constraints:

- economical – integrating other components or redesigning the system may be costly, and possibly cause shut-downs of the plant during the installation phase;
- technical – the structural design of the processing plant is partly fixed and bound by the field characteristics (e.g. temperatures and pressures) and the export conditions (e.g. purity);
- technological – the performance of a process component is limited by the current technological advances (e.g. state-of-the art centrifugal compressors).

These constraints imply that only a part of the thermodynamic inefficiencies taking place in petroleum separation processes can be reduced in practice, whereas another part cannot be avoided.

Bejan et al. [13] emphasised the difficulty of using the exergy efficiency for comparing systems with dissimilar functions, which is the case of oil and gas platforms. All platforms have the functions of separation, compression and pumping, but due to differences in their operating conditions (field conditions and product specifications), some platforms must do more compression (Platform A), while others mainly do pumping work (Platform D), and some may do less of compression and pumping, and thus almost only separation (Platform B). In general, pumps are characterised by a higher exergetic performance than compressors, which again are more exergy efficient than systems with separation tasks. Different systems present different potentials for improvement.

One way to overcome this problem may be to evaluate different subprocesses separately. If for instance the performance of separation was evaluated individually, or similarly the performance of compression or pumping, the platforms could be compared on a similar basis. The issue of comparing systems with dissimilar functions would be eliminated.

Another way to tackle this is to define an additional performance indicator that evalutes the performance related to what is practically achievable. The following resonings may be applied:

- Tsatsaronis and Park [121], who defined the unavoidable exergy destruction as the exergy that is destroyed when the current components are operated at their maximum efficiency, considering technological limitations that could not be overcome in the near future, regardless of the investment costs;
- Margarone et al. [58], who proposed to compare the current plant performance against that obtainable when integrating the state-of-the-art technologies present on the market;
- Johannessen et al. [40, 41], who suggested to set a state of minimum entropy production or minimum exergy destruction for a given operation target, and the difference between the current value and this minimum would be considered as an excess loss.

Such approaches could both give a more realistic target for each platform, and allow a comparison between them on how well they utilise their practically achievable potential. The main criticisms against these approaches are the degree of subjectivity when defining the state of unavoidable exergy destruction, and the high sensitivity of such targets to future technological achievements.

6.6.6 Performance and ageing

It is generally admitted that the performance of oil and gas platforms decreases with time, as a result of ageing and degradation of the on-site components and

processes. Meanwhile, the main function of an offshore platform may change over time due to changing operating conditions. For instance has an increased gas-to-oil ratio for Platform A resulted in more necessary compression work over the last 20 years, while increased water-to-oil ratio for Platform D has resulted in more pumping work necessary. Thus, using exergy efficiency to monitor installations over time may give results that are biased by the change in the relative importance of compression, pumping and separation over time, if not approaches such as those mentioned in Section 6.6.5 are taken into use.

Such issue may not be faced in the case of other petrochemical processes, since the variations over time of the gas and water contents of the feed are not as significant.

6.6.7 Significance

Exergy efficiency indicators may be coupled to other performance criteria, such as the specific power or exergy consumptions, which assess the expense of resources for a given unit of oil and gas. The latter illustrate different aspects of the current operations.

For instance, taking the *component-by-component* efficiency, one can conclude that Platform B presents the smallest exergy efficiency of the four investigated cases. It should be noticed that this facility has also the smallest specific power consumption, because there is very little need for compression. This characteristic illustrates the effects of the field conditions and export specifications, on the system performance.

6.6.8 Generalisation

The *component-by-component* efficiency presented in this paper may be of interest for petrochemical systems other than oil and gas platforms. It can be applied to industrial systems where petroleum is fractionated, since similar processes take place (compression, expansion, separation, distillation).

Some of the major differences are:

- the much greater amount of heat exergy consumed in some separation process, as large quantities of heat are required to preheat oil and to sustain the temperature gradient of distillation columns [83]. Separation of the oil fractions in refineries is therefore more temperature-driven than pressure-driven, at the difference of oil and gas platforms.
- the quantity of exergy destroyed in distillation columns in refineries represents a non-negligible part of the total exergy input, at the difference of oil and gas platforms where it represents less than 3% in any of the studied cases.

Although oil and gas platforms and oil refineries aim at separating the hydrocarbons composing the oil and gas mixtures, the performance of both systems may not be directly comparable since the structural design setup are fundamentally different.

6.7 Conclusion

Exergy efficiency definitions found in the scientific literature for similar systems had drawbacks such as (i) low sensitivity to efficiency improvements, (ii) calculation inconsistencies or (iii) favoured facilities with certain boundary conditions when applied to the four offshore processing plants. Based on these experiences, the *component-by-component* efficiency was proposed. This efficiency is sensitive to process improvements, gives consistent results and evaluates successfully the theoretical improvement potential. However, it requires high computational efforts. It ranges between 1.7 and 29.6% for our four cases. This efficiency is applicable also to other petroleum processes.

Acknowledgements

The motivation from Statoil's new-idea project of reducing CO_2 emissions from offshore oil and gas platforms is essential to this study. The Faculty of Natural Sciences and Technology at the Norwegian University of Science and Technology is acknowledged for financial support, as well as the funding from the Norwegian Research Council through the Petromaks programme, within the project 2034/E30 led by Teknova.

Nomenclature

e	specific exergy, J/kg
$\dot{E}$	exergy rate, W
h	specific enthalpy, J/kg
p	pressure, Pa
s	specific entropy, J/(kg·K)
$\dot{S}$	entropy rate, W/K
T	temperature, K
x	mass fraction, -
y	component/sub-system exergy ratio, -
β	chemical exergy correction factor, -
ε	exergy efficiency, -

Abbreviations

GOR	gas-to-oil ratio
LNG	liquefied natural gas
NHV	net heating value
OP	overall plant
PP	processing plant
TEG	triethylene glycol
WOR	water-to-oil ratio

Superscripts

ch	chemical
kin	kinetic
ph	physical
pot	potential
Q	heat
W	work
+	increase
-	decrease
$\hat{}$	partial molar
*	relative

Subscripts

cool	related to cooling
cv	control volume
d	destruction
f	fuel
feed	feed
gen	generation
h	hypothetical
heat	related to heating
i	chemical component i
in	inlet
j	stream j, feed stream j
k	heat transfer stream k, exergy stream k, product stream k
l	loss
mix	mixture
mt	metal
out	outlet
p	product
tr	transit
u	useful
w	waste
0	dead state

6.A Process details

The tables with pressures and temperatures in key streams are not included in this section, because they are identical to Tables 4.2 and 4.3 in Chapter 4.

6.B Process flowsheet

The process flowsheets are not included in this section, because they are identical to the flowsheets presented in Chapter 4. See Figs. 4.7–4.10 in Appendix 4.A.

Chapter 7

Conclusions and perspectives

This thesis presents the first exergy analyses of offshore oil and gas processing in the North Sea. In this chapter the different cases that are studied are summarised. Then conclusions are drawn separately for the exergy mapping, the considered improvement options and for the studies concerning performance indicators.

7.1 Case studies

Exergy analyses of the oil and gas processing plants of the following North Sea type offshore platforms were carried out:

- An oil platform with oil export and high gas injection rate. It is a real case based on measured data, and the analysis is presented in Chapters 2 and 4 (Platform A).
- An oil and gas platform that exports oil and dehydrated gas. This is a generic model based on literature data with six different feed compositions. The results are presented in Chapter 3 (generic model, Cases 1–6).
- A platform exporting condensate and gas. The reservoir pressure is high while the gas export pressure is low, and the gas is not dehydrated. It is a real case based on measured data, and the analysis is presented in Chapter 4 (Platform B).
- An oil platform exporting viscous oil. Gas is used for injection and gas lift. It is a real case based on measured data, and the analysis is presented in Chapter 4 (Platform C).

- An oil and gas platform with high water cut that exports oil and dehydrated gas, and has a separate condensate treatment section. It is a real case based on measured data. The analysis is presented in Chapter 4 (Platform D).

The exergy analysis of Platform A (Chapter 2) was performed with decomposition into pressure-based, temperature-based and chemical exergy, and a detailed uncertainty analysis was carried out. In the analysis of the generic model (Chapter 3), the impact of feed composition was examined in particular, and the utility plant was included in the analysis. Platforms B–D were analysed with focus on comparison of these platforms and Platform A (Chapter 4). The cases of Platforms A–D were then used to evaluate the applicability of different performance indicators to offshore oil and gas processing plants (Chapter 5), as well as different formulations of the exergy efficiency (Chapter 6).

7.2 Exergy consumption, destruction and losses

The processes taking place in the oil and gas processing system consume exergy in form of heat and power produced in the utility plant. For the cases studied in this work, the power consumption is in the range of 5.5–30 MW, or 20–660 MJ/Sm^{3}o.e. exported. The heat demand is for all cases low enough to be covered by utilising waste heat from the utility plant and/or by heat integration between process streams. Electric heating takes place to a minor extent (less than 0.4 MW).

The major power demand (40–78%) is associated with the compressors in the gas treatment system in all cases, with the exception of Platform B and Case 4 of the generic model. These differences can be explained by the gas export pressure, which is lower than the reservoir pressure in the case of Platform B, and by the large amount of heavy components in the feed, and thus the great power demand of the oil export pumps in Case 4. The recompression- and oil pumping sections appear to be the other significant power consumers, together with the seawater injection system for platforms where this process is installed.

For a complete offshore platform, the major part of the exergy destruction and exergy losses takes place in the utility system. In the analysis of the generic model, it was shown that 62–65% of the total exergy destruction occurs here, while 35–38% takes place in the oil and gas processing system. Out of the losses, 56–59% are lost with exhaust gases while the rest are lost with flared gas, cooling water and wastewater, and is therefore related to the oil and gas processing plant.

The total exergy destruction within the oil and gas processing plant is in the range of 12–32 MW, or 43–517 MJ/Sm^{3}o.e. exported. Most exergy destruction is related to pressure increase or decrease. Inefficiencies in the gas treatment section causes 8–57% of the total amount, destruction in the recompression section amounts to 11–29%, while irreversibilities in the production manifold accounts for 10–28% of

the total exergy destruction. The separation and oil/condensate export sections are of varying importance with 4–27% and 1–24%, respectively. The exergy destruction in the gas treatment and recompression sections appears partly in compressors, coolers and anti-surge recycle streams, while the exergy destruction in production manifolds is due to throttling. In the separation sections, the destruction appears due to throttling, mixing and heating, and in the oil/condensate export sections the destruction is mainly due to pumping and cooling.

Exergy losses due to flaring are significant on Platform A (5.0 MW), in the generic model (10–13 MW) and on Platform D (4.7 MW) for the studied production days. The exergy losses associated with flaring fluctuate with time, as flaring is practiced on a discontinuous basis. Exergy losses with produced water is significant on Platform C (5.6 MW) and Platform D (22 MW). Most of these losses are related to the chemical exergy of water and can hardly be utilised.

It was found in Chapter 3 that the variability of the feed composition has little effect on the split of thermodynamic inefficiencies between the oil and gas processing system and the utility plant, while the impact on the distribution of exergy destruction between subsystems in the oil and gas processing system was higher. In Chapter 4 it was pointed out that the gas treatment systems and production manifolds had high irreversibilities for the four platforms considered, while the contributions of the recompression, separation and oil export sections varied across the different platforms. Platforms with high gas-to-oil ratios and high pressures required in the gas product presented the highest power consumption and exergy destruction.

7.3 Measures for improving thermodynamic efficiency

Measures are proposed for reduction of exergy destruction and exergy losses. The following two points present mature technologies that can increase the thermodynamic performances of the oil and gas processing systems significantly:

- Limit flaring by installing flare gas recovery systems. The exergy losses due to flaring can then almost be eliminated under normal operation. A flare gas recovery system is already installed on Platform C.
- Improve gas compression performance. Compressor efficiencies are generally low on the studied platforms, and anti-surge recycling is frequently performed as a consequence of off-design conditions. Re-wheeling of existing compressors or installation of variable speed drive systems can improve compression efficiency and eliminate anti-surge recycling. In Chapter 3 the high impact of compressor efficiencies on total power demand was demonstrated, while in

Chapter 5 it was shown that the exergy consumption could be reduced to 62–79% with the use of best available technology for compression and pumping. However, it is unrealistic to aim for continuous operation with best available technology, due to varying feed compositions and flow rates.

The exergy destruction in the production manifolds may be reduced by integration of additional production manifolds and separators at higher pressure levels, integration of multiphase expanders or multiphase ejectors. Such solutions are not in common use yet, and multiphase expanders or ejectors face additional issues at the present conditions with sand and other impurities. However, multiphase expanders may also be an option in the separation sections. Exergy lost with cooling water can be reduced by better heat integration between process streams. The heat demand is low, and most of it is covered with heat integration or waste heat recovery already, but the small amounts of electric heating (Fig. 4.2, Chapter 4) can be reduced by heat integration, wich is done on Platform B. This picture may be different for offshore platforms in other parts of the world, where larger amounts of heat may be requred. It has been suggested to utilise physical exergy in the produced water or cooling water by injecting it to enhance oil recovery instead of treated seawater, and that varying feed flow rates and compositions can be handled by installing several compression trains in parallel. Looking at the whole offshore platform, utilisation of physical exergy in the exhaust gases from the utility plant in bottoming cycles present a significant improvement potential.

The benefits of the proposed measures will always be evaluated against investment costs and the general demand for simple, reliable and compact process equipment on offshore installations.

7.4 Performance indicators

Several thermodynamic performance indicators have been discussed (Chapter 5), but none of them could at the same time evaluate (i) utilisation of technical achievable potential, (ii) utilisation of theoretical achievable potential and (iii) total use of energy resources. Thus a set of indicators has to be used to evaluate the thermodynamic performance. The following indicators are suggested: specific exergy destruction, BAT efficiency on exergy basis, and exergy efficiency.

Different formulations of exergy efficiency for petroleum separation systems were obtained by applying approaches found in the literature for similar processes (Chapter 6). They all had drawbacks such as low sensitivity to efficiency improvements, calculation inconsistencies or that they favoured facilities with certain boundary conditions when applied to offshore processing plants. A new definition, called the *component-by-component* exergy efficiency, was suggested. This definition could sucessfully evaluate the theoretical improvement potential.

The challenges in defining performance indicators for evaluation of offshore oil and gas platforms lie mainly in the high variety in boundary conditions of the systems.

7.5 Further work

The exergy analyses and process data that now are published, opens for possible further work on this topic. It is suggested to perform advanced exergy analysis to quantify avoidable and unavodable exergy destruction, to gain further insight into the real improvement potential of the processes, and to further develop performance indicators for offshore oil and gas processing by applying this concept.

Furthermore, it would be interesting to quantify the effect of installing production manifolds and separators at higher pressure levels. The option is technically achievable today, but the potential to actually increase thermodynamic efficiency and decrease power demand is not known.

It would also be valuable to perform exergetic life cycle assessments of the studied processes. This option requires more data available from the industry, as the processes need to be evaluated at different life cycle stages. Such studies would give more insight into the performance of oilfields throughout their life cycles, and this knowledge will be useful under the planning of new installations. Examples of exergetic life cycle assessments of offshore oil and gas extraction can also motivate the industry to perform such analyses for expected life cycles in the planning stages of the development of new fields. By taking the production of process equipment into account in the analyses, alternatives with more complex processes can be evaluated against the standard solutions on a rational basis.

Bibliography

[1] H. K. Abdel-Aal, M. Aggour, and M. A. Fahim. *Petroleum and Gas Field Processing*. Chemical Industries. Marcel Dekker, New York, USA, 2003.

[2] F. Abdollahi-Demneh, M. A. Moosavian, M. R. Omidkhah, and H. Bahmanyar. Calculating exergy in flowsheeting simulators: A hysys implementation. *Energy*, 20:1061–1155, 1991.

[3] H. Al-Muslim and I. Dincer. Thermodynamic analysis of crude oil distillation systems. *International Journal of Energy Research*, 29:637–655, 2005.

[4] L.-J. Alveberg and E. V. Melberg, editors. *Facts 2013: The Norwegian Petroleum Sector*. Ministry of Petroleum and Energy and Norwegian Petroleum Directorate, 2013.

[5] P. Andreussi, S. Sodini, V. Faluomi, P. Ciandri, A. Ansiati, F. Paone, C. Battaia, and G. D. Ghetto. Multiphase ejector to boost production: First application in the gulf of mexico. In *Proceedings of Offshore Technology Conference, 5th–8th May 2003, Houston, Texas*, 2003.

[6] Aspen Technology. *Aspen Plus – Modelling Petroleum Processes*. Aspen Technology, Burlington, USA, 1999.

[7] Aspen Technology. *Aspen Hysys 2004.2 ®– User Guide*. Aspen Technology, Cambridge, USA, 2004.

[8] Aspen Technology. *Hysys 2004.2 ®– Operations Guide*. Aspen Technology, Cambridge, USA, 2004.

[9] Aspen Technology. *Aspen HYSYS Simulation Basis Guide*. Aspen Technology, Burlington, USA, 2011.

[10] H. D. Baehr. *Energie und Exergie – Die Anwendung des Exergiebegriffs in der Energietechnik*. VDI-Verlag, Düsseldorf, Germany, 1965.

[11] H. D. Baehr. Zur Definition exergetischer Wirkungsgrade – Eine systematische Untersuchung. *Brennstoff-Wärme-Kraft*, 20(5):197–200, 1968.

[12] A. Bejan. *Advanced Engineering Thermodynamics*. John Wiley & Sons, New York, USA, 3rd edition, 2006.

[13] A. Bejan, G. Tsatsaronis, and M. Moran. *Thermal Design & Optimization*. John Wiley & Sons, New York, USA, 1996.

[14] M. Bothamley. Offshore Processing Options for Oil Platforms. In *Proceedings of the SPE Annual Technical Conference and Exhibition*, pages 1–17 (Paper SPE 90325), Houston, USA, 2004. Society of Petroleum Engineers.

[15] BP. *BP Statistical Review of World Energy June 2013*. BP, London, England, United Kingdom, 2013.

[16] V. M. Brodyansky, M. V. Sorin, and P. Le Goff. *The Efficiency of Industrial Processes: Exergy Analysis and Optimization*. Elsevier, Amsterdam, The Netherlands, 1994.

[17] N. L. S. Carnot. Reflections on the motive-power of heat, and on machines fitted to develop that power. In R. H. Thurston, editor, *Reflections on the motive-power of heat. Accompanied by an account of carnot's theory*. John Wiley and sons, London, 2nd edition, 1897.

[18] Y. Charron, P. Pagnier, E. Marchetta, and S. Stihle. Multiphase flow helico-axial turbine: Applications and performance. In *Proceedings of the 11th Abu Dhabi international Petroleum Exhibition and Conference*, 2004.

[19] R. L. Cornelissen. *Thermodynamics and sustainable development*. PhD thesis, University of Twente, 1997.

[20] R. L. Cornelissen and G. G. Hirs. The value of the exergetic life cycle assessment besides the LCA. *Energy conversion and management*, 43:1417–1424, 2002.

[21] Danish Energy Agency. Danmarks olie og gas produktion. Technical report, Energistyrelsen, København, Denmark, 2011.

[22] S. de Oliveira Jr. and M. van Hombeeck. Exergy analysis of petroleum separation processes in offshore platforms. *Energy Conversion and Management*, 38(15–17):1577–1584, 1997.

[23] A. V. Delgado. *Exergy evaluation of the mineral capital on earth*. PhD thesis, University of Zaragoza, 2008.

[24] K. G. Denbigh. The second-law efficiency of chemical processes. *Chemical Engineering Science*, 6(1):1–9, 1956.

[25] A. C. Dimian. *Integrated Design and Simulation of Chemical Processes*. Elsevier, Amsterdam, The Netherlands, 2003.

[26] I. Dincer and M. A. Rosen. *Exergy: Energy, Environment and Sustainable Development*. Elsevier, Oxford, UK and Burlington, USA, 1. edition, 2007.

[27] B. Elmegaard and N. Houbak. DNA – A General Energy System Simulation Tool. In J. Amundsen, editor, *Proceedings of SIMS 2005 - 46th Conference on Simulation and Modeling*, pages 43–52, Trondheim, Norway, 2005. Tapir Academic Press.

[28] J. Falcimaigne and S. Decarre. *Multiphase Production: Pipeline Transport, Pumping and Metering*. Editions Technip, Paris, 2008.

[29] W. Fratzscher and J. Beyer. Stand und Tendenzen bei der Anwendung und Witerentwicklung des Exergiebegriffs. *Chemische Technik*, 33(1):1–10, 1981.

[30] W. Fratzscher, V. M. Brodjanskij, and K. Michalek. *Exergie: Theorie und Anwendung*. Deutscher Verlag für Grundstoffindustrie, Leipzig, Germany, 1986.

[31] V. P. Grassmann. Zur allgemeinen Definition des Wirkungsgrades. *Chemie Ingenieur Technik*, 4(1):77–80, 1950.

[32] W. P. Hancock. Development of a Reliable Gas Injection Operation for the North Sea's Largest-Capacity Production Platform, Statfjord A. *Journal of Petroleum Technology*, 35(11):1963–1972, 1983.

[33] W. He, G. Jacobsen, T. Anderson, F. Olsen, T. D. Hanson, M. Korpås, T. Toftevaag, J. Eek, K. Uhlen, and E. Johansson. The potential of integrating wind power with offshore oil and gas platforms. *Wind Engineering*, 34(2):125–138, 2010.

[34] O. K. Helgesen. Klimameldingen kan gi mindre utvinning. *Teknisk Ukeblad*, 16:14, 2012.

[35] Ingeniøren/bøger. *Pumpe Ståbi*. Ingeniøren A/S 2000, København, Denmark, 2000.

[36] International Energy Agency. *Energy Technology Perspectives 2012*. International Energy Agency, Paris, France, 2012.

[37] International Energy Agency. *World Energy Outlook 2012*. International Energy Agency, Paris, France, 2012.

[38] International Energy Agency. *CO_2 Emissions from Fuel Combusion*. International Energy Agency, Paris, France, 2013.

[39] International Energy Agency. *Redrawing the Energy-Climate Map*. International Energy Agency, Paris, France, 2013.

[40] E. Johannessen, L. Nummedal, and S. Kjelstrup. Minimizing the entropy production in heat exchange. *International Journal of Heat and Mass Transfer*, 45(13):2649–2654, 2002.

[41] E. Johannessen and A. Røsjorde. Equipartition of entropy production as an approximation to the state of minimum entropy production in diabatic distillation. *Energy*, 32(4):467–473, 2007.

[42] D. S. J. S. Jones and P. R. Pujadó, editors. *Handbook of Petroleum Processing*. Springer, Dordrecht, The Netherlands, 2006.

[43] K. Jøssang. Evaluation of a North Sea oil platform using exergy analysis. Master's thesis, Norwegian University of Science and Technology, 2013.

[44] S. Kelly, G. Tsatsaronis, and T. Morosuk. Advanced exergetic analysis: Approaches for splitting the exergy destruction into endogenous and exogenous parts. *Energy*, 34(3):384–391, 2009.

[45] S. Kjelstrup and E. Johannesen. *Non-equilibrium thermodynamics for engineers*. World Scientific, Singapore, 2010.

[46] P. Kloster. Energy Optimization on Offshore Installations with Emphasis on Offshore and Combined Cycle Plants. In *Proceedings of the Offshore Europe Conference*, pages 1–9 (Paper SPE 56964), Aberdeen, United Kingdom, 1999. Society of Petroleum Engineers.

[47] P. Kloster. Reduction of Emissions to Air Through Energy Optimisation on Offshore Installations. In *Proceedings of the SPE International Conference on Health, Safety, and the Environment in Oil and Gas Exploration and Production*, pages 1–7 (Paper SPE 61651), Stavanger, Norway, 2000. Society of Petroleum Engineers.

[48] T. J. Kotas. Exergy concepts for thermal plant: First of two papers on exergy techniques in thermal plant analysis. *International Journal of Heat and Fluid Flow*, 2(3):105–114, 1980.

[49] T. J. Kotas. Exergy Criteria of Performance for Thermal Plant: Second of two papers on exergy techniques in thermal plant analysis. *International Journal of Heat and Fluid Flow*, 2(4):147–163, 1980.

[50] T. J. Kotas. *The Exergy Method of Thermal Plant Analysis*. Krieger Publishing Company, Malabar, USA, 2nd edition, 1995.

[51] A. Lazzaretto and G. Tsatsaronis. On the calculation of efficiencies and costs in thermal systems. In S. M. Aceves, S. Garimella, and R. B. Peterson, editors, *Proceedings of the ASME Advanced Energy Systems Division*, volume 39, pages 421–430, New York, USA, 1999.

[52] A. Lazzaretto and G. Tsatsaronis. SPECO: A systematic and general methodology for calculating efficiencies and costs in thermal systems. *Energy*, 31:1257–1289, 2006.

[53] K. J. Li. Use of a Fractionation Column in an Offshore Environment. In *Proceedings of the SPE Annual Technical Conference and Exhibition*, pages 1–11 (Paper SPE 49121), New Orleans, USA, 1996. Society of Petroleum Engineers.

[54] S. Lieblein. *Analysis of experimental low-speed loss and stall characteristics of two-dimensional compressor blade cascades*. NACA RM E57A28, Washington, USA, 1957.

[55] N. Lior and N. Zhang. Energy, exergy, and Second Law performance criteria. *Energy*, 32(4):281–296, 2007.

[56] F. S. Manning and R. E. Thompson. *Oilfield processing of petroleum: Crude oil*, volume 2. PennWell Books, Tulsa, USA, 1991.

[57] F. S. Manning and R. E. Thompson. *Oilfield processing of petroleum: Natural Gas*, volume 1. PennWell Books, Tulsa, USA, 1991.

[58] M. Margarone, S. Magi, G. Gorla, S. Biffi, P. Siboni, G. Valenti, M. C. Romano, A. Giuffrida, E. Negri, and E. Macchi. Revamping, energy efficiency, and exergy analysis of an existing upstream gas treatment facility. *Journal of Energy Resources Technology*, 133:012001–1–012001–9, 2011.

[59] D. Marmolejo-Correa and T. Gundersen. A comparison of exergy efficiency definitions with focus on low temperature processes. *Energy*, 44:477–489, 2012.

[60] L. Meyer, G. Tsatsaronis, J. Buchgeister, and L. Schebek. Exergoenvironmental analysis for evaluation of the environmental impact of energy conversion systems. *Energy*, 34(1):75–89, 2009.

[61] M. J. Moran. *Availability analysis: a guide to efficient energy use*. ASME Press, New York, USA, 2nd edition, 1989.

[62] M. J. Moran. Fundamentals of exergy analysis and exergy-based thermal systems design. In A. Bejan and E. Mamut, editors, *Proceedings of the NATO Advanced Study Institute on Thermodynamic Optimization of Complex Energy Systems*, volume 69 of *NATO Science Series*, pages 73–92, Neptun, Romania, 1998. Kluwer Academic Publishers.

[63] M. J. Moran and H. N. Shapiro. *Fundamentals of Engineering Thermodynamics*. John Wiley & Sons, Inc, USA, 5 edition, 2004.

[64] D. Morris, F. Steward, and S. J. Technological assessment of chemical metallurgical processes. *Canadian Metallurgical Quarterly*, 33(4):289–295, 1994.

[65] D. R. Morris and J. Szargut. Standard chemical exergy of some elements and compounds on the planet earth. *Energy*, 11(8):733–755, 1986.

[66] D. E. Muir, H. I. H. Saravanamuttoo, and D. J. Marshall. Health Monitoring of Variable Geometry Gas Turbines for the Canadian Navy. *ASME Journal of Engineering for Gas Turbines and Power*, 111(2):244–250, 1989.

[67] K. Nesselmann. Über den thermodynamischen Begriff der Arbeitsfähigkeit. *Allgemeine Wärmetechnik*, 3(5–6):97–104, 1952.

[68] K. Nesselmann. Der Wirkungsgrad thermodynamischer Prozesse und sein Zusammenhang mit der Umgebungtemperatur. *Allgemeine Wärmetechnik*, 4(7):141–147, 1953.

[69] T.-V. Nguyen, T. Jacyno, P. Breuhaus, M. Voldsund, and B. Elmegaard. Thermodynamic analysis of an upstream petroleum plant operated on a mature field. *Energy*, xxx:1–16, 1014. In press. http://dx.doi.org/10.1016/j.energy.2014.02.040.

[70] T.-V. Nguyen, L. Pierobon, and B. Elmegaard. Exergy analysis of offshore processes on North Sea oil and gas platforms. In *Proceedings of CPOTE 2012 - The 3rd International Conference on Contemporary Problems of Thermal Engineering*, pages 1–9 (Paper 45), Gliwice, Poland, 2012.

[71] T.-V. Nguyen, L. Pierobon, B. Elmegaard, F. Haglind, P. Breuhaus, and M. Voldsund. Exergetic assessment of energy systems on North Sea oil and gas platforms. *Energy*, 62:23–36, 2013.

[72] F. M. Nordvik, S. B. Verlo, and E. Zenker, editors. *Facts 2011: The Norwegian petroleum sector*. Ministry of Petroleum and Energy and Norwegian Petroleum Directorate, 2010.

[73] Norwegian Meteorological Institute. Mean temperature – ordered report. http://eklima.met.no, October 2012.

[74] Norwegian Ministry of Petroleum and Energy. Facts 2012 – The Norwegian Petroleum Sector. Technical report, Norwegian Petroleum Directorate, Oslo, Norway, 2012.

[75] K. Oxley, J. Bennett, L. Fremin, J. Taylor, and G. Ross. Rst's mission to mars - the first commercial application of rotary separator turbine technology. In *Proceedings of Offshore Technology Conference, 5th.–8th May 2003, Houston, Texas*, 2003.

[76] V. P. Patel and H. E. Kimmel. Fifteen years of field experience in lng expander technology. In *Proceedings of the First Middle East Turbomachinery Symposium*, 2011.

[77] D.-Y. Peng and D. B. Robinson. A new two-constant equation of state. *Ind. Eng. Chem. Fundam.*, 15:59–64, 1976.

[78] W. C. L. Plisga and G. J., editors. *Standard Handbook of Petroleum & Natural Gas Engineering*. Gulf Professional Publishing, Burlington, USA, 2nd edition, 2004.

[79] T. Puntervold and T. Austad. Injection of seawater and mixtures with produced water into North Sea chalk formation: Impact on wettability, scale formation and rock mechanics caused by fluid-rock interaction. *Journal of Petroleum Science and Engineering*, 63(1-4):23–33, 2008.

[80] C. Rawlins and G. Ross. Design and analysis of a multiphase turbine for compact gas-liquid separation. *SPE Production & Facilities*, 17:47–52, 2002.

[81] H. Renon and J. M. Prausnitz. Local compositions in thermodynamic excess functions for liquid mixtures. *AIChE Journal*, 14(1):135–144, 1968.

[82] A. B. Rian and I. S. Ertesvåg. Exergy Evaluation of the Arctic Snøhvit Liquefied Natural Gas Processing Plant in Northern Norway – Significance of Ambient Temperature. *Energy & Fuels*, 26:1259–1267, 2012.

[83] R. Rivero. Application of the exergy concept in the petroleum refining and petrochemical industry. *Energy Conversion and Management*, 43(9-12):1199–1220, 2002.

[84] R. Rivero, C. Rendón, and S. Gallegos. Exergy and exergoeconomic analysis of a crude oil combined distillation unit. *Energy*, 29:1909–1927, 2004.

[85] R. Rivero, C. Rendon, and L. Monroy. The Exergy of Crude Oil Mixtures and Petroleum Fractions: Calculation and Application. *International Journal of Applied Thermodynamics*, 2(3):115–123, 1999.

[86] M. Rosen and I. Dincer. Exergy analysis of waste emissions. *International Journal of Energy Research*, 23(13):1153–1163, 1999.

[87] H. I. H. Saravanamuttoo, G. F. C. Rogers, H. Cohen, and P. Straznicky. *Gas Turbine Theory*. Pearson Prentice Hall, Upper Saddle River, USA, 6th edition, 2008.

[88] N. Sato. *Chemical Energy and Exergy: An Introduction to Chemical Thermodynamics for Engineers*. Elsevier, Amsterdam, The Netherlands, 1st edition, 2004.

[89] A. Satter, G. M. Iqbal, and J. L. Buchwalter. *Practical Enhanced Reservoir Engineering: Assisted With Simulated Software*. PennWell Books, Tulsa, USA, 2008.

[90] J. Schwartzentruber and H. Renon. Extension of UNIFAC to High Pressures and Temperatures by the Use of a Cubic Equation of State. *Industrial & Engineering Chemistry Research*, 28(7):1049–1055, 1989.

[91] J. Schwartzentruber, H. Renon, and S. Watanasiri. Development of a new cubic equation of state for phase equilibrium calculations. *Fluid Phase Equilibria*, 52:127–134, 1989.

[92] E. Sciubba. Beyond thermoeconomics? The concept of Extended Exergy Accounting and its application to the analysis and design of thermal systems. *Exergy, An International Journal*, 1(2):68–84, 2001.

[93] E. Sciubba. Extended exergy accounting applied to energy recovery from waste: The concept of total recycling. *Energy*, 28(13):1315–1334, 2003.

[94] E. Sciubba and G. Wall. A brief commented history of exergy from the beginnings to 2004. *International Journal of Thermodynamics*, 10(1):1–26, 2007.

[95] U. Setzmann and W. Wagner. A new equation of state and tables of thermodynamic properties for methane covering the range from the melting line to 625 K at pressures up to 1000 MPa. *J. Phys. Chem. Ref. Data*, 36:5320–5327, 2011.

[96] SIEMENS. SGT-500 Industrial Gas Turbine. Technical report, Siemens Industrial Turbomachinery AB, Finnspong, Sweden, 2011.

[97] G. Soave. Equilibrium constants from a modified Redlich–Kwong equation of state. *Chemical Engineering Science*, 27(6):1197–1203, 1972.

[98] G. Soave. 20 years of Redlich–Kwong equation of state. *Fluid Phase Equilibria*, 82:345–359, 1993.

[99] T. W. Song, T. S. Kim, J. H. Kim, and S. T. Ro. Performance prediction of axial flow compressors using stage characteristics and simultaneous calculation of interstage parameters. In *Proceedings of the Institution of Mechanical Engineers*, volume 215 Part A, pages 89–98, London, United Kingdom, 2001. Institution of Mechanical Engineers.

[100] M. V. Sorin, V. M. Brodyansky, and J. Paris. Observations on exergy efficiency coefficients. In E. Carnevale, G. Manfrida, and F. Martelli, editors, *Proceedings of the Florence World Energy Research Symposium*, volume 94, pages 941–949, Padova, Italy, 1994. SG Editoriali.

[101] M. V. Sorin, J. Paris, and V. M. Brodjanskij. Thermodynamic evaluation of a distillation. In *Thermodynamics and the Design, Analysis, and Improvement of Energy Systems*, volume 33, pages 125–134, New York, USA, 1994. ASME.

[102] J. G. Speight. *Handbook of petroleum product analysis*. Wiley, 2002.

[103] P. R. Spina. Gas Turbine performance prediction by using generalized performance curves of compressor and turbine stages. In *Proceedings of the ASME Turbo Expo 2002: Power for Land, Sea, and Air (GT2002)*, volume 2, pages 1073–1082, Amsterdam, The Netherlands, 2002.

[104] Statistics Norway. Greenhouse gases, by source, energy product and pollutant (1980–2011), November 2012. http://www.ssb.no/emner/01/04/10/klimagassn/.

[105] Statistics Norway. Emissions of greenhouse gases: Create your own tables and graphs, October 2013. http://www.ssb.no/emner/01/04/10/klimagassn/.

[106] Statistisk Sentralbyrå. Lavere klimagassutslipp i 2011, 2012.

[107] A. Stodola. *Dampf- und Gasturbinen*. Springer, Berlin, Germany, 6th edition, 1924.

[108] Sulzer Pumps. *Centrifugal Pump Handbook*. Elsevier, New York, USA, 3rd edition, 2010.

[109] S. M. Svalheim. Environmental Regulations and Measures on the Norwegian Continental Shelf. In *Proceedings of the SPE International Conference on Health, Safety and Environment in Oil and Gas Exploration and Production*, pages 1–10 (Paper SPE 73982), Kuala Lumpur, Malaysia, 2002. Society of Petroleum Engineers.

[110] S. M. Svalheim and D. C. King. Life of Field Energy Performance. In *Proceedings of the SPE Offshore Europe Conference*, pages 1–10 (Paper SPE 83993), Aberdeen, United Kingdom, 2003. Society of Petroleum Engineers.

[111] J. Szargut. International progress in second law analysis. *Energy*, 5:709–718, 1980.

[112] J. Szargut. Chemical exergies of the elements. *Applied Energy*, 32(4):269–286, 1989.

[113] J. Szargut. Exergy in the thermal systems analysis. In A. Bejan and E. Mamut, editors, *Proceedings of the NATO Advanced Study Institute on Thermodynamic Optimization of Complex Energy Systems*, volume 69 of *NATO Science Series*, pages 137–150, Neptun, Romania, 1998. Kluwer Academic Publishers.

[114] J. Szargut, D. Morris, and F. Steward. *Exergy analysis of thermal, chemical, and metallurgical processes*. Hemisphere, New York, USA, 1988.

[115] J. R. Taylor. *An Introduction to Error Analysis*. University Science Books, Sausalito, California, 2 edition, 1997.

[116] I. Templalexis, P. Pilidis, V. Pachidis, and P. Kotsiopoulos. Development of a two-dimensional streamline curvature code. *ASME Journal of Turbomachinery*, 133(1):011003, 2011.

[117] W. Traupel. *Thermische Turbomaschinen*. Springer, Berlin, Germany, 3rd edition, 1977.

[118] G. Tsatsaronis. Thermoeconomic analysis and optimization of energy systems. *Progress in Energy and Combustion Science*, 19:227–257, 1993.

[119] G. Tsatsaronis. Definitions and nomenclature in exergy analysis and exergoeconomics. *Energy*, 32:249–253, 2007.

[120] G. Tsatsaronis and F. Cziesla. *Encyclopedia of Physical Science and Technology*, volume 16, chapter Thermoeconomics, pages 659–680. Academic Press, 3rd edition, 2002.

[121] G. Tsatsaronis and M.-H. Park. On avoidable and unavoidable exergy destructions and investment costs in thermal systems. *Energy Conversion and Management*, 43:1259–1270, 2002.

[122] G. Tsatsaronis and M. Winhold. Exergoeconomic analysis and evaluation of energy-conversion plants – I. A new general methodology. *Energy*, 10(1):69–80, 1985.

[123] C. Tsonopoulos and J. Heidman. From Redlich-Kwong to the present. *Fluid phase equilibria*, 24(1):1–23, 1985.

[124] A. Valero and A. Valero. Exergoecology: A thermodynamic approach for accounting the earth's mineral capital. the case of bauxite-aluminium and limestone-lime chains. *Energy*, 35:229–238, 2010.

[125] E. A. Vik and A. J. Dinning. Produced Water Re-Injection - The Potential to Become an Improved Oil Recovery Method. Technical report, Aquatem A/S, Oslo, Norway, 2009.

[126] M. Voldsund, I. S. Ertesvåg, W. He, and S. Kjelstrup. Exergy analysis of the oil and gas processing a real production day on a North Sea oil platform. *Energy*, 55:716–727, 2013.

[127] M. Voldsund, I. S. Ertesvåg, A. Røsjorde, W. He, and S. Kjelstrup. Exergy analysis of the oil and gas separation processes on a North Sea oil platform. In D. Favrat, editor, *Proceedings of ECOS 2010: 23rd International Conference on Efficiency, Cost, Optimization, Simulation, and Environmental Impact of Energy Systems*, Lausanne, Switzerland, 2010.

[128] M. Voldsund, W. He, A. Røsjorde, I. S. Ertesvåg, and S. Kjelstrup. Evaluation of the oil and gas processing at a real production day on a north sea oil platform using exergy analysis. In U. Desideri, G. Manfrida, and E. Sciubba, editors, *Proceedings of ECOS 2012: 25th International Conference on Efficiency, Cost, Optimization, Simulation, and Environmental Impact of Energy Systems*, Perugia, Italy, 2012.

[129] M. Voldsund, T.-V. Nguyen, B. Elmegaard, I. S. Ertesvåg, A. Røsjorde, K. Jøssang, and S. Kjelstrup. Exergy destruction and losses on four north sea offshore platforms: A comparative study of the oil and gas processing plants. [under review], 2013 (submitted).

[130] G. Wall. Exergy flows in industrial processes. *Energy*, 13(2):197–208, 1988.

[131] G. Wall. Exergy. In *Encyclopedia of Energy*, volume 2, pages 593–606. Academic Press, 2004.

[132] C. H. Whitson and M. R. Brulé. *Phase Behavior*, volume 20 of *SPE Monograph Series*. Society of Petroleum Engineers, Richardson, USA, 2000.

[133] Ø. Wilhelmsen, E. Johannesen, and S. Kjelstrup. Energy efficient reactor design simplified by second law analysis. *International Journal of Hydrogen Energy*, 35(24):13213–13219, 2010.